論文 / 著書情報
Article / Book Information

題目(和文)	一般廃棄物焼却飛灰のマイクロスケールでの地球化学的特性評価
Title(English)	Micro-scale geochemical characterization of municipal solid waste incineration fly ash
著者(和文)	北村洋樹
Author(English)	Hiroki Kitamura
出典(和文)	学位:博士(工学), 学位授与機関:東京工業大学, 報告番号:甲第10841号, 授与年月日:2018年3月26日, 学位の種別:課程博士, 審査員:高橋 史武,吉川 邦夫,日野出 洋文,竹下 健二,時松 宏治
Citation(English)	Degree:Doctor (Engineering), Conferring organization: Tokyo Institute of Technology, Report number:甲第10841号, Conferred date:2018/3/26, Degree Type:Course doctor, Examiner:,,,,
学位種別(和文)	博士論文
Type(English)	Doctoral Thesis

Micro-scale Geochemical Characterization of Municipal Solid Waste Incineration Fly Ash

Hiroki Kitamura

Supervisor: Associate Professor Fumitake Takahashi

Doctoral Dissertation

Department of Environmental Science and Technology

Interdisciplinary Graduate School of Science and Engineering

Tokyo Institute of Technology

FY2017

一般廃棄物焼却飛灰のマイクロスケールでの
地球化学的特性評価

北村　洋樹

指導教員：高橋　史武　准教授

博士論文

東京工業大学　大学院総合理工学研究科

環境理工学創造専攻

平成 29 年度

Table of Contents

List of Figures

Chapter 1

Chapter 2

Chapter 3

Chapter 4

Chapter 5

Supplementary material

Chapter 6

List of Tables

Chapter 1

Chapter 2

Chapter 3

Chapter 4

Chapter 5

CHAPTER

1

INTRODUCTION

Abstract: This chapter presents background and objective of the present study. It summarizes municipal solid waste (MSW) management in Japan as well as intermediate treatment for municipal solid waste incineration (MSWI) fly ash. The objective of the present study is presented in this chapter.

1.1 Historical background and present situation of waste management in Japan

In Japan , the Waste Cleaning Act was legislated in 1900 as the first law relating to waste management [1–3]. The main objectives of the law were to improve public health and prevent from infectious disease. After World War II, the Public Cleansing Act was legislated in 1954 in order to clarify roles and encourage collaboration among national government, local governments, and consumers in waste management system. However, it was difficult to manage wastes since rapid economic growth because the amount of waste increased and various wastes were produced by corporate manufacturing activities. Therefore, the Waste Management and Public Cleaning Act was legislated in 1970 in order to handle various wastes. It categorized waste into municipal waste managed by municipalities and industrial waste managed by business operators.

The amount of municipal solid waste (MSW) generated in the last two decades is shown in Fig. 1.1 [4,5]. It had continuously increased from fiscal year (FY) 1996 to 2000. In 1990s, a large number of municipalities introduced unit-charging programs for waste

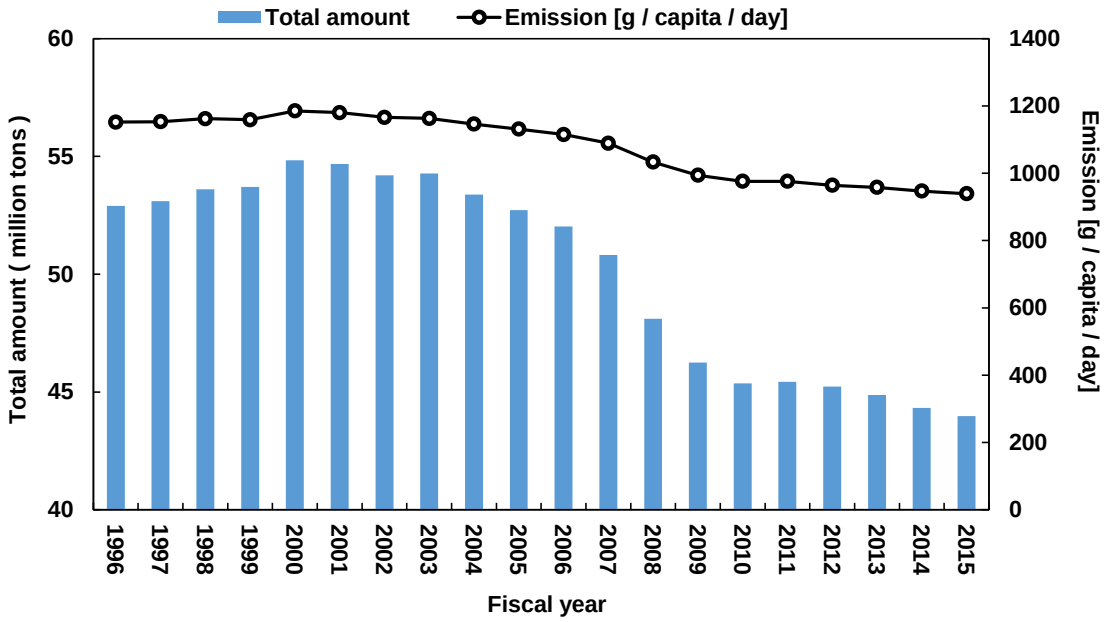

Fig. 1.1 Change in the amount of MSW generated in the last two decades

disposal known as pay-as-you-throw (PAYT) resulted from amendment to the Waste Management Law in 1991 [6]. Combination of PAYT programs and the Containers and Packaging Recycling Law legislated in 1995 promoted MSW reduction. The Basic Act on Establishing a Sound Material-Cycle Society legislated in 2000, which introduced the concept of 3R (reduce, reuse, and recycle), increased MSW recycling [7,8]. As a result, the amount of MSW generated has decreased from 54.83 to 43.98 million tons since FY2000.

The amount of MSW treated in the last decade is shown in Fig. 1.2 [5]. Recently, approximately 80 % of MSW is incinerated. Service lifetime for landfills remains only 20.4 year owing to limitedly available land space in Japan. However, it is difficult to construct new landfills owing to great difficulty of public acceptance [9]. Therefore, incineration has been accepted as main treatment method for MSW in order to reduce 90% of the volume and 70 % of the weight.

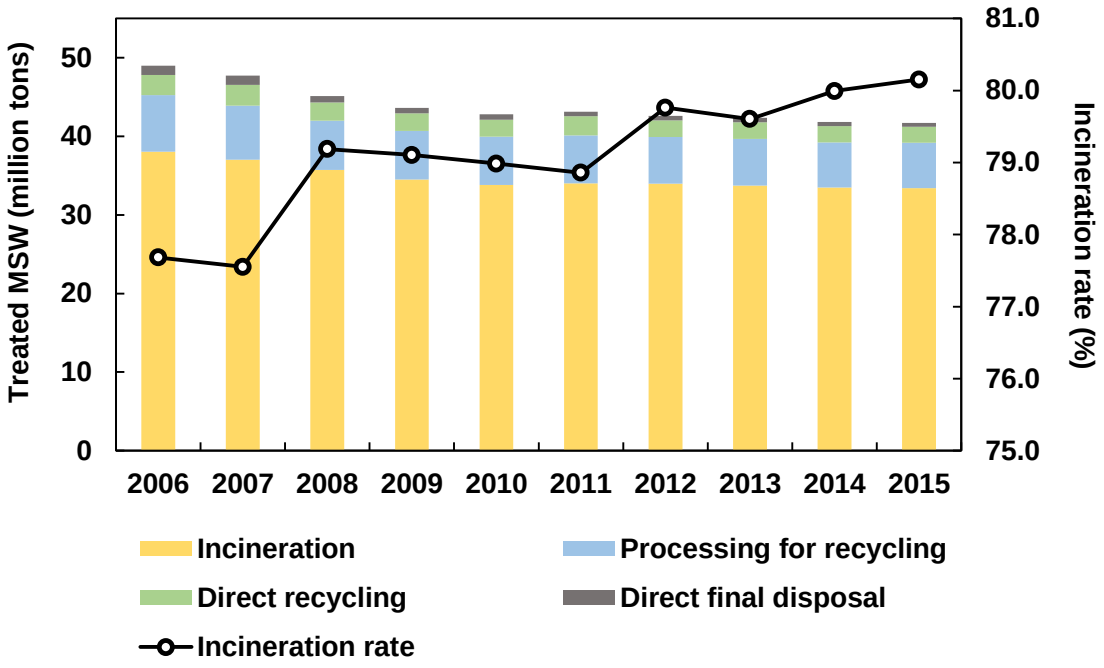

Fig. 1.2 Change in the amount of MSW treated in the last decade

1.2 Municipal solid waste incineration facility

In FY 2015, the number of municipal solid waste incineration (MSWI) facility was 1141 facilities. In Japan, three types of incinerators (stoker, fluidized bed, and gasification melting incinerator) are mainly used for MSWI. Particularly, stoker-type incinerator accounts for approximately 70 % of all incinerators owing to better processing performance, good environmental performance, and low maintenance and operating costs [5,10]. During MSWI process, exhaust gas including toxic substances such as hydrochloric acid (HCl), sulfur oxide (SO_x), nitrogen oxide (NO_x), dioxin, and dust should be carefully controlled for environmental preservation [11].

For acidic gas (HCl and SO_x) treatment, lime for dry and semi-dry process or sodium hydroxide (NaOH) for wet process is injected into exhaust gas in order to neutralize acidic gas (see Eqs (1) to (6) shown in table 1.1) [12,13]. For NO_x treatment, ammonia (NH_3) or urea ($(NH_2)_2CO$) is injected for catalytic or non-catalytic reduction process (see Eqs (7) and (8) shown in table 1.1) [12]. For dioxin control, complete combustion with higher than 850 ˚C, rapid cooling of exhaust gas with lower than 200 ˚C, and injection of

Table 1.1 Representative chemical reaction for exhaust gas treatment

Gas		Representative chemical reaction	Eqs
HCl and SO_x	Dry process and Semi-dry process	$CaO + 2HCl \rightarrow CaCl_2 + H_2O$	(1)
		$CaO + SO_2 \rightarrow CaSO_3$	(2)
		$Ca(OH)_2 + 2HCl \rightarrow CaCl_2 + 2H_2O$	(3)
		$Ca(OH)_2 + SO_2 + 1/2O_2 \rightarrow CaSO_4 + H_2O$	(4)
	Wet process	$NaOH + HCl \rightarrow NaCl + H_2O$	(5)
		$2NaOH + SO_2 + 1/2O_2 \rightarrow Na_2SO_4 + H_2O$	(6)
NO_x	Reduction	$4NO + 4NH_3 + O_2 \rightarrow 4N_2 + 6H_2O$	(7)
		$4NO + 2(NH_2)_2CO + O_2 \rightarrow 4N_2 + 4H_2O + 2CO_2$	(8)

activated carbon for adsorption are required [14]. The detoxified substances in exhaust gas are then collected together with dust by air pollution control devices (APCDs) such as fabric filter.

1.3 MSWI residues (bottom ash and fly ash)

As mentioned before, incineration has some advantages such as significant volume and weight reduction as well as energy recovery, and destruction of pathogens and other organic toxic compounds, and so on [15]. In contrast to these advantages, one of the inconvenience is that MSWI incineration residues such as bottom ash and fly ash are generated as by-products. The amounts of the bottom ash generated from incinerator is 10–15 % of MSW and that of the fly ash collected from APCDs is 2–3 % of MSW [16]. In FY 2015, approximately 3.2 million tons of MSWI residues were generated and the disposal volume accounted for approximately 76 % of total disposal volume [5]. The amount of heavy metals in bottom ash is lower than that in fly ash because volatilized heavy metals concentrated to fly ash during MSWI process [17]. Furthermore, leachability of heavy metals in bottom ash is lower than that in fly ash [16–18]. As a result, MSWI bottom ash is classified as non-hazardous materials while MSWI fly ash is classified as hazardous materials [16,19]. Therefore, intermediate treatment is required in order to reduce leachability of heavy metals in MSWI fly ash before landfill disposal.

Physical, chemical, mineralogical, and geochemical characteristics of MSWI fly ash have been investigated by comprehensive approaches [20]. However, such characteristics of MSWI fly ash depend on compositions of feeding MSW, types of incinerator, APCDs, operation conditions, and so on [21,22]. Furthermore, metal species in MSWI fly ash also depend on many factors such as affinities of elements and flue gas compositions (e.g. contents of chlorine, moisture, sulfur, and inorganic particulates) [23–30]. Therefore,

appropriate treatment and the treatment conditions are different for each MSWI fly ash.

1.4 Regulatory intermediate treatment for MSWI fly ash

Intermediate treatments for MSWI fly ash are required before landfill disposal in order to prevent from leaching of heavy metals to the environment. In Japan, melting and cement solidification/stabilization (S/S), chemical immobilization, and extraction with acid or other solvents are legislated by the government [11,31]. After the intermediate treatments, MSWI fly ashes are subjected to leaching experiment in order to confirm leaching concentration level of regulated toxic heavy metals (see Table 1.2). MSWI fly ash, which can satisfy the regulation standard after the intermediate treatment, can be disposed. Each intermediate treatments are introduced in following sections.

1.4.1 Cement solidification/stabilization

Cement S/S process is that cement and water are added to MSWI fly ash and

Table 1.2 Regulation standard of toxic metals for landfill disposal

Toxic metals	Regulation standard [mg/L]
Alkyl mercury compounds	To be non-detected
Mercury (Hg) and its compounds	0.005
Cadmium (Cd) and its compounds	0.3
Lead (Pb) and its compounds	0.3
Hexavalent chromium (Cr^{6+}) and its compounds	1.5
Arsenic (As) and its compounds	0.3
Selenium (Se) and its compounds	0.3

sufficiently mixed in order to contact the cement and the fly ash. Immobilization mechanisms of heavy metals are considered as adsorption to calcium silicate hydrates (C-S-H) and formation of insoluble metal hydroxides [32–34]. C-S-H gel is major product of cement which contains bulk of micro-porosity with high surface area. The microstructural characteristics promote sorption properties of heavy metals. Heavy metals are also incorporated into ettringite ($3CaO{\cdot}Al_2O_3{\cdot}3CaSO_4{\cdot}32H_2O$) in cement by substitution reaction of Ca^{2+}, Al^{3+}, and SO_4^{2-} site. Thus, heavy metals in MSWI fly ash can be immobilized physically and chemically. However, the final disposal volume is increased by addition of cement. Therefore, cement S/S process is combined with chemical immobilization in order to prevent from volume increase in some cases.

1.4.2 Melting solidification/stabilization

Melting S/S is that MSWI fly ash is melted at high temperature in excess 1200 ˚C in order to produce inert glass material called slag [35,36]. The volume of MSWI fly ash can be reduced to 15-25% by the melting [37]. Toxic substances can be destructed during the melting. Volatile heavy metals in MSWI fly ash concentrate to molten fly ash. On the other hand, heavy metals remained in slag are incorporated into glass matrix of slag consisting mainly of Al_2O_3, CaO, SiO_2, and Fe_2O_3. The slag can be recycled as landscaping and building materials. In contrast to these advantages, additional treatment for molten fly ash containing high amount of volatile heavy metals are required. Furthermore, operating cost is quite expensive in comparison with other intermediate treatments [31].

1.4.3 Extraction with acid or other solvents

Extraction with acid solution is that heavy metals in MSWI fly ash are extracted by

acid and immobilized by sodium hydrogensulfide (NaHS) [38]. Firstly, MSWI fly ash and water are mixed in order to make fly ash slurry. In this process, water soluble salt such as $CaCl_2$, KCl, and NaCl as well as parts of heavy metals are extracted. Secondary, HCl is added to the slurry in order to adjust pH to 6.0 and extract heavy metals. After the extraction, NaHS is added to the slurry in order to adjust pH to 8.0 and immobilize heavy metals. Thirdly, the immobilized slurry is coagulated with polymer flocculant and dewatered by centrifugal separator. However, pH of MSWI fly ash is usually high alkaline owing to lime injection during exhaust gas treatment. This means that large amounts of acid addition is required. Therefore, chelate reagent such as ethylendiaminetetraacetate (EDTA), which can extract heavy metals in the wide range of pH, is also used as extract solution [37,39].

1.4.4 Chemical immobilization

Chemical immobilization is that heavy metals in MSWI fly ash are immobilized by inorganic or organic reagent. In the case of inorganic reagent, phosphoric acid (H_3PO_4) is mainly used in order to immobilize heavy metals as stable metal phosphate minerals [40–42]. In the case of organic reagent, chelate reagent using dithiocarbamic salt, which called chelate treatment, is preferred by a number of municipalities [43]. The advantages of chelate treatment are as follows: (1) simple treatment (chelate reagent and water for kneading are mixed with MSWI fly ash), (2) additional pretreatment such as pH control is not required regardless of the high alkalinity of MSWI fly ash [43], (3) heavy metals can be immobilized at wide range of pH value [44,45]. The main immobilization mechanism of chelate treatment is considered as water-insoluble complexation of heavy metals with organic sulfide functional group as shown in Fig 1.3 [43]. The stability of metal chelate complex of diethyldithiocarbamate decreases in following order: Hg > Cu

> Pb > Ni > Cd > Fe > Co > Zn > Mn [46]. Chelate treatment is one of the most used intermediate treatment for MSWI fly ash in Japan. However, long-term stability of the metal chelate complex under the air contact conditions has been concerned [43,47].

1.5 Previous researches on MSWI fly ash

Mineralogical characteristics of MSWI fly ash are usually investigated by X-ray diffraction (XRD) analysis. However, it has some difficulties for mineralogical characterization because MSWI fly ash consists of complex crystalline and non-crystalline phases [21,48]. Metal species in MSWI fly ash are also identified by XRD analysis. However, it is also difficult to identify metal-bearing minerals in MSWI fly ash owing to their presence in amorphous phase and/or their low concentration level [49–52]. Morphological characteristics of MSWI fly ash are usually investigated by microscopic observation equipped with elemental analyzer. However, structural characteristics of MSWI fly ash particles are still uncertain. In addition, MSWI fly ash is naturally considered as homogeneous owing to fine particles although no researches investigated heterogeneity of MSWI fly ash quantitatively. Geochemical modeling approaches also simulate leaching behaviors of heavy metals without considering the impacts of heterogeneous characteristics of MSWI fly ash. Therefore, previous studies on MSWI fly

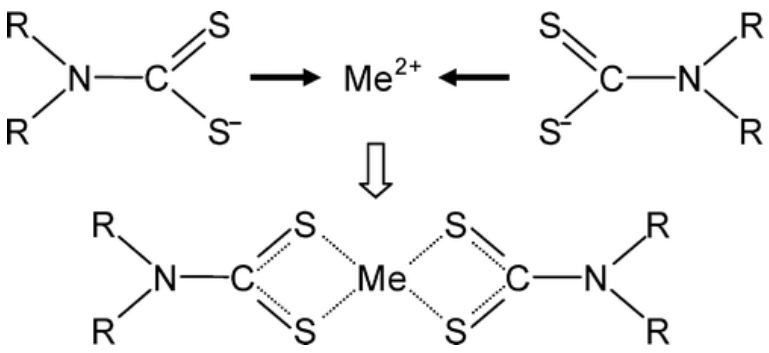

Fig. 1.3 Immobilization mechanism of chelate treatment (R: carbon chain) [43]

ash still have some uncertain points for characterization.

As described in previous section, various intermediate treatments for MSWI fly ash have been proposed [53,54]. Chelate treatment is preferred than other treatments in Japan although cement solidification/stabilization is the most used among various treatments in the world owing to low treatment costs and ease of application [54–56]. Therefore, only a few studies have been focused on chelate-treated MSWI fly ash [44,45,57]. However, these studies only focused on leachability of heavy metals after chelate treatment because its immobilization mechanism is considered as complexation without change of material structure [57]. Therefore, the impacts of chelate treatment on micro-scale characteristics (e.g. morphological, mineralogical, heterogeneous characteristics) of MSWI fly ash still have not been investigated.

1.6 Objective of the present study

As described in previous section, micro-scale characteristics of MSWI fly ash have been ignored because MSWI fly ash is naturally considered as homogeneous owing to fine particles. In this context, this study aims to geochemically characterize MSWI fly ash at micro-scale level. Furthermore, chelate treatment is major intermediate treatment for MSWI fly ash in Japan. However, the impacts of chelate treatment on characteristics of MSWI fly ash still have not been investigated because the metal immobilization mechanism is simply considered as complexation. Therefore, this study also focused on characteristics of chelate-treated MSWI fly ash.

1.7 Outline of the thesis

Fig. 1.4 shows the thesis structure. The contents of this study are divided into seven chapters as follows:

Chapter 1: Introduction

In chapter 1, firstly present situation of MSW management in Japan are introduced. Secondary, advantages and inconveniences of MSWI process are explained. Thirdly, intermediate treatment for MSWI fly ash are literature reviewed. Finally, objective of the present study is presented.

Chapter 2: Morphological characteristics of MSWI fly ash particles

In chapter 2, morphological characteristics of raw and chelate-treated MSWI fly ash were mainly investigated. XRD analysis showed that raw and chelate-treated MSWI fly

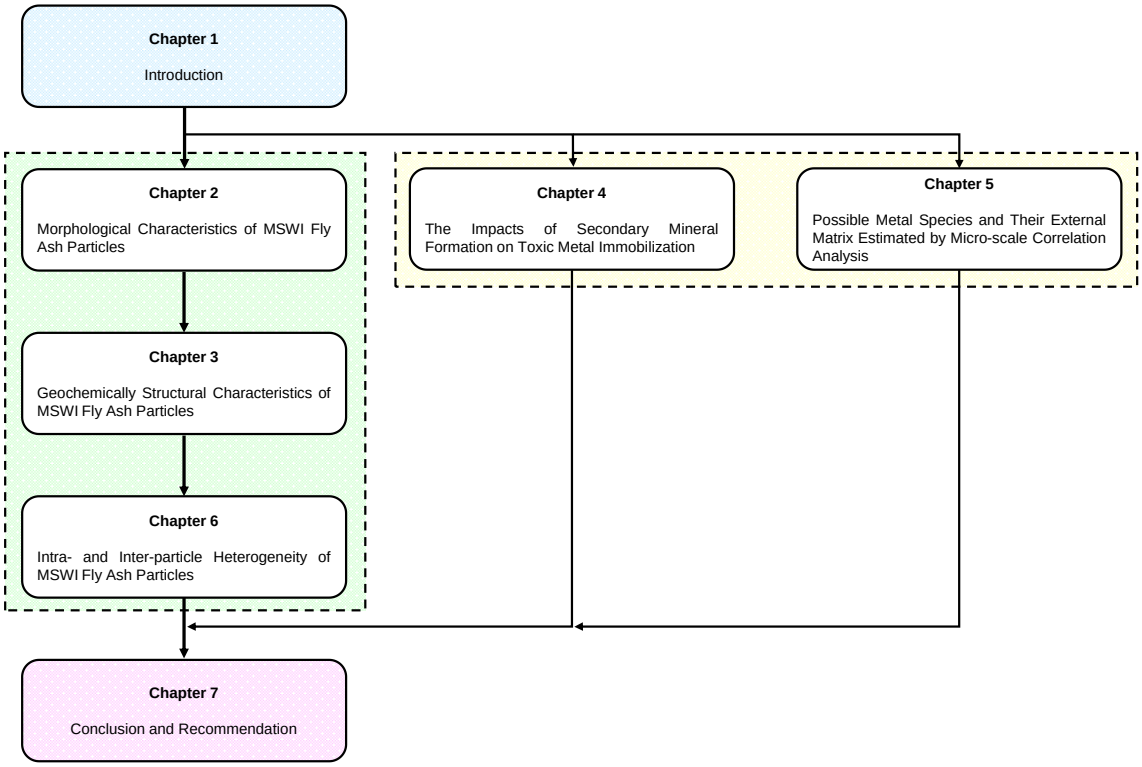

Fig. 1.4 Structure of the thesis

ash consists of similar minerals such as sylvite (KCl), halite (NaCl), anhydrite ($CaSO_4$), gypsum ($CaSO_4 \cdot 2H_2O$), calcite ($CaCO_3$), and quartz (SiO_2). It suggests that chelate treatment did not generate new secondary minerals in detectable level of XRD analysis (approximately 5–10 wt%) for MSWI fly ash. Scanning electron microscope (SEM) observations showed that raw MSWI fly ash could be categorized to 4 types according to their morphological characteristics; Larger particles (L.P.), smaller particles (S.P.), aggregates of smaller particles (A.S.P.), and fibrous particles (F.B.). SEM observations of chelate-treated MSWI fly ash showed that morphological characteristics of MSWI fly ash particles changed dramatically by secondary mineral formations such as cubic crystals (C.C.) and specular crystals (S.P.). This means that MSWI fly ash particles have mineralogically active surface. The morphological characteristics of raw and chelate-treated MSWI fly ash depend on particle formation processes.

Chapter 3: Geochemically structural characteristics of MSWI fly ash particles

In chapter 3, structural characteristics of MSWI fly ash particles were investigated employing 3 types of leaching experiments; Japan Leaching Test 46th (JLT46), Toxicity Characteristic Leaching Procedure (TCLP, US EPA Method 1311), and Japan Leaching Test 19th (JLT19). SEM-EDX analysis showed that a MSWI fly ash particle likely consists of Si-based insoluble core structure, Al/Ca/Si-based semi-soluble matrices inside the body, and soluble KCl/NaCl-based aggregates on the surface. The smooth and non-porous matrix surface might contribute to heavy metal immobilization to some extent.

Chapter 4: The impacts of secondary mineral formation on toxic metal immobilization

In chapter 4, the impacts of secondary mineral formation on toxic metal immobilization

were investigated. Point analysis of SEM-EDX analysis could not find metal-rich points in ettringite structure. It means that mineralogical immobilization of heavy metals by the encapsulation to ettringite structure seems to be limited. SEM observation of the same MSWI fly ash particles before and after the moistening treatment showed that transfer of soluble components was inhibited only when insoluble minerals such as gypsum were generated and covered the particle surface. However, such physical immobilization seems to be limited because insoluble mineral formation with surface coverage was monitored only one time of more than 20 observations. According to the results, mineralogical and physical immobilization of heavy metals by secondary generated minerals seem to be limited although secondary minerals are always generated on the surface of MSWI fly ash particle during chelate treatment. Therefore, the durability of toxic metal immobilization by chelate treatment is almost equal to the stability of metal chelate complex.

Chapter 5: Possible metal species and their external matrix estimated by micro-scale correlation analysis

In chapter 5, micro-scale correlation analysis was applied to estimate metal species and their external matrix in MSWI fly ash. Target metals were Cu, Cr, Fe, Mn, Ti, and Zn. Dominant metal species and their bonding states with fly ash matrix are different in each individual fly ash particle. For example, major Ti forms are perovskite ($CaTiO_3$) in some particles and rutile (TiO_2) in others. Micro-scale correlation analysis also suggests heavy metal behaviors in fly ash formation processes. Metal oxides (Ti, Cu, Fe, Mn and Zn) likely react with and/or are trapped in Al/Ca/Si-based matrix like aluminosilicate in the gas phase and then followed by KCl/NaCl adsorption on the surface. On the other hand, Cr oxide is not incorporated in Al/Ca/Si-based matrix. Zn can possibly form other species

depending on combustion condition. Zn chlorides ($ZnCl_2$ and/or K_2ZnCl_4) and Zn spinels ($ZnAl_2O_4$ and $ZnFe_2O_4$) are not trapped in Al/Ca/Si-based matrix but adsorbed on the surface together with KCl/NaCl-based aggregates. Because metal oxides basically combine with and/or are trapped in Al/Ca/Si-based matrix, metal leachability might be controlled by not only metal oxide leachability but also leachability of Al/Ca/Si-based matrix around metal oxides.

Chapter 6: Intra- and inter-particle heterogeneity of MSWI fly ash particles

In chapter 6, elemental heterogeneity of MSWI fly ash particles was investigated. On the surface of fly ash particles, Cl, K, and Na have 0-82% larger intra-particle heterogeneities than Al, Ca, and Si owing to KCl/NaCl-based aggregates. Smaller intra-particle heterogeneity of Ca in semi-soluble component than those of Al and Si suggest that semi-soluble Al/Ca/Si-based matrices around insoluble cores are Ca-based materials including aluminosilicate domains. It was also supported by inter-particle heterogeneity analysis of fly ash particle surfaces. Inter-particle heterogeneities of Al, Ca, and Si in semi-soluble components and insoluble components are 9-40% and 49-352% higher than those of fly ash particle surface, respectively. Inter-particle heterogeneity analysis clearly suggests that insoluble components are not only Si-rich cores but also Al-rich and Ca-rich cores. MSWI fly ash particles have both internal heterogeneities inside their bodies and also are heterogeneous in inter-particle level. When MSWI fly ash becomes wet during chelate-treatment, it decreased intra-particle heterogeneities of Cl, K, and Na by 2-54%. In addition, wet condition also increased inter-particle heterogeneities of Al, Ca, and Si by 30-61% but decrease those of Cl, K, and Na by 61-75%.

Chapter 7: Conclusion and recommendation

In chapter 7, the findings from the present study are summarized as conclusions. Following the conclusions, recommendations in association with conclusions are outlined.

1.8 References

[1] T. Urabe, M. Inamura, History of waste management research in Japan : 1920-1970, Waste Manag. Res. 17 (2006) 360–366. doi:10.3985/wmr.17.360 (in Japanese).

[2] Y. Yagi, Changes in Japan's waste management administration after World War II, Waste Manag. Res. 17 (2006) 249–359. doi:10.3985/wmr.17.349 (in Japanese).

[3] M. Osawa, T. Shimaoka, H. Nakayama, Waste management roles in the improvement of public hygiene, J. Japan Soc. Mater. Cycles Waste Manag. 20 (2009) 291–302. doi:10.3985/jjsmcwm.20.291 (in Japanese).

[4] Ministry of the Environment, Annual report of waste management in Japan ("Nihon no Haikibutu Shori"), Japan, 2007 (in Japanese).

[5] Ministry of the Environment, Annual report of waste management in Japan ("Nihon no Haikibutu Shori"), 2017 (in Japanese).

[6] S. Sakai, T. Ikematsu, Y. Hirai, H. Yoshida, Unit-charging programs for municipal solid waste in Japan, Waste Manag. 28 (2008) 2815–2825. doi:10.1016/j.wasman.2008.07.010.

[7] T. Eguchi, Outline of the Basic Law for Establishing a Recycling-based Society, Waste Manag. Res. 12 (2001) 281–285. doi:10.3985/wmr.12.281 (in Japanese).

[8] H. Takiguchi, Progress in the 3R initiative, Waste Manag. Res. 17 (2006) 60–68. doi:10.3985/wmr.17.60 (in Japanese).

[9] T. Akiyama, S. Harashina, M. Osako, How public opposition and distance affect

waste management facility siting, J. Japan Soc. Waste Manag. Expert. 16 (2005) 429–440. doi:10.3985/jswme.16.429 (in Japanese).

[10] X. Su, L. Zhang, Y. Xiao, M. Sun, X. Gao, J. Su, Evaluation of a flue gas cleaning system of a circulating fluidized bed incineration power plant by the analysis of pollutant emissions, Powder Technol. 286 (2015) 9–15. doi:10.1016/j.powtec.2015.07.038.

[11] S. Sakai, Municipal solid waste management in Japan, Waste Manag. 16 (1996) 395–405. doi:10.1016/S0956-053X(96)00107-9.

[12] S. Matsuura, T. Inada, Removal technologies for noxious gases controlled by regulations, Waste Manag. Res. 2 (1991) 318–330. doi:10.3985/wmr.2.318 (in Japanese).

[13] N. Tanikawa, K. Urano, Emitted and removed levels of HCl and SO_2 from municipal waste incinerators, J. Japan Soc. Waste Manag. Expert. 8 (1997) 261–269. doi:10.3985/jswme.8.261 (in Japanese).

[14] S. Sakai, Reduction of PCDDs/DFs Emission and environmental cycle control, Waste Manag. Res. 8 (1997) 322–335. doi:10.3985/wmr.8.322 (in Japanese).

[15] M.J. Quina, J.C.M. Bordado, R.M. Quinta-Ferreira, Chemical stabilization of air pollution control residues from municipal solid waste incineration, J. Hazard. Mater. 179 (2010) 382–392. doi:10.1016/j.jhazmat.2010.03.016.

[16] F.Y. Chang, M.Y. Wey, Comparison of the characteristics of bottom and fly ashes generated from various incineration processes, J. Hazard. Mater. 138 (2006) 594–603. doi:10.1016/j.jhazmat.2006.05.099.

[17] A. Kida, Y. Noma, T. Imada, Chemical speciation and leaching properties of elements in municipal incinerator ashes, Waste Manag. 16 (1996) 527–536. doi:10.1016/S0956-053X(96)00094-3.

[18] Y. Shim, S. Rhee, W. Lee, Comparison of leaching characteristics of heavy metals from bottom and fly ashes in Korea and Japan, Waste Manag. 25 (2005) 473–480. doi:10.1016/j.wasman.2005.03.002.

[19] Y. Pan, Z. Wu, J. Zhou, J. Zhao, X. Ruan, J. Liu, G. Qian, Chemical characteristics and risk assessment of typical municipal solid waste incineration (MSWI) fly ash in China, J. Hazard. Mater. 261 (2013) 269–276. doi:10.1016/j.jhazmat.2013.07.038.

[20] T.T. Eighmy, J.D. Eusden, J.E. Krzanowski, D.S. Domingo, D. Stampfli, J.R. Martin, P.M. Erickson, Comprehensive approach toward understanding element speciation and leaching behavior in municipal solid waste incineration electrostatic precipitator ash, Environ. Sci. Technol. 29 (1995) 629–646. doi:10.1021/es00003a010.

[21] M. Li, S. Hu, J. Xiang, L.S. Sun, P.S. Li, S. Su, X.X. Sun, Characterization of fly ashes from two chinese municipal solid waste incinerators, Energy & Fuels. 17 (2003) 1487–1491. doi:10.1021/ef030092o.

[22] M. Li, J. Xiang, S. Hu, L.S. Sun, S. Su, P.S. Li, X.X. Sun, Characterization of solid residues from municipal solid waste incinerator, Fuel. 83 (2004) 1397–1405. doi:10.1016/j.fuel.2004.01.005.

[23] H. Raclavská, A. Corsaro, S. Hartmann-Koval, D. Juchelková, Enrichment and distribution of 24 elements within the sub-sieve particle size distribution ranges of fly ash from wastes incinerator plants, J. Environ. Manage. 203 (2017) 1169–1177. doi:10.1016/j.jenvman.2017.03.073.

[24] F. Jiao, L. Zhang, W. Song, Y. Meng, N. Yamada, A. Sato, Y. Ninomiya, Effect of inorganic particulates on the condensation behavior of lead and zinc vapors upon flue gas cooling, Proc. Combust. Inst. 34 (2013) 2821–2829.

doi:10.1016/j.proci.2012.07.062.

[25] Y. Zhang, Q. Li, J. Jia, A. Meng, Thermodynamic analysis on heavy metals partitioning impacted by moisture during the MSW incineration, Waste Manag. 32 (2012) 2278–2286. doi:10.1016/j.wasman.2012.07.007.

[26] Z. Youcai, S. Stucki, C. Ludwig, J. Wochele, Impact of moisture on volatility of heavy metals in municipal solid waste incinerated in a laboratory scale simulated incinerator, Waste Manag. 24 (2004) 581–587. doi:10.1016/j.wasman.2004.01.004.

[27] K.S. Wang, K.Y. Chiang, S.M. Lin, C.C. Tsai, C.J. Sun, Effects of chlorides on emissions of toxic compounds in waste incineration: Study on partitioning characteristics of heavy metal, Chemosphere. 38 (1999) 1833–1849. doi:10.1016/S0045-6535(98)00398-1.

[28] J.C. Chen, M.Y. Wey, J.L. Su, S.M. Hsieh, Two-stage simulation of the major heavy-metal species under various incineration conditions, Environ. Int. 24 (1998) 451–466. doi:10.1016/S0160-4120(98)00025-7.

[29] K. Chiang, K. Wang, F. Lin, W. Chu, Chloride effects on the speciation and partitioning of heavy metal during the municipal solid waste incineration process, Sci. Total Environ. 203 (1997) 129–140. doi:10.1016/S0048-9697(97)00140-X.

[30] S.K. Durlak, P. Biswas, J. Shi, Equilibrium analysis of the affect of temperature, moisture and sodium content on heavy metal emissions from municipal solid waste incinerators, J. Hazard. Mater. 56 (1997) 1–20. doi:10.1016/S0304-3894(97)00002-2.

[31] H. Ecke, H. Sakanakura, T. Matsuto, N. Tanaka, A. Lagerkvist, State-of-the-art treatment processes for municipal solid waste incineration residues in Japan, Waste Manag. Res. 18 (2000) 41–51. doi:10.1177/0734242X0001800106.

[32] T. Shimaoka, M. Hanashima, The behavior of fly ash stabilized by cement solidification in landfills, Waste Manag. Res. 5 (1994) 32–45. doi:10.3985/wmr.5.32 (in Japanese).

[33] M.L.D. Gougar, B.E. Scheetz, D.M. Roy, Ettringite and C-S-H portland cement phases for waste ion immobilization: A review, Waste Manag. 16 (1996) 295–303. doi:10.1016/S0956-053X(96)00072-4.

[34] Q.Y. Chen, M. Tyrer, C.D. Hills, X.M. Yang, P. Carey, Immobilisation of heavy metal in cement-based solidification/stabilisation: A review, Waste Manag. 29 (2009) 390–403. doi:10.1016/j.wasman.2008.01.019.

[35] Y.J. Park, J. Heo, Vitrification of fly ash from municipal solid waste incinerator, J. Hazard. Mater. 91 (2002) 83–93. doi:10.1016/S0304-3894(01)00362-4.

[36] H. Fujiyoshi, Trends of MSW-Ash melting technology in Japan, Waste Manag. Res. 16 (2005) 98–110. doi:10.3985/wmr.16.98 (in Japanese).

[37] K. Hong, S. Tokunaga, T. Kajiuchi, Extraction of heavy metals from MSW incinerator fly ashes by chelating agents, J. Hazard. Mater. 75 (2000) 57–73. doi:10.1016/S0304-3894(00)00171-0.

[38] H. Katsuura, T. Inoue, M. Hiraoka, S. Sakai, Full-scale plant study on fly ash treatment by the acid extraction process, Waste Manag. 16 (1996) 491–499. doi:10.1016/S0956-053X(96)00091-8.

[39] Y. Zhao, L. Song, G. Li, Chemical stabilization of MSW incinerator fly ashes, J. Hazard. Mater. 95 (2002) 47–63. doi:10.1016/S0304-3894(02)00002-X.

[40] T. Uchida, I. Itoh, K. Harada, Immobilization of heavy metals contained in incinerator fly ash by application of soluble phosphate - Treatment and disposal cost reduction by combined use of “High Specific Surface Area Lime,” Waste Manag. 16 (1996) 475–481. doi:10.1016/S0956-053X(96)00101-8.

[41] T.T. Eighmy, B.S. Crannell, L.G. Butler, F.K. Cartledge, E.F. Emery, D. Oblas, J.E. Krzanowski, J.D. Eusden, E.L. Shaw, C.A. Francis, Heavy metal stabilization in municipal solid waste combustion dry scrubber residue using soluble phosphate, Environ. Sci. Technol. 31 (1998) 3330–3338. doi:10.1021/es970407c.

[42] P. Piantone, F. Bodénan, R. Derie, G. Depelsenaire, Monitoring the stabilization of municipal solid waste incineration fly ash by phosphation: Mineralogical and balance approach, Waste Manag. 23 (2003) 225–243. doi:10.1016/S0956-053X(01)00058-7.

[43] H. Sakanakura, Formation and durability of dithiocarbamic metals in stabilized air pollution control residue from municipal solid waste incineration and melting processes, Environ. Sci. Technol. 41 (2007) 1717–1722. doi:10.1021/es062077e.

[44] S. Mizutani, H.A. van der Sloot, S. Sakai, Evaluation of treatment of gas cleaning residues from MSWI with chemical agents, Waste Manag. 20 (2000) 233–240. doi:10.1016/S0956-053X(99)00317-7.

[45] J. Jianguo, W. Jun, X. Xin, W. Wei, D. Zhou, Z. Yan, Heavy metal stabilization in municipal solid waste incineration flyash using heavy metal chelating agents, J. Hazard. Mater. 113 (2004) 141–146. doi:10.1016/j.jhazmat.2004.05.030.

[46] H. Cesur, Ç. Akus, Determination of cadmium and zinc in fertilizer samples by FAAS after solid-phase extraction with freshly precipitated manganese-diethyldhithiocarbamate, Anal. Sci. 22 (2006) 727–730. doi:10.2116/analsci.22.727.

[47] H. Sakanakura, N. Tanaka, T. Matsuto, Later stage release of heavy metals from municipal solid waste incinerator fly ash stabilized with chelating agent, J. Japan Soc. Waste Manag. Expert. 16 (2005) 214–222. doi:10.3985/jswme.16.214 (in Japanese).

[48] M.C. Hsiao, H.P. Wang, Y.L. Wei, J.E. Chang, C.J. Jou, Speciation of copper in the incineration fly ash of a municipal solid waste, J. Hazard. Mater. 91 (2002) 301–307. doi:10.1016/S0304-3894(02)00015-8.

[49] T. Mangialardi, A.E. Paolini, A. Polettini, P. Sirini, Optimization of the solidification/stabilization process of MSW fly ash in cementitious matrices, J. Hazard. Mater. 70 (1999) 53–70. doi:10.1016/S0304-3894(99)00132-6.

[50] M.C. Hsiao, H.P. Wang, Y.W. Yang, EXAFS and XANES studies of copper in a solidified fly ash, Environ. Sci. Technol. 35 (2001) 2532–2535. doi:10.1021/es001374v.

[51] R.P.W.J. Struis, C. Ludwig, H. Lutz, A.M. Scheidegger, Speciation of zinc in municipal solid waste incineration fly ash after heat treatment: An X-ray absorption spectroscopy study, Environ. Sci. Technol. 38 (2004) 3760–3767. doi:10.1021/es0346126.

[52] R.P.W.J. Struis, M. Pasquali, L. Borgese, A. Gianoncelli, M. Gelfi, P. Colombi, D. Thiaudière, L.E. Depero, G. Rizzo, E. Bontempi, Inertisation of heavy metals in municipal solid waste incineration fly ash by means of colloidal silica – a synchrotron X-ray diffraction and absorption study, RSC Adv. 3 (2013) 14339–14351. doi:10.1039/c3ra41792a.

[53] M.J. Quina, J.C. Bordado, R.M. Quinta-Ferreira, Treatment and use of air pollution control residues from MSW incineration: An overview, Waste Manag. 28 (2008) 2097–2121. doi:10.1016/j.wasman.2007.08.030.

[54] T. Sabbas, A. Polettini, R. Pomi, T. Astrup, O. Hjelmar, P. Mostbauer, G. Cappai, G. Magel, S. Salhofer, C. Speiser, S. Heuss-Assbichler, R. Klein, P. Lechner, Management of municipal solid waste incineration residues, Waste Manag. 23 (2003) 61–88. doi:10.1016/S0956-053X(02)00161-7.

[55] A. Polettini, R. Pomi, P. Sirini, F. Testa, Properties of Portland cement - Stabilised MSWI fly ashes, J. Hazard. Mater. 88 (2001) 123–138. doi:10.1016/S0304-3894(01)00292-8.

[56] L. Benassi, M. Pasquali, A. Zanoletti, R. Dalipi, L. Borgese, L.E. Depero, I. Vassura, M.J. Quina, E. Bontempi, Chemical Stabilization of Municipal Solid Waste Incineration Fly Ash without Any Commercial Chemicals: First Pilot-Plant Scaling Up, ACS Sustain. Chem. Eng. 4 (2016) 5561–5569. doi:10.1021/acssuschemeng.6b01294.

[57] B. Zhang, W. Zhou, H. Zhao, Z. Tian, F. Li, Y. Wu, Stabilization/solidification of lead in MSWI fly ash with mercapto functionalized dendrimer Chelator, Waste Manag. 50 (2016) 105–112. doi:10.1016/j.wasman.2016.02.001.

CHAPTER

2

MORPHOLOGICAL CHARACTERISTICS OF MSWI FLY ASH PARTICLES

Abstract: In this chapter, morphological characteristics of raw and chelate chelate-treated MSWI fly ash particles were investigated. According to SEM observations, raw MSWI fly ash particles could be categorized to 4 types based on their shapes. Because chelate treatment changed the surface of fly ash particles dramatically owing to secondary mineral formations, two more types could be categorized for chelate-treated MSWI fly ash particles.

2.1 Introduction

Leaching behaviors of heavy metals in MSWI fly ash depend on mineral dissolution/precipitation [1–4], particle size and morphology [5–7], pH [8,9], and so on. Hence, chemical, mineralogical, and morphological characterization of MSWI fly ash are important for effective management [10]. As described in subsection 1.4.4, main immobilization mechanism of chelate treatment is simply considered as complexation between heavy metals and chelating substances. Therefore, leaching behaviors of heavy metals in chelate-treated MSWI fly ash have been interested in previous studies [11–13]. On the other hand, the impacts of chelate treatment on characteristics of MSWI fly ash have been ignored although it might have non-negligible impacts on leaching behaviors of heavy metals. In this context, chemical, mineralogical, and morphological characteristics of raw and chelate-treated MSWI fly ash are investigated in this chapter.

2.2 Materials and methods

2.2.1 MSWI fly ash samples

Raw and chelate-treated MSWI fly ash samples used in this study were taken from a MSWI facility plant equipped with stoker-type incinerator (incineration capacity: 250 Mg/d). In this MSWI facility plant, $Ca(OH)_2$ slurry and pulverized activated carbon are injected into flue gas for acidic gas neutralization and dioxin control, respectively. Raw MSWI fly ash, trapped by APCDs (fabric filter), were transferred to a storage tank by an air pressure feeder and stored there temporally. Then raw MSWI fly ash was conveyed from the storage tank to a chelate treatment apparatus. Raw MSWI fly ash samples were collected between the storage tank and the chelate treatment apparatus. About 100 to 300 g of raw MSWI fly ash sample increment was taken from the ash conveyer and the increment sampling was repeated more than 9 times at the interval of about 10 minutes.

All of sampled fly ash were mixed to make the composite sample.

Chelate-treated MSWI fly ash samples were collected from the chelate treatment apparatus. Chelate reagent used in this facility consisted mainly of potassium diethyldithiocarbamate ($KS_2CN(C_2H_5)_2$). After 0.45 L of chelate reagent solution with about 50 wt% chelate concentration was sprayed to approximately 30 kg of raw MSWI fly ash, fly ash was mixed by screw feeder for about 10 minutes. Chelate-treated MSWI fly ash was also sampled as the same with raw MSWI fly ash (random increment sampling and 9 time repetition). All increments were finally mixed to make the composite sample as well as raw fly ash. Total sampling time was 4 hours. Therefore, raw and chelate-treated MSWI fly ash can be regarded as the same lot at 4-hour interval. After drying all samples under room condition for 1 week or longer, fly ash samples were observed and analyzed.

It should be noted that the present study tested only one sample lot intentionally. Composite samples made of different sample lots are usually recommended to generalize analysis results because characteristics of MSWI fly ash depend on waste stream and incineration conditions. However, a composite sample made of several sample lots is not appropriate in this case. This study would observe and analyze each MSWI fly ash particle (one by one). It is needed to know possible diversity of micro-characteristics of fly ash particles from the same sample lot.

2.2.2 Elemental and mineralogical analysis

Elemental compositions of raw and chelate-treated MSWI fly ash samples were determined by energy dispersive X-ray fluorescence spectrometer (EDXRF: S2 RANGER/LE, BRUKER AXS).

Mineral composition of raw and chelate-treated MSWI fly ash samples were analyzed

by X-ray diffraction (XRD: MultiFlex, Rigaku Co., Japan). MSWI fly ash samples were ground with pestle in a mortar in order to make their powder for XRD analysis. The analysis conditions are as follows; 40kV accelerating voltage, 25 mA current, 5-75° 2θ scanning range, 0.01° step, and 1°/min scan speed. Possible mineral compositions were identified based on database of analysis software.

2.2.3 Microscopic observation

Morphological characteristics of raw and chelate-treated MSWI fly ash particles were observed by scanning electron microscope (SEM: SS-550, Shimadzu Co., Japan). Before the SEM observation, MSWI fly ash samples were fixed on specimen holder using double-sided adhesive carbon tape. MSWI fly ash samples on specimen holder were coated by Pt thin layer using vapor deposition apparatus in order to avoid surface charging during SEM observation. Elemental compositions of MSWI fly ash particles were analyzed by point analysis using energy dispersive X-ray analyzer attached to SEM (SEM-EDX: Genesis2000, EDAX Co., Japan). It should be noted that carbon tape used to fix fly ash particles on the specimen holder might cause overestimation of carbon content. In addition, point analysis data include Pt concentration owing to pretreatment. Therefore, Pt concentration was excluded during the point analysis.

2.3 Results and discussion

2.3.1 Elemental compositions of raw and chelate-treated MSWI fly ash

Table 2.1 shows elemental compositions of raw and chelate-treated MSWI fly ash samples determined by EDXRF analysis. The constituent elements in both MSWI fly ash samples are Ca, Cl, K (> approximately 10 wt%), Si, Zn, Al, S, Ti, Fe (> 1 wt%), and other heavy metals (less than 1 wt%). Especially, the contents of Ca and Cl were

significantly high. The high Ca content mainly results from injection of lime slurry for acidic gas neutralization [14]. The high Cl content mainly results from incineration of salty food waste and plastics such as polyvinyl chloride (PVC) in MSW [10,14–18]. It also suggests that higher efficiency of lime to neutralize acidic gas (HCl) in exhaust gas [14]. The contents of volatile metals such as Zn and Pb were a little higher than other heavy metals. The contents of non-volatile metals such as Fe and Ti were also high although they usually transfer to bottom ash during MSWI process [19,20].

2.3.2 Mineral compositions of raw and chelate-treated MSWI fly ash

XRD patterns of raw and chelate-treated MSWI fly ash are shown in Fig. 2.1. XRD analysis show that raw MSWI fly ash consists of sylvite (KCl), halite (NaCl), anhydrite ($CaSO_4$), gypsum ($CaSO_4 \cdot 2H_2O$), calcite ($CaCO_3$) and quartz (SiO_2). XRD pattern of chelate-treated MSWI fly ash is almost the same with that of raw MSWI fly ash. These

Table 2.1 Elemental compositions of raw and chelate treated MSWI fly ash

Elements	**Ca**	**Cl**	**K**	**Si**	**Zn**	**Al**	**S**
Raw fly ash	34.25	30.41	14.73	4.864	3.642	3.15	2.414
Chelated fly ash	45.51	21.71	7.297	5.996	3.813	4.645	2.546

Elements	**Ti**	**Fe**	**Pb**	**Mg**	**Br**	**Sb**	**Cu**
Raw fly ash	1.697	1.55	0.775	0.622	0.432	0.263	0.1937
Chelated fly ash	2.406	1.928	0.779	1.19	0.419	0.299	0.2

Elements	**Sn**	**Ba**	**Mn**	**Cr**	**Sr**	**Cd**	**Zr**
Raw fly ash	0.193	0.14	0.103	0.0828	0.0566	0.0317	0.0264
Chelated fly ash	0.225	0.225	0.125	0.0968	0.0701	0.037	0.0311

Unit: weight percent [wt%]

results suggest that chelate treatment did not generate new secondary minerals in detectable level of XRD analysis (approximately 5-10 wt%) for MSWI fly ash.

2.3.3 Morphological characteristics of raw and chelate-treated MSWI fly ash

According to SEM observations, raw MSWI fly ash particles could be categorized to 4 types based on their morphological characteristics as follows: larger particles (L.P.), smaller particles (S.P.), aggregates of smaller particles (A.S.P.), and fibrous particles (F.P.) (see Fig. 2.2). Among 4 particle types, L.P., S.P., and A.S.P were found at greatly higher frequency than F.P. The larger and smaller particle size were several ten to several hundred micrometer and several micrometer, respectively. Larger spherical particles were always attached with smaller particles on their surface (L.P with S.P., see Fig. 2.2-A). Fig. 2.3 shows the average elemental contents of each particle type. Larger particles consisted mainly of Al, C, Ca, O, and Si (see Table in Fig. 2.3: Point analysis number (N) = 13). On the other hand, smaller particles consisted mainly of C, Ca, Cl, K, Na, and O (see Table in Fig. 2.3: N = 22). Therefore, larger particles are considered as oxides and/or carbonates of Al, Ca, and Si. Smaller particles seem to be chlorides and/or carbonates of

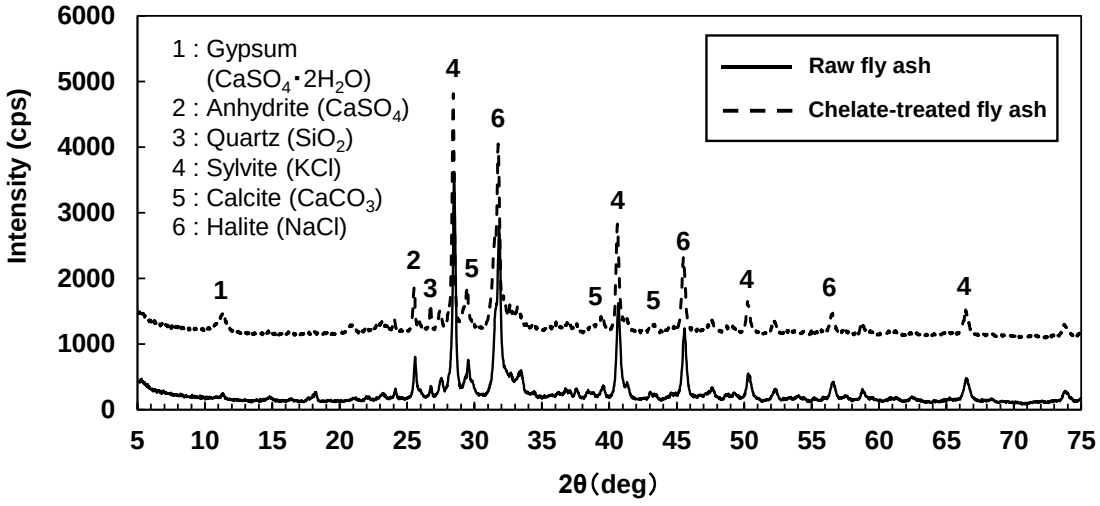

Fig. 2.1 XRD patterns of raw and chelate-treated MSWI fly ash

Ca, K, and Na. The other major type is aggregates of smaller particles (A.S.P., see Fig. 2.2-B). They consisted mainly of C, Ca, Cl, K, Na, and O (see Table in Fig. 2.3: N = 51). Therefore, they are considered as carbonates and/or chlorides of Ca, K, and Na. According to elemental composition of these major types, it is found that elemental

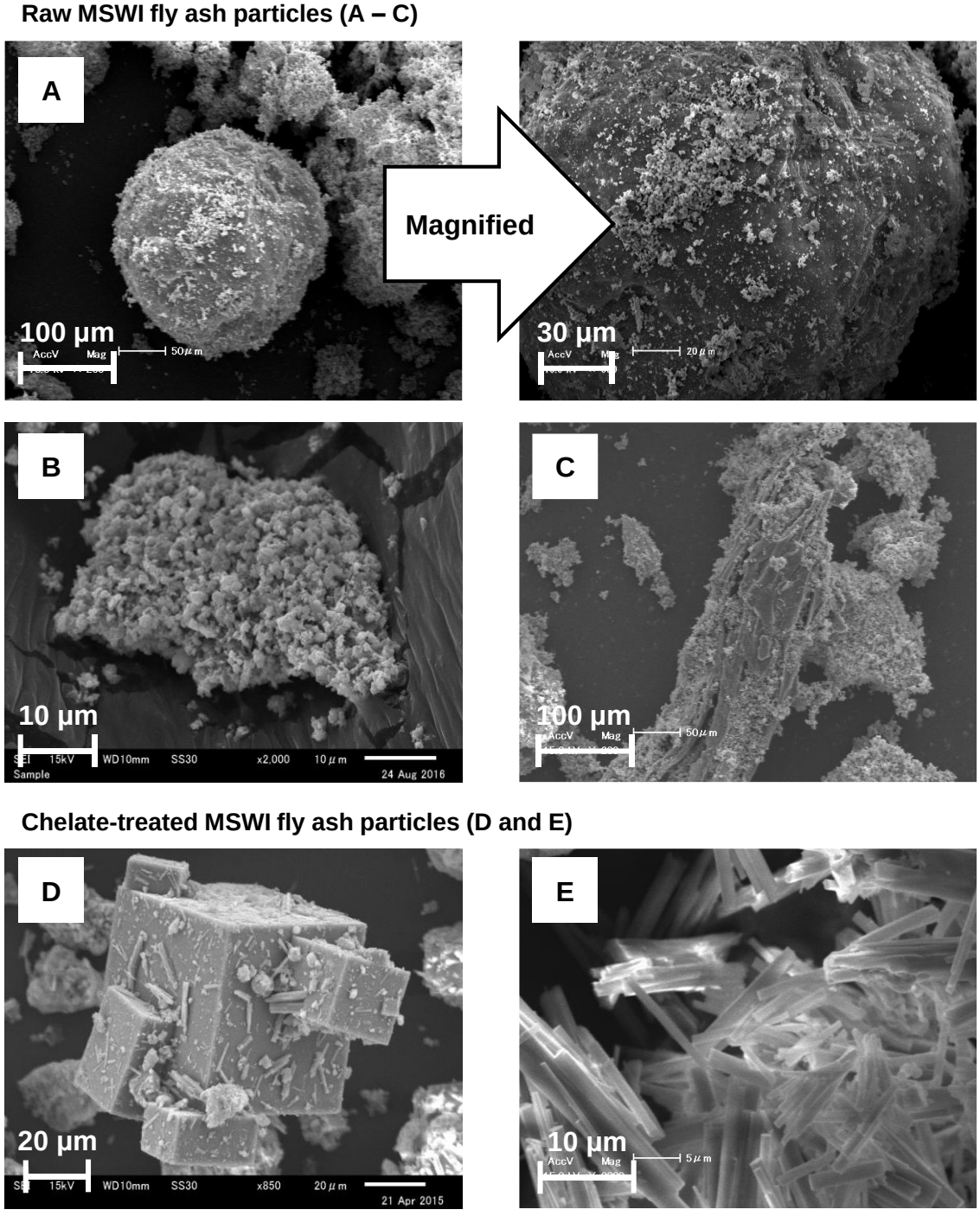

Fig. 2.2 SEM images of raw and chelate-treated MSWI fly ash particles

composition of raw MSWI fly ash particles was strongly dependent on particle size. Fibrous particles consisted mainly of C, Ca, and O (see Fig. 2.2-C and Table in Fig. 2.3: N = 20). Furthermore, atomic percent of carbon exceeded 50 at% at some analysis points. Consequently, they are considered as organic residues due to incomplete combustion and/or activated carbon for dioxin emission control [6].

As described in the previous subsection, there is no large difference of XRD patterns between raw and chelate-treated MSWI fly ash (see Fig. 2.1). However, SEM observation of chelate-treated MSWI fly ash showed that morphological characteristics of MSWI fly ash particles changed dramatically by the generation of secondary minerals. This means that MSWI fly ash particles have mineralogically active surfaces. According to secondary mineral formation and/or re-crystallization, two more types could be added to the categorization. One is cubic crystals (C.C., see Fig. 2.2-D) and the other is spicular crystals (S.C., see Fig. 2.2-E). They were observed on the surface of chelate-treated MSWI fly ash particles at high frequency. Cubic crystals consisted mainly of C, Ca, Cl,

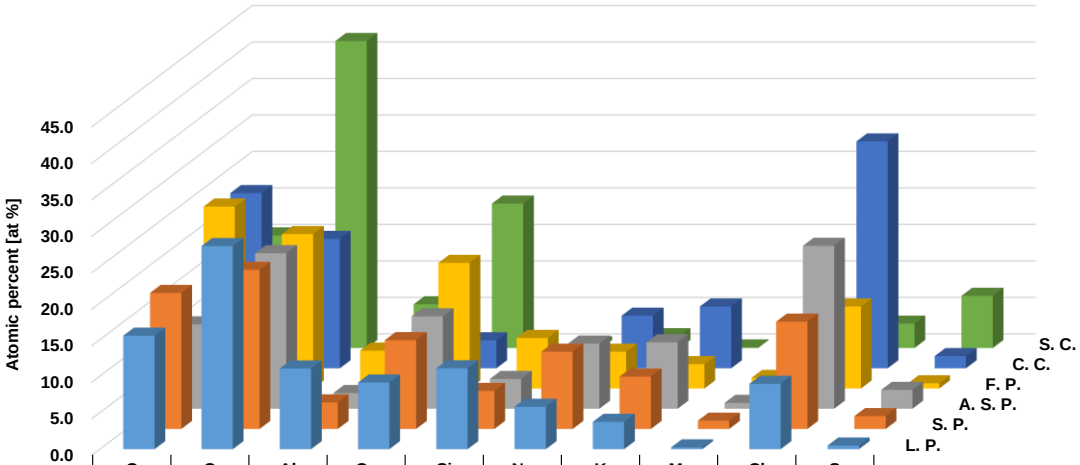

	C	O	Al	Ca	Si	Na	K	Mg	Cl	S
L. P.	15.55	27.83	11.05	9.14	11.08	5.81	3.74	0.24	8.95	0.50
S. P.	18.63	21.80	3.64	12.16	5.21	10.58	7.17	1.13	14.70	1.76
A. S. P.	11.56	21.31	2.15	12.66	4.08	8.92	9.10	0.80	22.32	2.58
F. P.	24.92	21.15	5.18	17.21	6.93	5.03	3.33	1.45	11.23	0.71
C. C.	24.00	17.72	1.05	3.83	1.66	7.20	8.46	1.02	31.08	1.66
S. C.	15.42	42.06	5.99	19.79	0.50	1.62	0.08	0.03	3.33	7.15

Fig. 2.3 Average elemental contents of raw and chelate-treated MSWI fly ash particles

K, Na, and O (see Table in Fig. 2.3: N = 6). According to elemental composition and crystal shape, they are considered as K and Na chlorides (sylvite and halite) and Ca carbonates (calcite). Spicular crystals consisted mainly of Al, Ca, O, and S (see Table in Fig. 2.3: N = 39). According to the elemental composition and crystal shape, they are considered as ettringite ($3CaO{\cdot}Al_2O_3{\cdot}3CaSO_4{\cdot}32H_2O$) [21].

2.3.4 Particle formation processes of each particle type

Larger spherical particles are usually found in MSWI fly ash [6,10,14,15,22,23]. They are considered as calcium aluminosilicate compounds produced from melt droplets during MSWI process [6,22,24,25]. Furthermore, smaller particles consisted of KCl and NaCl are also found on the particle surfaces [22,26]. According to literature review, elements with high boiling points such as Al, Ca, and Si are not volatilized in the incineration area, but can be droplets that form matrix of fly ash particle [6,27,28]. Elements with high vapor pressures and low boiling points (e.g. Cl, K, Na, Cd, Pb, and Zn) are volatilized and transported together with ash matrix in the flue gas [18]. When the flue gas cools down, volatile substances form fine particles [19,29,30]. The formation of KCl and NaCl is promoted because affinities among Cl, K, and Na are stronger than those of volatile metals [31]. Thus, KCl and NaCl attach on the surface of ash matrix and/or form aggregates of smaller particles. As described in previous subsection, fibrous particles consisted mainly of carbon are considered as unburnt carbon [6].

According to elemental compositions and crystal shape, cubic crystals are considered as calcite, halite, and sylvite. Halite and sylvite crystals are generated by dissolution and recrystallization by moistening during chelate treatment. The moistening condition promotes carbonation reaction via CO_2 in atmosphere. Calcite is the predominant mineral formed during the carbonation as follows Eq (1) [32]. During the storage of fly ash,

$Ca(OH)_2$ also reacts with moisture and CO_2 in atmosphere and then forms calcite [18]. Thus, calcite was identified in raw and chelate-treated MSWI fly ash by XRD analysis (see Fig. 2.1). The moistening condition also promotes spicular crystals (ettringite) formation via hydration reaction as follows Eq (2) [33]. Ettringite formation was promoted rapidly by the moisture added to fly ash during chelate treatment (moistening), not by chelate reagent itself [34]. These literature reviews suggested that morphological characteristics of raw and chelate-treated MSWI fly ash particles depend on particle formation processes.

$$Ca(OH)_2 + CO_2 \rightarrow CaCO_3 + H_2O \quad \cdots\cdots (1)$$

$$3(CaSO_4 \cdot 2H_2O) + 3CaO \cdot Al_2O_3 + 26H_2O \rightarrow 3CaO \cdot Al_2O_3 \cdot 3CaSO_4 \cdot 32H_2O \quad \cdots\cdots (2)$$

2.4 Conclusion

Morphological characteristics of raw and chelate-treated MSWI fly ash particles were investigated. Raw MSWI fly ash particles were categorized to larger spherical particles with smaller particles on the surface, aggregates of smaller particles, and fibrous particles according to their morphological characteristics. Elemental compositions of raw MSWI fly ash particles were strongly dependent on particle size in this observation. Secondary minerals such as halite (NaCl), sylvite (KCl) and ettringite ($3CaO \cdot Al_2O_3 \cdot 3CaSO_4 \cdot 32H_2O$) were generated on the surface of fly ash particles by moistening in chelate treatment. This means that MSWI fly ash particles have mineralogically active surface. These results suggest that chelate treatment has non-negligible impacts on morphological and mineralogical characteristics of MSWI fly ash. Literature review suggested that morphological characteristics of raw and chelate-treated MSWI fly ash particles depend on particle formation processes.

2.5 References

[1] T. Astrup, J.J. Dijkstra, R.N.J. Comans, H.A. Van Der Sloot, T.H. Christensen, Geochemical modeling of leaching from MSWI air-pollution-control residues, Environ. Sci. Technol. 40 (2006) 3551–3557. doi:10.1021/es052250r.

[2] Y. Zhang, J. Jiang, M. Chen, MINTEQ modeling for evaluating the leaching behavior of heavy metals in MSWI fly ash, J. Environ. Sci. 20 (2008) 1398–1402. doi:10.1016/S1001-0742(08)62239-1.

[3] J. Hyks, T. Astrup, T.H. Christensen, Long-term leaching from MSWI air-pollution-control residues: Leaching characterization and modeling, J. Hazard. Mater. 162 (2009) 80–91. doi:10.1016/j.jhazmat.2008.05.011.

[4] H. Zhang, Y. Zhao, J. Qi, Characterization of heavy metals in fly ash from municipal solid waste incinerators in Shanghai, Process Saf. Environ. Prot. 88 (2010) 114–124. doi:10.1016/j.psep.2010.01.001.

[5] S. Mizutani, N. Watanabe, S. Sakai, H. Takatsuki, Influence of particle size preparation of MSW incineration residues on heavy metal leaching behavior in leaching tests., Environ. Sci. 13 (2006) 363–370.

[6] A. Bogush, J.A. Stegemann, I. Wood, A. Roy, Element composition and mineralogical characterisation of air pollution control residue from UK energy-from-waste facilities, Waste Manag. 36 (2015) 119–129. doi:10.1016/j.wasman.2014.11.017.

[7] A. Ramesh, J.A. Koziński, Investigations of ash topography/morphology and their relationship with heavy metals leachability, Environ. Pollut. 111 (2001) 255–262. doi:10.1016/S0269-7491(00)00062-2.

[8] M.J. Quina, J.C.M. Bordado, R.M. Quinta-Ferreira, The influence of pH on the leaching behaviour of inorganic components from municipal solid waste APC

residues, Waste Manag. 29 (2009) 2483–2493. doi:10.1016/j.wasman.2009.05.012.

[9] Y. Zhang, B. Cetin, W.J. Likos, T.B. Edil, Impacts of pH on leaching potential of elements from MSW incineration fly ash, Fuel. 184 (2016) 815–825. doi:10.1016/j.fuel.2016.07.089.

[10] N. Saikia, S. Kato, T. Kojima, Compositions and leaching behaviours of combustion residues, Fuel. 85 (2006) 264–271. doi:10.1016/j.fuel.2005.03.035.

[11] S. Mizutani, H.A. van der Sloot, S. Sakai, Evaluation of treatment of gas cleaning residues from MSWI with chemical agents, Waste Manag. 20 (2000) 233–240. doi:10.1016/S0956-053X(99)00317-7.

[12] J. Jianguo, W. Jun, X. Xin, W. Wei, D. Zhou, Z. Yan, Heavy metal stabilization in municipal solid waste incineration flyash using heavy metal chelating agents, J. Hazard. Mater. 113 (2004) 141–146. doi:10.1016/j.jhazmat.2004.05.030.

[13] F.H. Wang, F. Zhang, Y.J. Chen, J. Gao, B. Zhao, A comparative study on the heavy metal solidification/stabilization performance of four chemical solidifying agents in municipal solid waste incineration fly ash, J. Hazard. Mater. 300 (2015) 451–458. doi:10.1016/j.jhazmat.2015.07.037.

[14] M. Li, J. Xiang, S. Hu, L.S. Sun, S. Su, P.S. Li, X.X. Sun, Characterization of solid residues from municipal solid waste incinerator, Fuel. 83 (2004) 1397–1405. doi:10.1016/j.fuel.2004.01.005.

[15] L. Le Forestier, G. Libourel, Characterization of Flue Gas Residues from Municipal Solid Waste Combustors, Environ. Sci. Technol. 32 (1998) 2250–2256. doi:10.1021/es980100t.

[16] Y.J. Park, J. Heo, Vitrification of fly ash from municipal solid waste incinerator, J. Hazard. Mater. 91 (2002) 83–93. doi:10.1016/S0304-3894(01)00362-4.

[17] Y.J. Park, Stabilization of a chlorine-rich fly ash by colloidal silica solution, J.

Hazard. Mater. 162 (2009) 819–822. doi:10.1016/j.jhazmat.2008.05.143.

[18] G. Weibel, U. Eggenberger, S. Schlumberger, U.K. Mäder, Chemical associations and mobilization of heavy metals in fly ash from municipal solid waste incineration, Waste Manag. 62 (2016) 147–159. doi:10.1016/j.wasman.2016.12.004.

[19] H. Belevi, H. Moench, Factors determining the element behavior in municipal solid waste incinerators. 1. Field studies, Environ. Sci. Technol. 34 (2000) 2501–2506. doi:10.1021/es991078m.

[20] C.H. Jung, T. Matsuto, N. Tanaka, T. Okada, Metal distribution in incineration residues of municipal solid waste (MSW) in Japan, Waste Manag. 24 (2004) 381–391. doi:10.1016/S0956-053X(03)00137-5.

[21] Q.Y. Chen, M. Tyrer, C.D. Hills, X.M. Yang, P. Carey, Immobilisation of heavy metal in cement-based solidification/stabilisation: A review, Waste Manag. 29 (2009) 390–403. doi:10.1016/j.wasman.2008.01.019.

[22] T.T. Eighmy, J.D. Eusden, J.E. Krzanowski, D.S. Domingo, D. Stampfli, J.R. Martin, P.M. Erickson, Comprehensive approach toward understanding element speciation and leaching behavior in municipal solid waste incineration electrostatic precipitator ash, Environ. Sci. Technol. 29 (1995) 629–646. doi:10.1021/es00003a010.

[23] P.Y. Mahieux, J.E. Aubert, M. Cyr, M. Coutand, B. Husson, Quantitative mineralogical composition of complex mineral wastes - Contribution of the Rietveld method, Waste Manag. 30 (2010) 378–388. doi:10.1016/j.wasman.2009.10.023.

[24] C.S. Kirby, J.D. Rimstidt, Mineralogy and surface properties of municipal solid waste ash, Environ. Sci. Technol. 27 (1993) 652–660. doi:10.1021/es00001a601.

[25] A.P. Bayuseno, W.W. Schmahl, Characterization of MSWI fly ash through

mineralogy and water extraction, Resour. Conserv. Recycl. 55 (2011) 524–534. doi:10.1016/j.resconrec.2011.01.002.

[26] J.L. Ontiveros, T.L. Clapp, D.S. Kosson, Physical properties and chemical species distributions within municipal waste combuster ashes, Environ. Prog. 8 (1989) 200–206. doi:10.1002/ep.3300080319.

[27] D.H. Klein, A.W. Andren, J.A. Carter, J.F. Emery, C. Feldman, W. Fulkerson, W.S. Lyon, J.C. Ogle, Y. Talmi, R.I. Van Hook, N. Bolton, Pathways of Thirty-seven Trace Elements Through Coal-Fired Power Plant, Environ. Sci. Technol. 9 (1975) 973–979. doi:10.1021/es60108a007.

[28] M.A. Fernandez, L. Martinez, M. Segarra, J.C. Garcia, F. Espiell, Behavior of heavy metals in the combustion gases of urban waste incinerators, Environ. Sci. Technol. 26 (1992) 1040–1047. doi:10.1021/es00029a026.

[29] H. Belevi, M. Langmeier, Factors determining the element behavior in municipal solid waste incinerators. 2. Laboratory experiments, Environ. Sci. Technol. 34 (2000) 2507–2512. doi:10.1021/es991079e.

[30] J. Zhou, S. Wu, Y. Pan, L. Zhang, Z. Cao, X. Zhang, S. Yonemochi, S. Hosono, Y. Wang, K. Oh, G. Qian, Enrichment of heavy metals in fine particles of municipal solid waste incinerator (MSWI) fly ash and associated health risk, Waste Manag. 43 (2015) 239–246. doi:10.1016/j.wasman.2015.06.026.

[31] K. Chiang, K. Wang, F. Lin, W. Chu, Chloride effects on the speciation and partitioning of heavy metal during the municipal solid waste incineration process, Sci. Total Environ. 203 (1997) 129–140. doi:10.1016/S0048-9697(97)00140-X.

[32] J.A. Meima, R.N.J. Comans, Geochemical modeling of weathering reactions in municipal solid waste incinerator bottom ash, Environ. Sci. Technol. 31 (1997) 1269–1276. doi:10.1021/es9603158.

[33] M. Collepardi, A state-of-the-art review on delayed ettringite attack on concrete, Cem. Concr. Compos. 25 (2003) 401–407. doi:10.1016/S0958-9465(02)00080-X.

[34] P. Ubbrìaco, P. Bruno, A. Traini, D. Calabrese, Fly ash reactivity: Formation of hydrate phases, J. Therm. Anal. Calorim. 66 (2001) 293–305. doi:10.1023/A:1012468505722.

CHAPTER

3

GEOCHEMICALLY STRUCTURAL CHARACTERISTICS OF MSWI FLY ASH PARTICLES

Abstract: In this chapter, structural characteristics of MSWI fly ash particles were investigated employing 3 types of leaching experiments. According to SEM-EDX analysis, a MSWI fly ash particle likely consists of Si-based insoluble core structure, Al/Ca/Si-based semi-soluble matrices inside the body, and soluble KCl/NaCl-based aggregates on the surface.

3.1 Introduction

In chapter 2, morphological characteristics on the surface of raw and chelate-treated MSWI fly ash particles were investigated. According to SEM-EDX analysis and literature review of particle formation processes, it seems that MSWI fly ash particles likely consist of Al/Ca/Si-based inner matrices attached with KCl/NaCl-based aggregates on the surface. However, structural characteristics of MSWI fly ash particles are still uncertain. A few studies investigated morphological characteristics of MSWI fly ash particles employing water or acidic leaching experiments [1,2]. After the leaching experiments, elemental compositions of ash matrix could be analyzed owing to leaching out of soluble salts. Leaching experiments are usually used in order to investigate leachabilities of toxic substances in hazardous materials [3]. However, they also seem to be useful for removal of soluble and semi-soluble components from the surface of MSWI fly ash particles. In this context, structural characteristics of MSWI fly ash particles were investigated employing water and acidic leaching experiments.

3.2 Materials and methods

3.2.1 Residual materials

Raw and chelate-treated MSWI fly ash samples were subjected to 3 types of leaching experiments. The first leaching experiment is Japan Leaching Test 46th (JLT46). JLT46 was conducted as water extraction in order to remove soluble components from the surface of MSWI fly ash particles. Extracting solvent is pure water. The liquid to solid (fly ash sample) weight ratio (L/S) is 10. After leaching test bottles were shaken at 200 rpm for 6 hours, residual materials were collected by filtration using membrane filter (0.45 μm mesh). The second leaching experiment is Toxicity Characteristic Leaching Procedure (TCLP, US EPA Method 1311). TCLP was conducted as weakly acidic

extraction in order to remove soluble and part of semi-soluble components from the surface of MSWI fly ash particle. Extracting solvent is 0.57 v/v% of acetic acid (CH_3COOH) solution (L/S = 20). After leaching test bottles were shaken at 30 rpm for 18 hours, residual materials were collected by filtration using 0.6-0.8 μm glass fiber filter. The third leaching experiment is Japan Leaching Test 19th (JLT19). JLT19 was conducted as strongly acidic extraction in order to remove soluble and semi-soluble components from MSWI fly ash particles completely. Extracting solvent is 1.0 mol/L hydrochloric acid (HCl) solution (L/S = 33.3). After leaching test bottles were shaken at 200 rpm for 2 hours, residual materials were collected by filtration using membrane filter (0.45 μm mesh). Experimental conditions of each leaching experiment are summarized in Table 3.1. After residual materials collected from each leaching experiment were dried sufficiently under room condition, they were observed and analyzed by SEM-EDX.

3.2.2 Mineralogical analysis

Mineral compositions of residual materials collected from each leaching experiment were analyzed by XRD (MultiFlex, Rigaku Co., Japan). Residual materials were ground

Table 3.1 Experimental conditions of each leaching experiment

	JLT46	**TCLP**	**JLT19**
Extractant	Water (H_2O)	Acetic acid (CH_3COOH)	Hydrochloric acid (HCl)
L/S [mL/g]	10	20	33.3
Shaking speed [rpm]	200	30	200
Shaking time [hour]	6	18	2
Filtration paper [μm]	0.45 MF	0.6-0.8 GF	0.45 MF

MF：Membrane Filter, GF：Glass fiber Filter

with pestle in a mortar in order to make their powder for XRD analysis. The analysis conditions are as follows; 40kV accelerating voltage, 25 mA current, 5-75° 2θ scanning range, 0.01° step, and 1°/min scan speed. Possible mineral compositions were identified based on database of analysis software.

3.2.3 Microscopic observation and elemental analysis

It should be noted that SEM-EDX used in this and following chapters is different from that used in chapter 2 owing to difficulty of continued use of the same SEM-EDX. Therefore, analysis condition is little bit different from chapter 2.

Morphological characteristics of residual materials were observed by SEM (JSM-6610LA, JEOL Ltd., Japan). Residual materials collected from each leaching experiment were fixed on specimen holder using double-sided adhesive carbon tape. Residual materials on the specimen holder were coated by Pt-Pd thin layer using vapor deposition apparatus (MSP-1S, Vacuum device Ltd., Japan) in order to avoid surface charging during the SEM observation. Elemental compositions and the distributions of residual materials were analyzed by elemental mapping using SEM-EDX (SEM-EDX: EX-94300S4L1Q, JEOL Ltd., Japan). The carbon tape and sputtering treatment cause overestimation of C, Pd, and Pt concentration. Therefore, these elemental concentration data were excluded during SEM-EDX analysis.

3.3 Results and discussion

3.3.1 Mineral compositions of residual materials

In this and following chapters, residual materials collected after JLT46 (or TCLP) and JLT19 were defined as semi-soluble and insoluble fraction, respectively. Fig. 3.1 shows XRD patterns of residual materials of chelate-treated MSWI fly ash collected after each

leaching experiment. After JLT46 and TCLP, soluble components such as sylvite and halite disappeared owing to leaching out. Semi-soluble fractions consist mainly of Al/Ca/Si-based minerals such as gehlenite ($Ca_2Al_2SiO_7$). Gehlenite can be formed by grain-boundary reaction between Al_2O_3, CaO, and SiO_2 at 800 ˚C [4]. Lime is reacting with quartz and Al from Al-foil particles, melt droplets to form gehlenite in the hot flue gas [5]. After JLT19, XRD peaks of Al/Ca/Si-based semi-soluble minerals were disappeared. Insoluble faction consists mainly of silicon dioxides such as quartz and cristobalite (SiO_2) as other insoluble minerals. Furthermore, Ti-bearing minerals such as

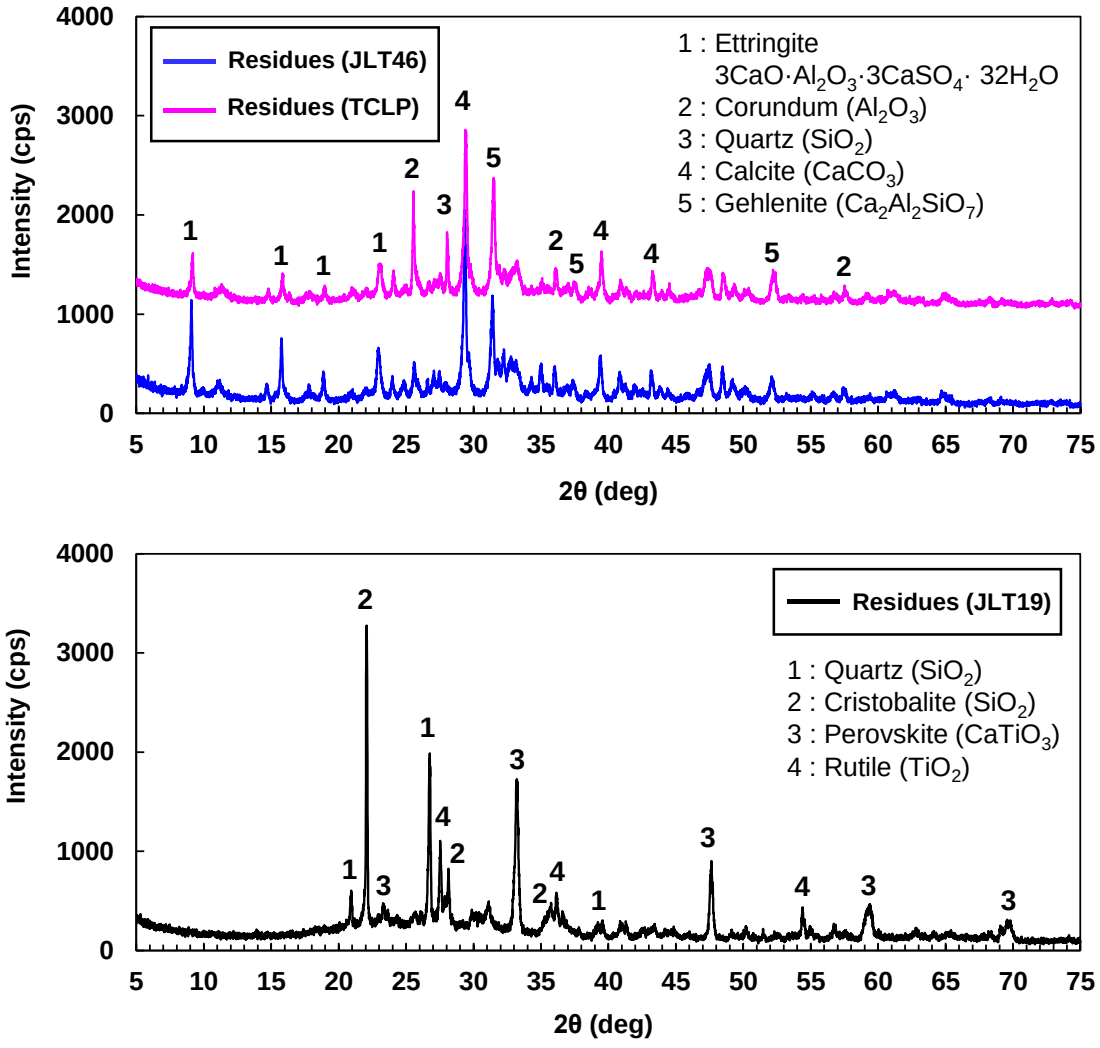

Fig. 3.1 XRD patterns of residual materials collected after leaching experiments

rutile (TiO_2) and perovskite ($CaTiO_3$) could be identified as metal-bearing minerals.

3.3.2 Inner structure of MSWI fly ash particle

Morphological characteristics and elemental distributions of residual materials collected after JLT46 and TCLP are shown in Figs. 3.2 and 3.3, respectively. SEM observation showed that smaller particles (KCl/NaCl-based aggregates) were removed sufficiently from the surface of MSWI fly ash particles. SEM-EDX analysis showed that residual materials had coarse or smooth surface consisted mainly of Al, Ca, and Si. They are considered as Al/Ca/Si-based semi-soluble minerals such as gehlenite as identified by XRD analysis.

Morphological characteristics of residual materials collected after JLT19 are shown in Fig. 3.4. Some residual materials had smooth surface with or without hollows (see Fig. 3.4-A and B). On the other hand, other residual materials had complicated 3-dimensional structure such as skeleton (see Fig. 3.4-C). SEM-EDX analysis showed that soluble

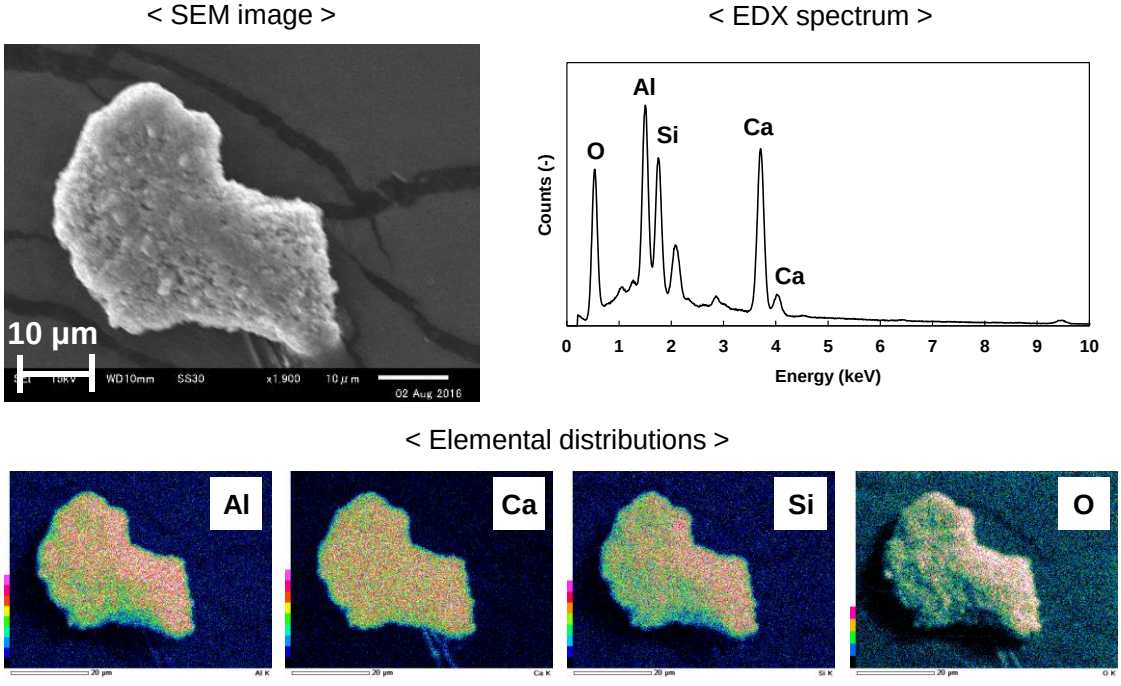

Fig. 3.2 SEM image and elemental distributions of residue collected after LT46

components (KCl/NaCl) and semi-soluble components (Al/Ca/Si-based matrices) were removed sufficiently. Thus, some residual materials consisted mainly of Si (see Fig. 3.5).

As summarized these results, a MSWI fly ash particle used in this study likely consists of Si-based insoluble core structure, Al/Ca/Si-based matrices inside the body, and soluble KCl/NaCl-based aggregates on the surface (see Fig. 3.6). SEM-EDX analysis showed that structural characteristics of chelate-treated MSWI fly ash particles were similar to that of raw MSWI fly ash particles. As concluded in chapter 2, chelate treatment has non-negligible impacts on morphological characteristics of MSWI fly ash, in particular formation of cubic and spicular crystals. However, the impacts on Al/Ca/Si-based

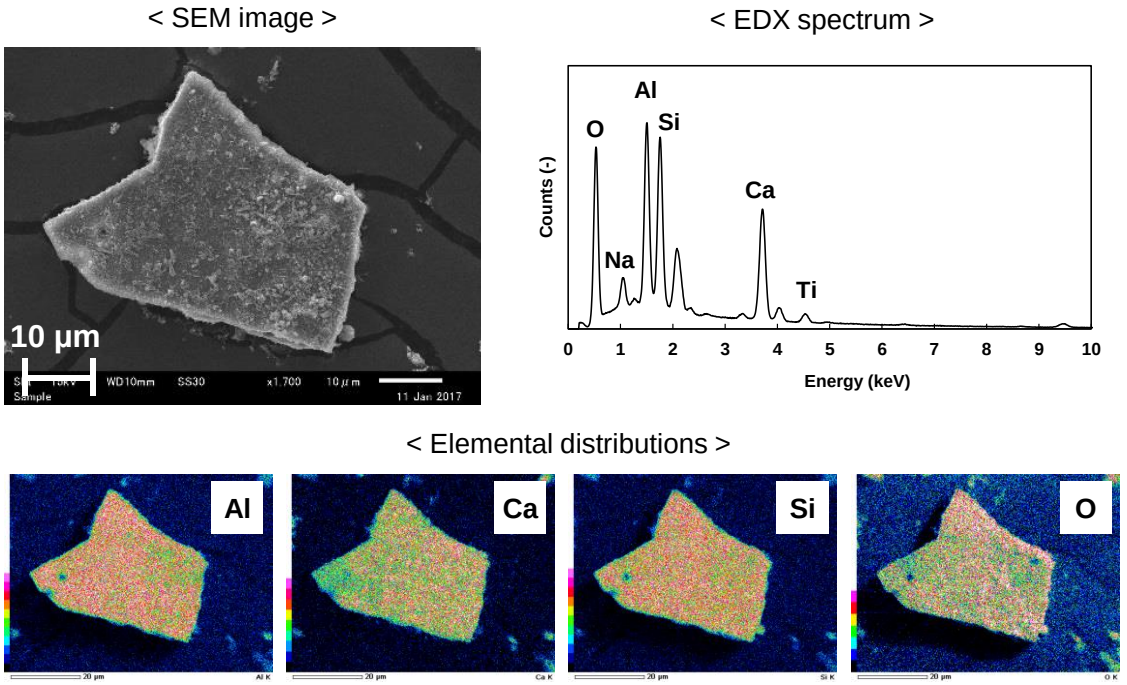

Fig. 3.3 SEM image and elemental distributions of residue collected after TCLP

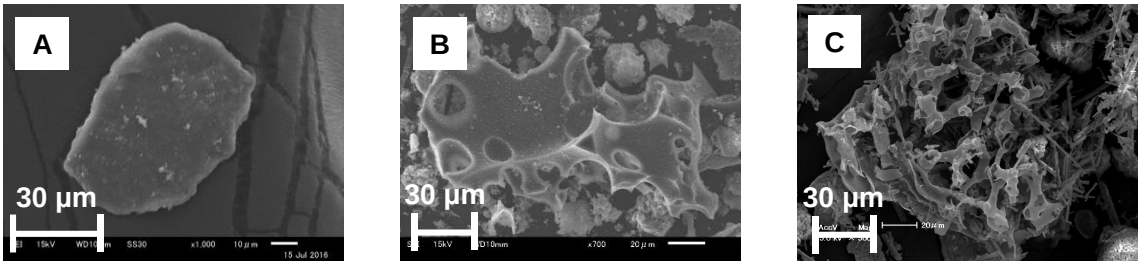

Fig. 3.4 Morphological characteristics of residues collected after JLT19

matrices might be limited. Furthermore, heavy metals can be incorporated into Al/Ca/Si-based matrix [5–9]. MSWI fly ash particles with non-porous and smooth surface as shown in Fig. 3.4-A might prevent infiltration of water into the matrix and thus reduce the leachabilities of heavy metals [10]. It is considered that such structural characteristics of MSWI fly ash particles contribute to heavy metal immobilization to some extent. The relationship between heavy metals and Al/Ca/Si-based matrices is presented in chapter 5.

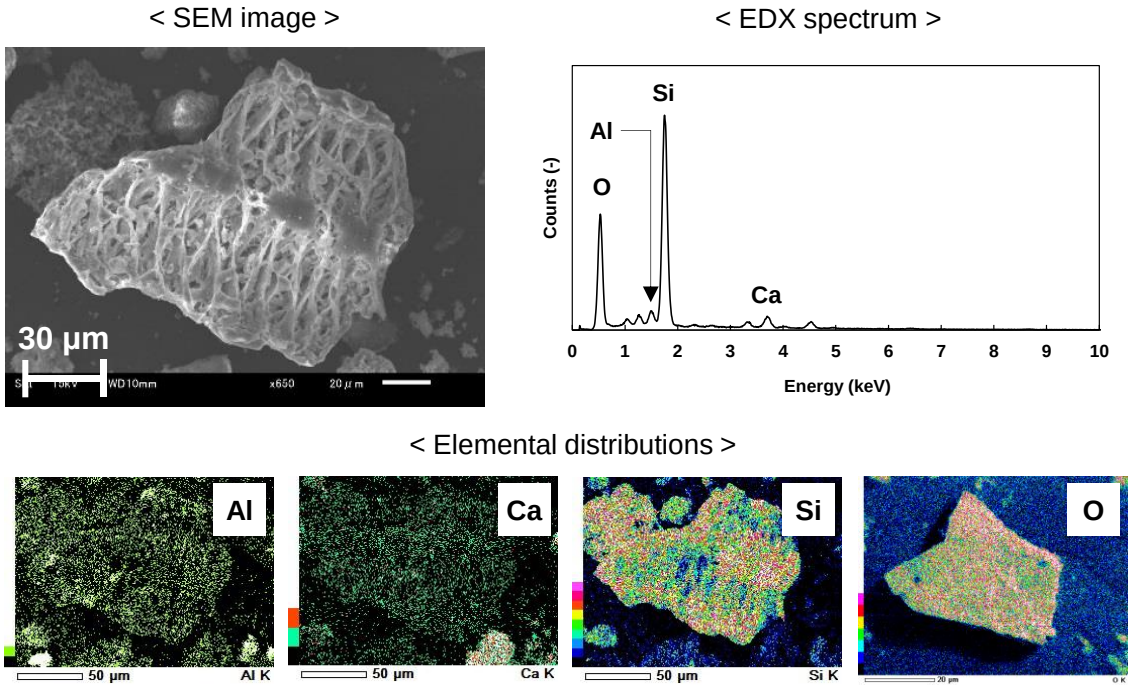

Fig. 3.5 SEM image and elemental distributions of residue collected after JLT19

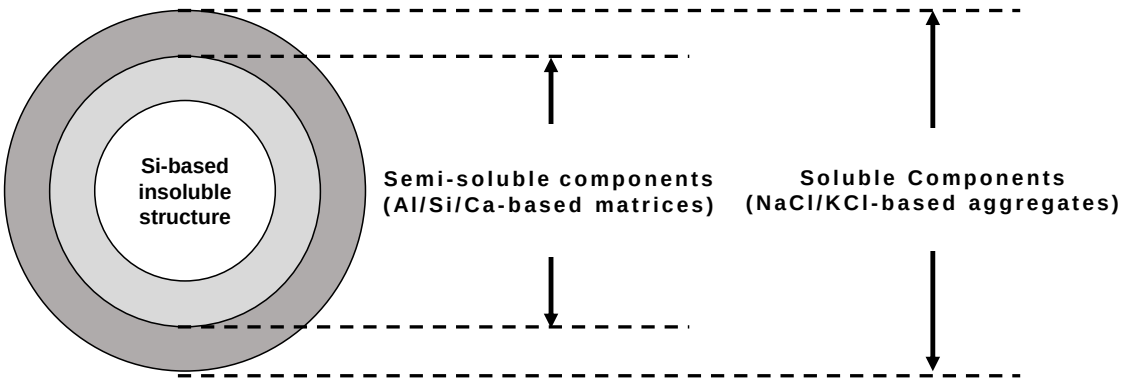

Fig. 3.6 Component model of a MSWI fly ash particle

3.4 Conclusion

Structural characteristics of MSWI fly ash particles were investigated employing 3 types of leaching experiments. Soluble components (KCl/NaCl) and semi-soluble components (Al/Ca/Si-based matrices) were removed sufficiently from MSWI fly ash particles by water and acidic leaching experiments, respectively. SEM-EDX analysis showed that residual materials collected after JLT46 and TCLP consisted of Al/Ca/Si-based matrices. Residual materials collected after JLT19 consisted mainly of Si. Therefore, a MSWI fly ash particle likely consists of Si-based insoluble core structure, Al/Ca/Si-based semi-soluble matrices inside the body, and soluble KCl/NaCl-based aggregates on the surface.

3.5 References

[1] N. Saikia, S. Kato, T. Kojima, Compositions and leaching behaviours of combustion residues, Fuel. 85 (2006) 264–271. doi:10.1016/j.fuel.2005.03.035.

[2] M.J. Quina, R.C. Santos, J.C. Bordado, R.M. Quinta-Ferreira, Characterization of air pollution control residues produced in a municipal solid waste incinerator in Portugal, J. Hazard. Mater. 152 (2008) 853–869. doi:10.1016/j.jhazmat.2007.07.055.

[3] P. Quevauviller, H. a Van Der Sloot, A. Ure, H. Muntau, A. Gomez, G. Rauret, Conclusions of the workshop: harmonization of leaching / extraction tests for environmental risk assessment, Sci. Total Environ. 178 (1996) 133–139. doi:10.1016/0048-9697(95)04805-7.

[4] G. Cultrone, E. Rodriguez-Navarro, Carlos Sebastian, O. Cazalla, M.J. De La Torre, Carbonate and silicate phase reactions during ceramic firing, Eur. J. Mineral. 13 (2001) 621–634. doi:10.1127/0935-1221/2001/0013-0621.

[5] G. Weibel, U. Eggenberger, S. Schlumberger, U.K. Mäder, Chemical associations and mobilization of heavy metals in fly ash from municipal solid waste incineration, Waste Manag. 62 (2016) 147–159. doi:10.1016/j.wasman.2016.12.004.

[6] K. Karlfeldt Fedje, S. Rauch, P. Cho, B.M. Steenari, Element associations in ash from waste combustion in fluidized bed, Waste Manag. 30 (2010) 1273–1279. doi:10.1016/j.wasman.2009.09.012.

[7] H. Zhang, Y. Zhao, J. Qi, Characterization of heavy metals in fly ash from municipal solid waste incinerators in Shanghai, Process Saf. Environ. Prot. 88 (2010) 114–124. doi:10.1016/j.psep.2010.01.001.

[8] A. Bogush, J.A. Stegemann, I. Wood, A. Roy, Element composition and mineralogical characterisation of air pollution control residue from UK energy-from-waste facilities, Waste Manag. 36 (2015) 119–129. doi:10.1016/j.wasman.2014.11.017.

[9] F. Jiao, L. Zhang, Z. Dong, T. Namioka, N. Yamada, Y. Ninomiya, Study on the species of heavy metals in MSW incineration fly ash and their leaching behavior, Fuel Process. Technol. 152 (2016) 108–115. doi:10.1016/j.fuproc.2016.06.013.

[10] A. Ramesh, J.A. Koziński, Investigations of ash topography/morphology and their relationship with heavy metals leachability, Environ. Pollut. 111 (2001) 255–262. doi:10.1016/S0269-7491(00)00062-2.

CHAPTER

4

THE IMPACTS OF SECONDARY MINERAL FORMATION ON TOXIC METAL IMMOBILIZATION

Abstract: In this chapter, the impacts of secondary mineral formation on toxic metal immobilization were investigated. Point analysis of SEM-EDX showed that mineralogical immobilization of toxic metals by ettringite seems to be limited. SEM observation showed that element mobility on the surface of MSWI fly ash particles depends on secondary mineral formation by the moistening. Although insoluble mineral formation prevented from the leaching of soluble elements, its immobilization effect seems to be limited. It is considered that additional immobilization effects of secondary mineral formation are limited for chelate-treated MSWI fly ash. Therefore, the durability of toxic metal immobilization by chelate treatment is almost equal to the stability of metal chelate complex.

4.1 Introduction

Chelate treatment makes MSWI fly ash wet and it promotes secondary mineral formation. Although mineralogical characteristic of MSWI fly ash changed dramatically by secondary mineral formation in chelate treatment, its impact on toxic metal immobilization has been ignored. In contrast to MSWI fly ash, previous studies on MSWI bottom ash already focused on the impact of secondary minerals, which were generated by weathering, on leaching behaviors of toxic metals [1–5]. Previous studies revealed that toxic metals in MSWI bottom ash can be adsorbed and/or incorporated to secondary minerals (e.g. calcite, ettringite, and goethite (α-FeOOH)) through the weathering process. In the weathering process, calcite formation via CO_2 absorption is considered as primary weathering reaction [6]. Therefore, accelerated carbonation has been investigated in order to decrease the leaching potential of toxic metals in MSWI bottom ash [7–12] as well as MSWI fly ash [13–17]. Toxic metal immobilization by cement solidification also suggests that secondary mineral formation might have non-negligible impact on toxic metal immobilization for chelate-treated MSWI fly ash. In cement solidification, adsorption to C-S-H gel and formation of insoluble metal hydroxide are major immobilization mechanisms of toxic metals as well as encapsulation to cement matrices [18,19]. In addition, ettringite is also generated by hydration reaction in cement systems. It has been reported that toxic metals can be incorporated into ettringite structure by substitute reaction (see Table 4.1) [18–21]. Although ettringite is not usually confirmed in fresh fly ash, formation of ettringite in fly ash is immediately promoted when water added to fly ash [22].

It has been simply considered that complexation between chelating substances and toxic metals contributed mainly to toxic metal immobilization by chelate treatment. However, decomposition of chelate-metal complex under air-contact condition has been

reported [23]. The stability is also not so high owing to single dithiocarboxy chelating group [24]. Therefore, long-term stability of metal-chelate complex has been concerned after landfill disposal. On the other hand, mineralogical and physical immobilization of toxic elements by secondary mineral formation owing to chelate treatment has been ignored. In contrast, previous studies as described above imply non-negligible impact of secondary mineral formation on toxic element immobilization in weathered bottom ash. This means that secondary minerals generated by chelate treatment might contribute into metal immobilization even after decomposition of chelate-metal complex. In this context, secondary mineral formation by chelate treatment and its impact on toxic element immobilization were investigated. This chapter would focus on micro-scale neoformed minerals such as ettringite, gypsum, and calcite on the surfaces and inside of chelate-treated MSWI fly ash particles.

4.2 Materials and methods

4.2.1 Experimental samples

In this chapter, chelate-treated MSWI fly ash samples were analyzed in order to

Table 4.1 Ion substitution in ettringite

Ca^{2+} site	Al^{3+} site	SO_4^{2-} site
Sr^{2+}	Cr^{3+}	CO_3^{2-}
Ba^{2+}	Si^{4+}	Cl^-
Pb^{2+}	Fe^{3+}	OH^-
Cd^{2+}	Mn^{3+}	CrO_4^{2-}
Co^{2+}	Ni^{3+}	AsO_4^{3-}
Ni^{2+}	Co^{3+}	NO_3^-
Zn^{2+}	Ti^{3+}	SO_3^{2-}

investigate neoformed minerals on the particle surface. Chelate-treated MSWI fly ash samples were subjected to JLT46 and TCLP in order to remove soluble components (KCl/NaCl) and semi-soluble components (a part of Al/Ca/Si-base matrices) from fly ash particle surface, respectively. Furthermore, leaching experiments also make MSWI fly ash wet and it promotes further formation of secondary minerals via hydration, hydrolysis, carbonation, and so on. Therefore, residual materials collected after JLT46 and TCLP were also analyzed in order to investigate neoformed minerals on inner matrices. Therefore, 3 types of experimental samples (chelate-treated MSWI fly ash, residual materials collected after JLT46 and TCLP) were used in this chapter.

4.2.2 Microscopic observation and metal distribution analysis

Point analysis of SEM-EDX was conducted 500 times in order to detect metal-rich point on spicular crystals (ettringite) in all experimental samples. In addition, other particulate matters of all experimental samples were also analyzed 500 times by point analysis, respectively (see Fig. 4.1). Therefore, 3000 times point analysis were conducted in total. In this analysis, analysis points on the particles were selected randomly (see Fig.

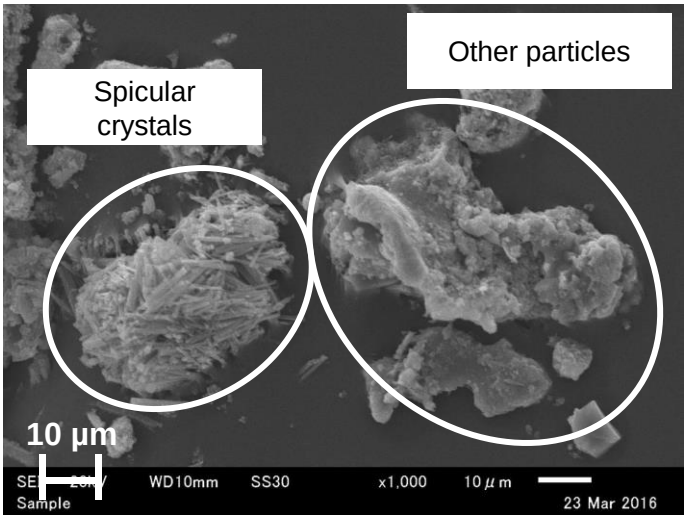

Fig. 4.1 Analyzed experimental samples by point analysis of SEM-EDX

4.2). When metal-rich points on the particle surfaces were detected by point analysis, the particle surfaces were analyzed further by elemental mapping using SEM-EDX.

4.2.3 Observation of the same MSWI fly ash particle

Micro-scale leaching behaviors of soluble components were investigated in order to evaluate the impact of secondary mineral formation on leaching behaviors of heavy metals. Before and after the moistening treatment, leaching and transfer of soluble elements on the surface of the same MSWI fly ash particles were monitored exactly by elemental mapping and line profile analysis of SEM-EDX. At first, MSWI fly ash particles at the corner of carbon tape on the specimen holder were observed individually by SEM-EDX (Fig. 4.3-A and A'). After the first observation, MSWI fly ash particles on the carbon tape were moistened by a humidifier (KZ-550A-BB, CCP Co., Ltd., Japan) and dried under room condition over 24 hours or longer. Approximately 1 mL of pure water was sprayed to fly ash particles for 30 seconds. Moistened MSIW fly ash particles at the corner of carbon tape were observed again (Fig. 4.3-B and B'). In this observation, moistening and drying were repeated twice. Therefore, the same MSWI fly ash particles were monitored before the moistening treatment, after the first and the second moistening

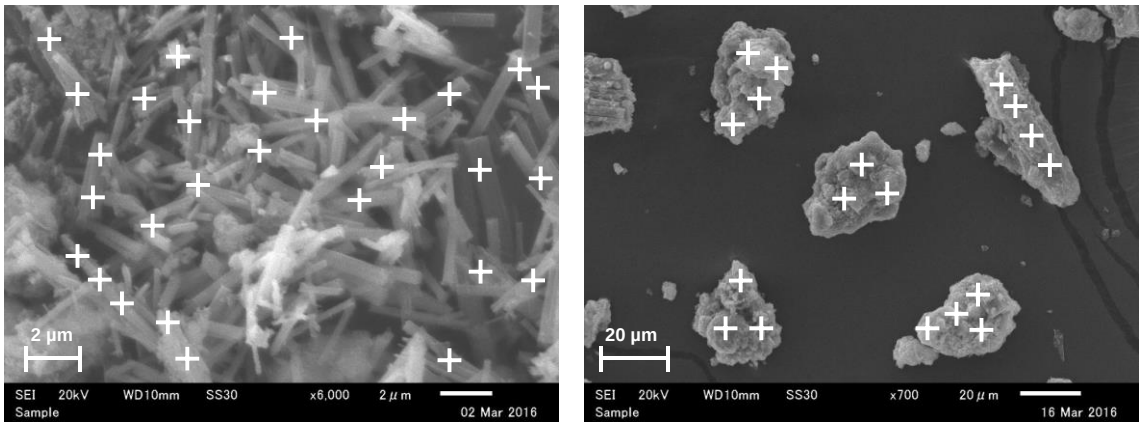

Fig. 4.2 Examples of analysis point on spicular crystals and other particles (white cross mark; analysis point)

treatment (Fig. 4.3-C and C').

4.3 Results and discussion

4.3.1 The impacts of neoformed ettringite and secondary iron-based minerals on metal immobilization

SEM-EDX analysis of chelate-treated MSWI fly ash particles showed that metal-rich points in ettringite structure could not be found during 500 times point analysis although incorporation of toxic metals into ettringite structure has been reported [18–21]. Although concentration of toxic metals in secondary minerals such as calcite, ettringite and iron-based minerals on the surface of chelate-treated MSWI fly ash particles is expected, limited number of metal-rich points on other particles were found contrary to the expectation (88 metal-rich points found in 500 times analysis). In most cases, toxic metals were not concentrated in the spots but distributed on entire surface of MSWI fly ash particles uniformly (see Fig. 4.4-A). Metal-rich and metal-poor fly ash particles consist

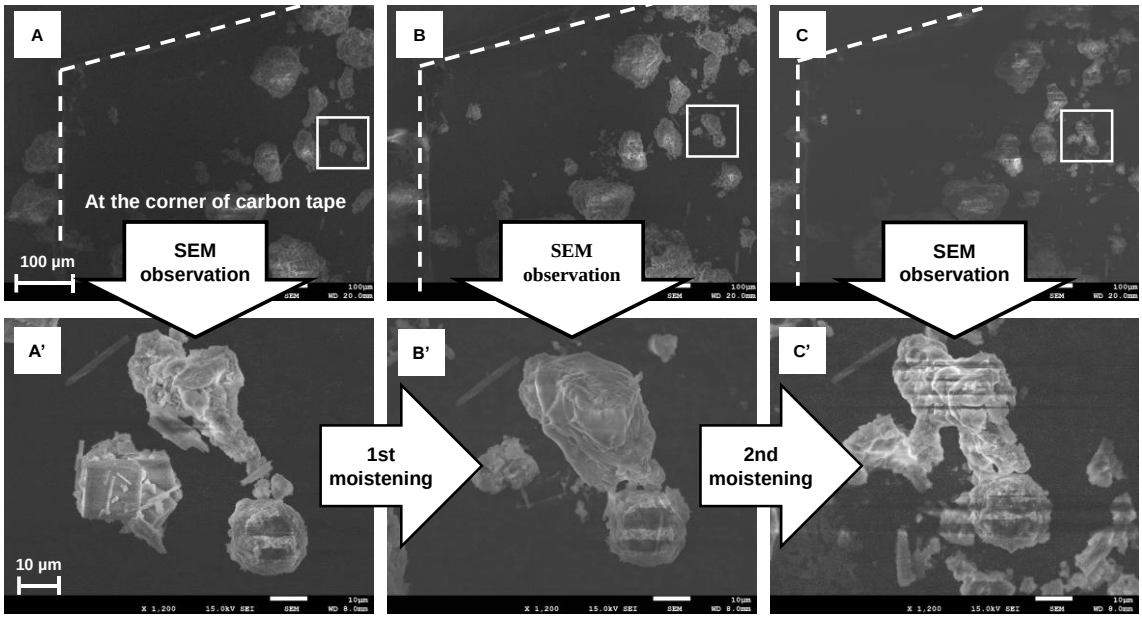

Fig. 4.3 The observation process of the same MSWI fly ash particles before and after the moistening (white broken line; at the corner of carbon tape, white square; observation area by SEM)

mainly of similar elements such as Al, Ca, Cl, Na, O, and Si. There was no significant difference of weight percent in both fly ash particles (see Fig. 4.5). It is considered that these results support evaporation and condensation of metal oxides and chlorides in air pollution control processes of MSW incinerators [25]. Although it is expected that chemisorption of volatilized metal species onto the fly ash particle surface and it generates metal-rich spots, heavy metal accumulation via chemisorption was not observed.

Ettringite was also observed on residual materials collected after JLT46 and TCLP. These seem to be original ettringite unremoved from the particle surface during leaching experiments or newly generated ettringite by moistening in leaching experiments. Metal-rich points were also not observed on ettringite crystals in residual materials collected after JLT46 and TCLP, respectively. On the other hand, some toxic metals were observed on residual materials except for ettringite (see Figs. 4.4-B, C, and D). These toxic metals

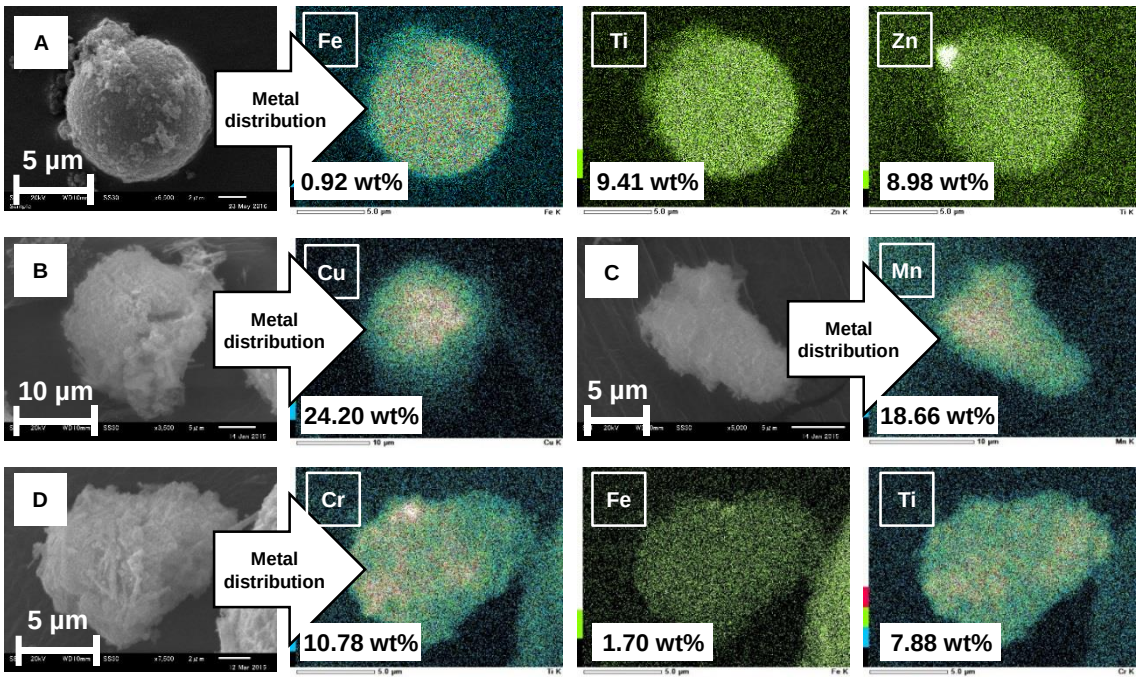

Fig. 4.4 SEM images and metal distributions of metal-rich particles. (A) Chelate-treated MSWI fly ash particles, (B and C) Residual materials collected after JLT46, (D) Residual materials collected after TCLP

also distributed uniformly on entire surface of residual materials as well as chelate-treated MSWI fly ash particles. Metal-rich and metal-poor residual materials consist mainly of semi-soluble components (Al, Ca and Si) and O. There was no significant difference of weight percent between metal-rich and metal-poor points of JLT46 and TCLP (see Fig. 4.5). Because some toxic metals with Al/Ca/Si-based matrices remained even after leaching experiments, they seem to be encapsulated in the Al/Ca/Si-based matrices of MSWI fly ash particles [26–30].

These observation and analysis are summarized as follows. Ettringite, which has metal immobilization effect, was generated on MSWI fly ash particle surface as well as residual materials by the moistening. However, mineralogical metal immobilization such as incorporation of toxic metals into ettringite structure was not confirmed. Additionally, ettringite is stable under alkaline condition at over pH 10.5 [31], whereas it is unstable under carbonation process at the presence of water [3,9]. Nishikawa et al. and Grounds et

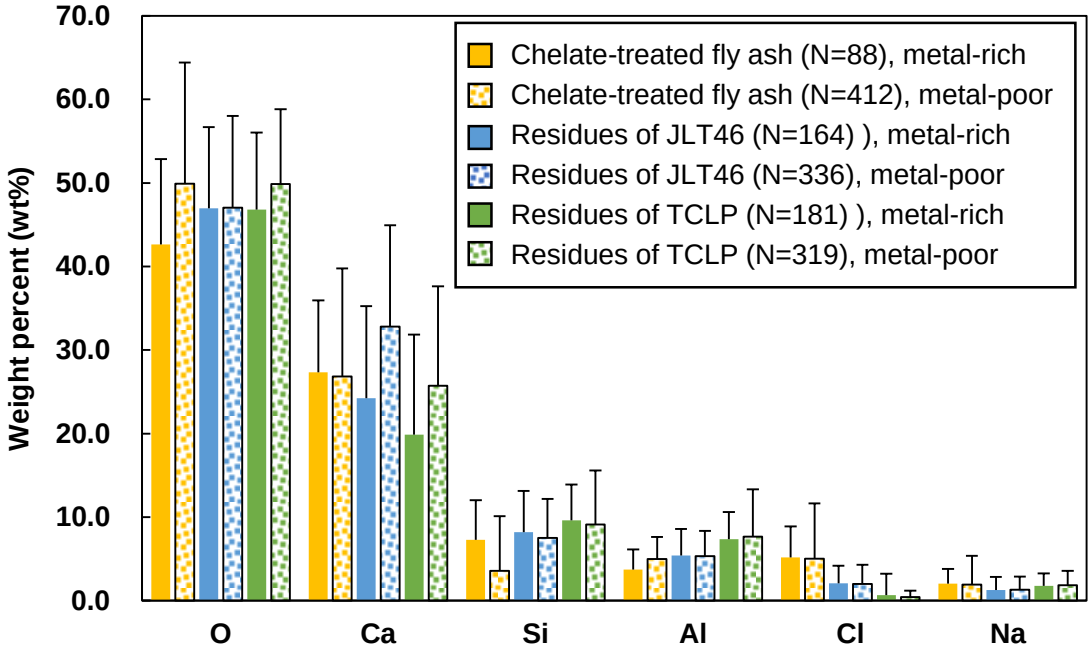

Fig. 4.5 Elemental compositions of metal-rich and metal-poor points (Normal bar: metal rich point, Dotted bar: metal-poor point, N: Number of point analysis)

al. suggest decomposition of ettringite through attack by atmospheric CO_2 as follows [32,33]:

$$3CaO{\cdot}Al_2O_3{\cdot}3CaSO_4{\cdot}32H_2O + 3CO_2 \rightarrow 3CaCO_3 + 3(CaSO_4{\cdot}2H_2O) + Al_2O_3{\cdot}xH_2O + (26-x)H_2O$$

Therefore, mineralogical immobilization of toxic elements by neoformed ettrigite seems to be limited. In the previous studies, adsorption of toxic metals to iron-based minerals in the weathered bottom ash has been reported [3–5]. In this study, Cr, Ti, and Zn were distributed with Fe on the same particle in some cases (see Fig. 4.4-A and D). Jiao et al. reported that Fe is one of the host for heavy metals in fly ash particles [29]. Zhou et al. also reported that enrichment of heavy metal is probably relative to Fe in fine fly ash particles [34]. If iron-based minerals are generated in MSWI fly ash during the weathering process, it might promote mineralogical immobilization to some extent. However, iron content in fly ash is usually much lower than that of bottom ash [35]. Therefore, such immobilization effect in MSWI fly ash seems to be limited.

4.3.2 Physical immobilization of soluble elements by secondary insoluble mineral formation

During the moistening and drying treatment of the same fly ash particle, soluble components (KCl/NaCl) leached and transferred to different places on the particle surface although morphological surface conversions were small (see Fig. 4.6). Fig. 4.7 shows intensity of major elements before and after the first moistening between the point A to point B in Fig. 4.6. After the first moistening, smaller particles (KCl/NaCl) on the surface of the fly ash particle were leached. Then, Cl, K, and Na moved and concentrated at

middle part of the particle. Intensity of soluble components (Cl, K, and Na) slightly increased between 10 to 30 μm of the distance although intensity of Ca, O, and S remained the same level. After the second moistening, Cl, K, and Na transferred to the right side of the particle and concentrated. Soluble components could leach and transfer on the surface under wet condition. Therefore, this observation suggests that toxic metals, which have high solubility such as Zn, can also leach and transfer on the particle surface. In addition, exposure of metal-rich Al/Ca/Si-based matrices owing to leaching of soluble components might promote toxic metal leaching.

In most observations, leaching and transfer of soluble components were always observed. On the other hand, movement of soluble components was inhibited by secondary mineral formation in one case (see Fig. 4.8). After the first moistening, smaller

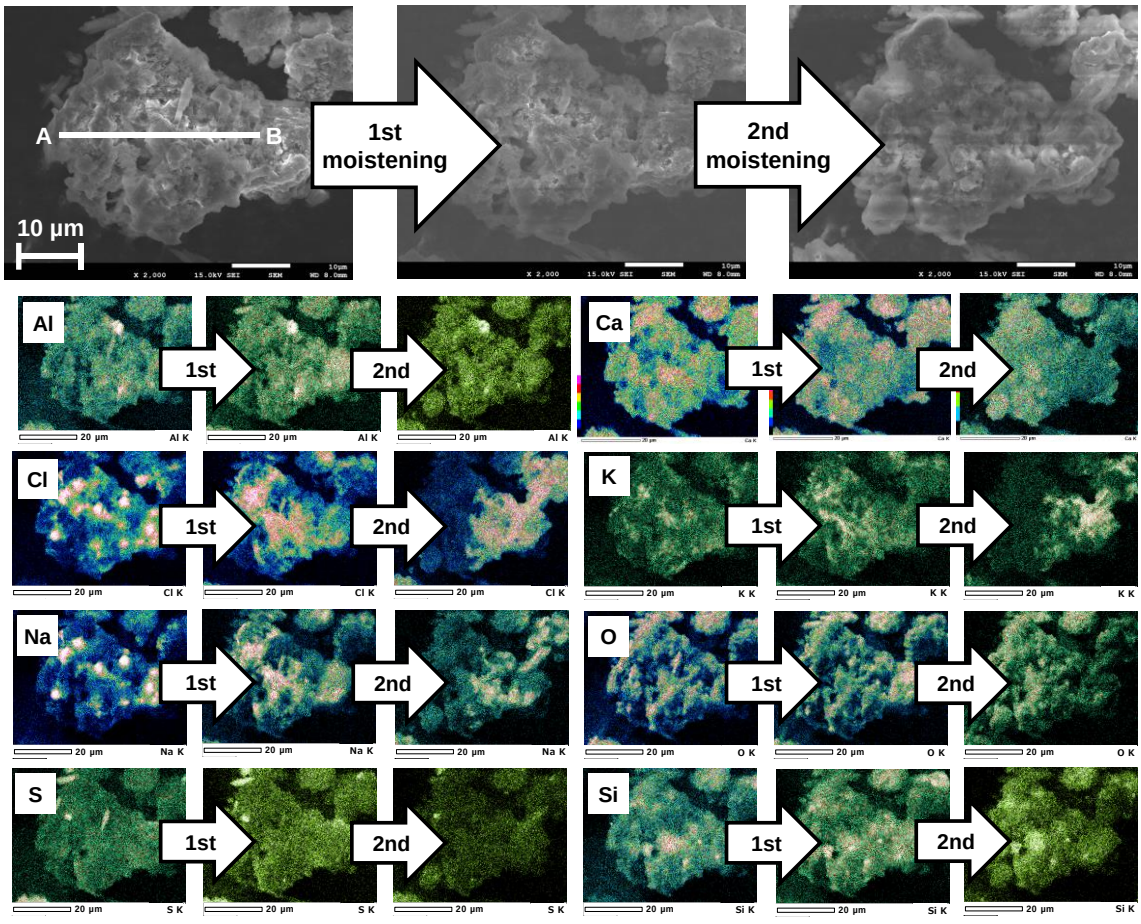

Fig. 4.6 Transfer of soluble components of the same fly ash particle surface

particles (KCl/NaCl) on the surface leached as well as the previous observation. However,

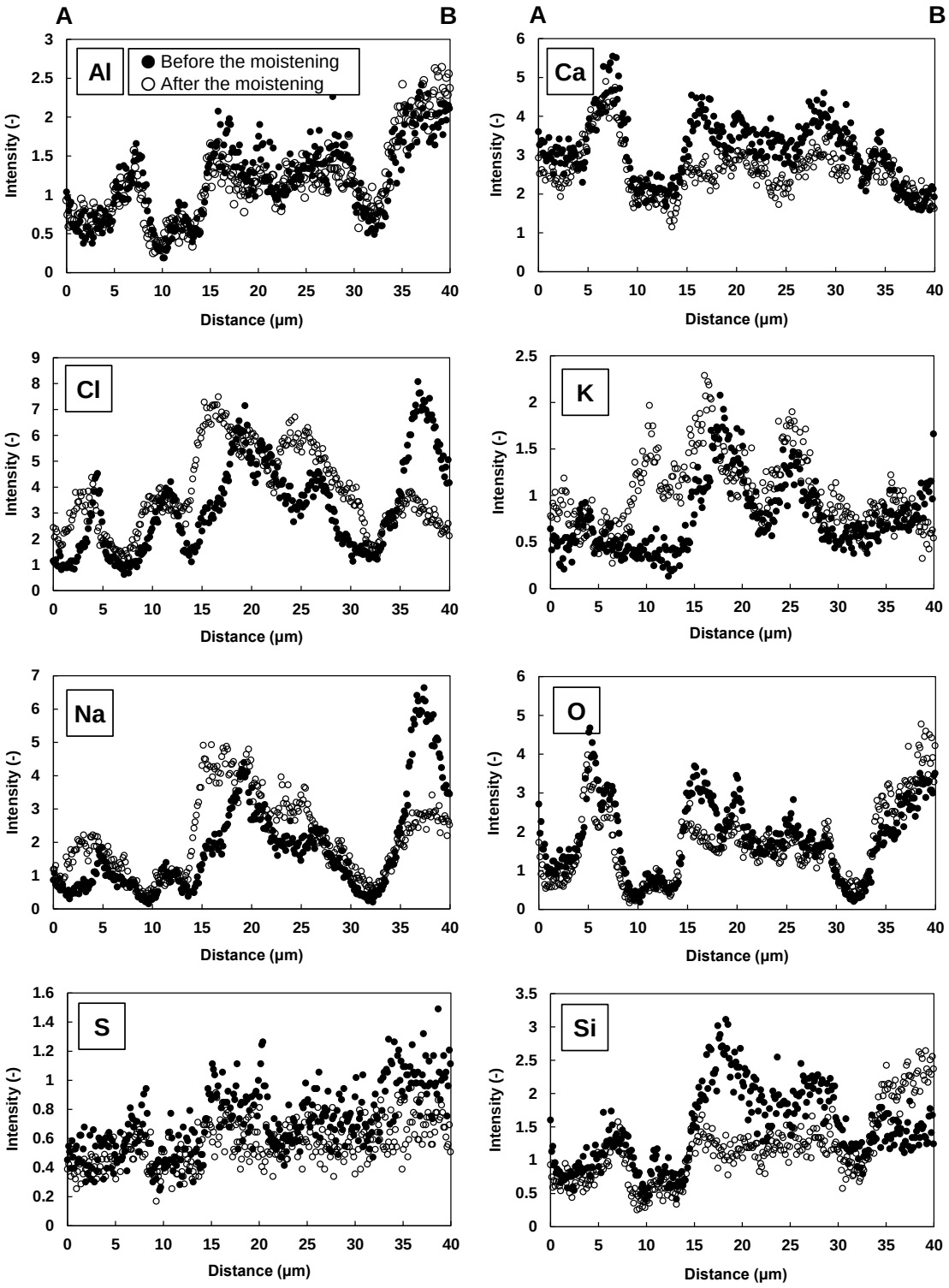

Fig. 4.7 Intensity changes of major elements by transfer of soluble components before and after the first moistening

Cl, K, and Na did not concentrate on fly ash particle surface. Alternatively, concentration of Ca, O, and S increased. Intensity of Cl, K, and Na decreased dramatically while intensity of Ca, O, and S increased (see Fig. 4.9). This means that secondary minerals containing Ca, O, and S such as gypsum ($CaSO_4 \cdot 2H_2O$) were generated on the particle surface after the first moistening. After the second moistening, transfers of soluble elements (Cl, K, and Na) were not observed. This suggests that newly generated gypsum (and/or other calcium sulfate minerals) reduced water infiltration during the second moistening treatment and thus inhibited the leaching of KCl/NaCl. Such physical immobilization of soluble elements by secondary gypsum formation (and other insoluble minerals) seems to be limited because such physical immobilization was monitored only one time of more than 20 observations. On the other hand, calcite should be also

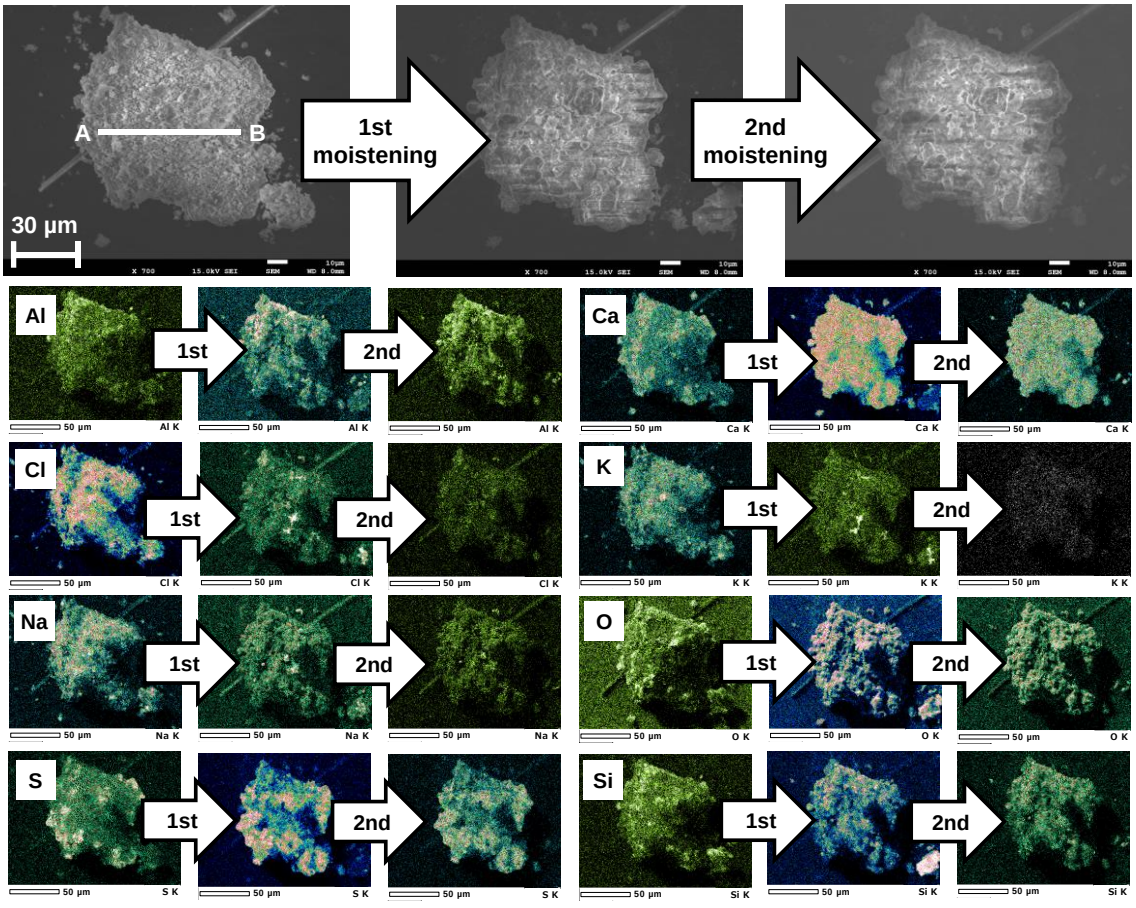

Fig. 4.8 Inhibited transfer of Cl, K and Na by gypsum generation

concerned in terms of physical immobilization. In general, calcite can be generated by

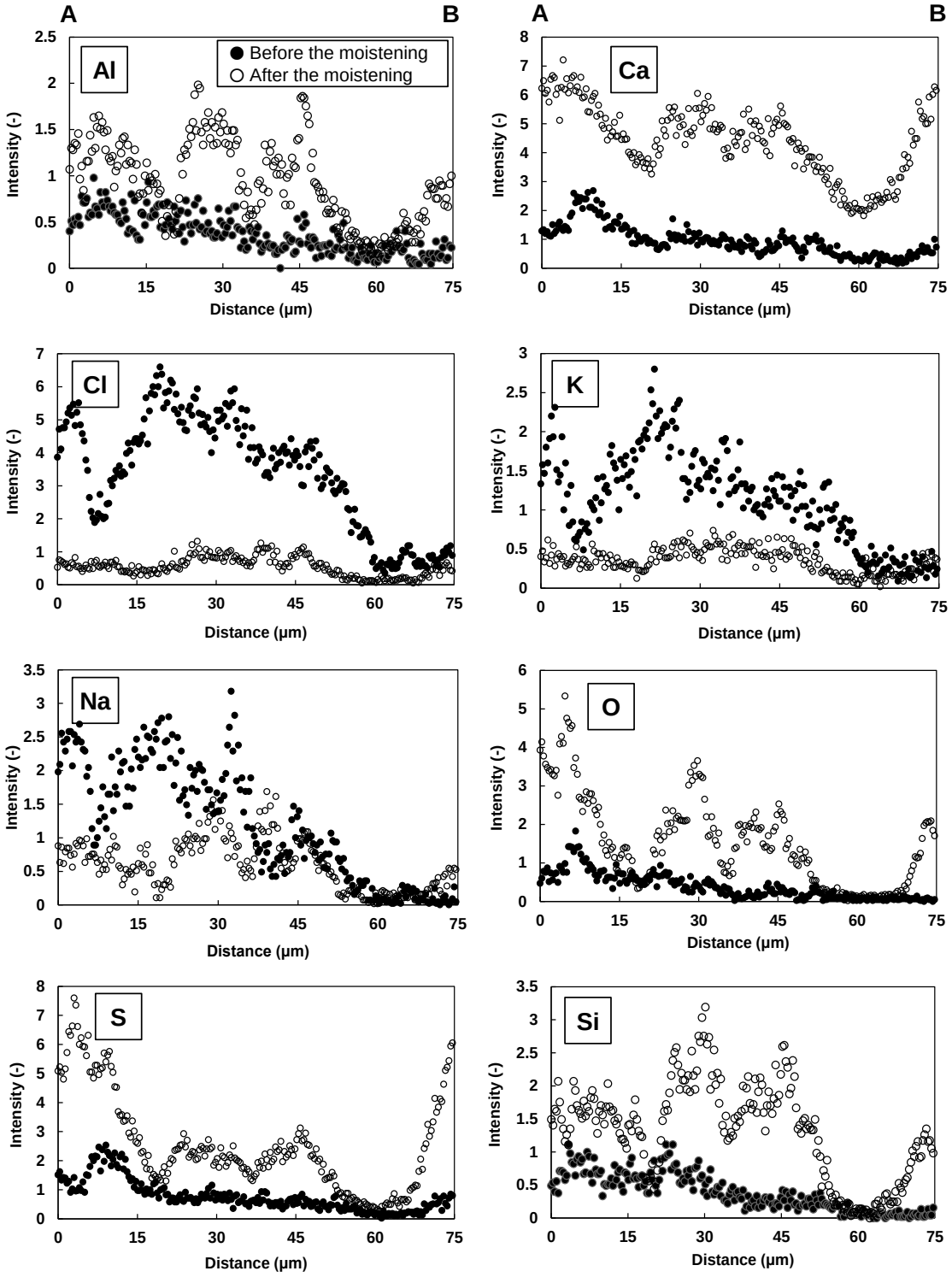

Fig. 4.9 Intensity changes of major elements by gypsum generation before and after the first moistening

the carbonation with atmospheric CO_2 when high alkaline materials such as fly ash are wetted. Calcite can incorporate toxic metals into its structure [1–4]. However, remarkable generation of calcite was not found in this observation. It is considered that high water contents hinder the diffusion of CO_2 because diffusion of CO_2 in water is slower than that in atmosphere [36,37]. Therefore, the observations in this study could not conclude negligible or non-negligible effect of calcite formation on metal immobilization.

These observations are summarized as follows. Element mobility on the surface of MSWI fly ash particles depends on secondary mineral formation by the moistening. Generated gypsum (and/or other calcium sulfate minerals) inhibited leaching and transfer of soluble components. This means that secondary generated mineral has physical immobilization effect for toxic metals. However, generation of insoluble minerals (gypsum, calcite and others) on the fly ash particle surface was rare in this observation. This suggests that physical immobilization of toxic metals by secondary mineral formations is limited.

4.4 Conclusion

In this chapter, mineralogical and physical effects of secondary mineral formation on toxic element immobilization for chelate-treated MSWI fly ash were investigated. SEM observation showed that ettringite, which has metal immobilization effect, was generated on the surface of chelate-treated MSWI fly ash particles and residual materials after leaching experiments. However, metal-rich points could not be found in ettringite structure. This suggests that mineralogical immobilization of toxic elements by ettringite formation seems to be limited. On the other hand, Cr, Ti, and Zn were found with Fe on the same particle in some cases. This suggests that toxic metals in MSWI fly ash can be adsorbed to iron-based secondary minerals generated during the weathering. SEM

observation of the same MSWI fly ash particles showed that element mobility on the surface of MSWI fly ash particles depends on secondary mineral formation by the moistening. Although insoluble mineral formation such as gypsum prevented from the leaching of soluble elements, its immobilization effect seems to be limited because surface coverage by secondary mineral formation occurred with low frequency. As a conclusion, additional immobilization effects of secondary mineral formation are limited for chelate-treated MSWI fly ash. The durability of toxic metal immobilization by chelate treatment is almost equal to the stability of metal chelate complex.

4.5 References

[1] P. Freyssinet, P. Piantone, M. Azaroual, Y. Itard, B. Clozel-Leloup, D. Guyonnet, J.C. Baubron, Chemical changes and leachate mass balance of municipal solid waste bottom ash submitted to weathering, Waste Manag. 22 (2002) 159–172. doi:10.1016/S0956-053X(01)00065-4.

[2] P. Piantone, F. Bodenan, L. Chatelet-Snidaro, Mineralogical study of secondary mineral phases from weathered MSWI bottom ash: Implications for the modelling and trapping of heavy metals, Appl. Geochemistry. 19 (2004) 1891–1904. doi:10.1016/j.apgeochem.2004.05.006.

[3] A. Saffarzadeh, T. Shimaoka, Y. Wei, K.H. Gardner, C.N. Musselman, Impacts of natural weathering on the transformation/neoformation processes in landfilled MSWI bottom ash: A geoenvironmental perspective, Waste Manag. 31 (2011) 2440–2454. doi:10.1016/j.wasman.2011.07.017.

[4] Y. Wei, T. Shimaoka, A. Saffarzadeh, F. Takahashi, Mineralogical characterization of municipal solid waste incineration bottom ash with an emphasis on heavy metal-bearing phases, J. Hazard. Mater. 187 (2011) 534–543.

doi:10.1016/j.jhazmat.2011.01.070.

[5] Y. Wei, T. Shimaoka, A. Saffarzadeh, F. Takahashi, Alteration of municipal solid waste incineration bottom ash focusing on the evolution of iron-rich constituents, Waste Manag. 31 (2011) 1992–2000. doi:10.1016/j.wasman.2011.04.021.

[6] J.A. Meima, R.N.J. Comans, Geochemical modeling of weathering reactions in municipal solid waste incinerator bottom ash, Environ. Sci. Technol. 31 (1997) 1269–1276. doi:10.1021/es9603158.

[7] S. Arickx, T. Van Gerven, C. Vandecasteele, Accelerated carbonation for treatment of MSWI bottom ash, J. Hazard. Mater. 137 (2006) 235–243. doi:10.1016/j.jhazmat.2006.01.059.

[8] M. Nilsson, L. Andreas, A. Lagerkvist, Effect of accelerated carbonation and zero valent iron on metal leaching from bottom ash, Waste Manag. 51 (2016) 97–104. doi:10.1016/j.wasman.2015.12.028.

[9] A. Polettini, R. Pomi, The leaching behavior of incinerator bottom ash as affected by accelerated ageing, J. Hazard. Mater. 113 (2004) 209–215. doi:10.1016/j.jhazmat.2004.06.009.

[10] E. Rendek, G. Ducom, P. Germain, Carbon dioxide sequestration in municipal solid waste incinerator (MSWI) bottom ash, J. Hazard. Mater. 128 (2006) 73–79. doi:10.1016/j.jhazmat.2005.07.033.

[11] R.M. Santos, G. Mertens, M. Salman, Ö. Cizer, T. Van Gerven, Comparative study of ageing, heat treatment and accelerated carbonation for stabilization of municipal solid waste incineration bottom ash in view of reducing regulated heavy metal/metalloid leaching, J. Environ. Manage. 128 (2013) 807–821. doi:10.1016/j.jenvman.2013.06.033.

[12] T. Van Gerven, E. Van Keer, S. Arickx, M. Jaspers, G. Wauters, C. Vandecasteele,

Carbonation of MSWI-bottom ash to decrease heavy metal leaching, in view of recycling, Waste Manag. 25 (2005) 291–300. doi:10.1016/j.wasman.2004.07.008.

[13] G. Cappai, S. Cara, A. Muntoni, M. Piredda, Application of accelerated carbonation on MSW combustion APC residues for metal immobilization and CO2 sequestration, J. Hazard. Mater. 207–208 (2012) 159–164. doi:10.1016/j.jhazmat.2011.04.013.

[14] J. Jiang, M. Chen, Y. Zhang, X. Xu, Pb stabilization in fresh fly ash from municipal solid waste incinerator using accelerated carbonation technology, J. Hazard. Mater. 161 (2009) 1046–1051. doi:10.1016/j.jhazmat.2008.04.051.

[15] J. Jiang, X. juan Du, M. zhe Chen, C. Zhang, Continuous CO2 capture and MSWI fly ash stabilization, utilizing novel dynamic equipment, Environ. Pollut. 157 (2009) 2933–2938. doi:10.1016/j.envpol.2009.06.007.

[16] X. Li, M.F. Bertos, C.D. Hills, P.J. Carey, S. Simon, Accelerated carbonation of municipal solid waste incineration fly ashes, Waste Manag. 27 (2007) 1200–1206. doi:10.1016/j.wasman.2006.06.011.

[17] L. Wang, Y. Jin, Y. Nie, Investigation of accelerated and natural carbonation of MSWI fly ash with a high content of Ca, J. Hazard. Mater. 174 (2010) 334–343. doi:10.1016/j.jhazmat.2009.09.055.

[18] M.L.D. Gougar, B.E. Scheetz, D.M. Roy, Ettringite and C-S-H portland cement phases for waste ion immobilization: A review, Waste Manag. 16 (1996) 295–303. doi:10.1016/S0956-053X(96)00072-4.

[19] Q.Y. Chen, M. Tyrer, C.D. Hills, X.M. Yang, P. Carey, Immobilisation of heavy metal in cement-based solidification/stabilisation: A review, Waste Manag. 29 (2009) 390–403. doi:10.1016/j.wasman.2008.01.019.

[20] M. Chrysochoou, D. Dermatas, Evaluation of ettringite and hydrocalumite

formation for heavy metal immobilization: Literature review and experimental study, J. Hazard. Mater. 136 (2006) 20–33. doi:10.1016/j.jhazmat.2005.11.008.

[21] G. Cornelis, C.A. Johnson, T. Van Gerven, C. Vandecasteele, Leaching mechanisms of oxyanionic metalloid and metal species in alkaline solid wastes: A review, Appl. Geochemistry. 23 (2008) 955–976. doi:10.1016/j.apgeochem.2008.02.001.

[22] P. Ubbrìaco, P. Bruno, A. Traini, D. Calabrese, Fly ash reactivity: Formation of hydrate phases, J. Therm. Anal. Calorim. 66 (2001) 293–305. doi:10.1023/A:1012468505722.

[23] H. Sakanakura, Formation and durability of dithiocarbamic metals in stabilized air pollution control residue from municipal solid waste incineration and melting processes, Environ. Sci. Technol. 41 (2007) 1717–1722. doi:10.1021/es062077e.

[24] F.H. Wang, F. Zhang, Y.J. Chen, J. Gao, B. Zhao, A comparative study on the heavy metal solidification/stabilization performance of four chemical solidifying agents in municipal solid waste incineration fly ash, J. Hazard. Mater. 300 (2015) 451–458. doi:10.1016/j.jhazmat.2015.07.037.

[25] M.A. Fernandez, L. Martinez, M. Segarra, J.C. Garcia, F. Espiell, Behavior of heavy metals in the combustion gases of urban waste incinerators, Environ. Sci. Technol. 26 (1992) 1040–1047. doi:10.1021/es00029a026.

[26] K. Karlfeldt Fedje, S. Rauch, P. Cho, B.M. Steenari, Element associations in ash from waste combustion in fluidized bed, Waste Manag. 30 (2010) 1273–1279. doi:10.1016/j.wasman.2009.09.012.

[27] H. Zhang, Y. Zhao, J. Qi, Characterization of heavy metals in fly ash from municipal solid waste incinerators in Shanghai, Process Saf. Environ. Prot. 88 (2010) 114–124. doi:10.1016/j.psep.2010.01.001.

[28] A. Bogush, J.A. Stegemann, I. Wood, A. Roy, Element composition and mineralogical characterisation of air pollution control residue from UK energy-from-waste facilities, Waste Manag. 36 (2015) 119–129. doi:10.1016/j.wasman.2014.11.017.

[29] F. Jiao, L. Zhang, Z. Dong, T. Namioka, N. Yamada, Y. Ninomiya, Study on the species of heavy metals in MSW incineration fly ash and their leaching behavior, Fuel Process. Technol. 152 (2016) 108–115. doi:10.1016/j.fuproc.2016.06.013.

[30] G. Weibel, U. Eggenberger, S. Schlumberger, U.K. Mäder, Chemical associations and mobilization of heavy metals in fly ash from municipal solid waste incineration, Waste Manag. 62 (2016) 147–159. doi:10.1016/j.wasman.2016.12.004.

[31] G. Cornelis, T. Van Gerven, C. Vandecasteele, Antimony leaching from uncarbonated and carbonated MSWI bottom ash, J. Hazard. Mater. 137 (2006) 1284–1292. doi:10.1016/j.jhazmat.2006.04.048.

[32] T. Grounds, H. G Midgley, D. V Novell, Carbonation of ettringite by atmospheric carbon dioxide, Thermochim. Acta. 135 (1988) 347–352. doi:10.1016/0040-6031(88)87407-0.

[33] T. Nishikawa, K. Suzuki, S. Ito, K. Sato, T. Takebe, Decomposition of synthesized ettringite by carbonation, Cem. Concr. Res. 22 (1992) 6–14. doi:10.1016/0008-8846(92)90130-N.

[34] J. Zhou, S. Wu, Y. Pan, L. Zhang, Z. Cao, X. Zhang, S. Yonemochi, S. Hosono, Y. Wang, K. Oh, G. Qian, Enrichment of heavy metals in fine particles of municipal solid waste incinerator (MSWI) fly ash and associated health risk, Waste Manag. 43 (2015) 239–246. doi:10.1016/j.wasman.2015.06.026.

[35] A. Kida, Y. Noma, T. Imada, Chemical speciation and leaching properties of elements in municipal incinerator ashes, Waste Manag. 16 (1996) 527–536.

doi:10.1016/S0956-053X(96)00094-3.

[36] W.Y. Lin, K.S. Heng, X. Sun, J.Y. Wang, Influence of moisture content and temperature on degree of carbonation and the effect on Cu and Cr leaching from incineration bottom ash, Waste Manag. 43 (2015) 264–272. doi:10.1016/j.wasman.2015.05.029.

[37] J. Sun, M.F. Bertos, S.J.R. Simons, Kinetic study of accelerated carbonation of municipal solid waste incinerator air pollution control residues for sequestration of flue gas CO2, Energy Environ. Sci. 1 (2008) 370–377. doi:10.1039/B804165M.

CHAPTER

5

POSSIBLE METAL SPECIES AND THEIR EXTERNAL MATRIX ESTIMATED BY MICRO-SCALE CORRELATION ANALYSIS

Abstract: In this chapter, micro-scale correlation analysis was applied to estimate metal species and their external matrix in MSWI fly ash. The analysis method could estimate dominant metal species and their external matrix of each individual fly ash particle regardless of crystalline or non-crystalline forms. However, it should be conducted at appropriate scale level to prevent from detecting pseudo-correlation.

5.1 Introduction

Metal species in MSWI fly ash depend on affinities of elements and flue gas compositions such as contents of chlorine, moisture, sulfur, and inorganic particulates [1–8]. Main immobilization mechanism of chelate treatment is complexation between heavy metal and chelating substances. However, it does not mean that all heavy metals in MSWI fly ash can react with chelate reagent. For examples, Sakanakura reported that approximately 70 % of Pb in air pollution control residues from MSWI plant formed lead chelate complex [9]. Therefore, it is necessary to identify metal species in MSWI fly ash in order to understand leaching behaviors of heavy metals.

Generally, XRD analysis has been used to identify mineral compositions including metal-bearing minerals in MSWI fly ash. In some cases, however, metal-bearing minerals cannot be identified by XRD analysis owing to their low concentration levels, their presence in amorphous or poor crystalline phases, and complex matrix of fly ash [10–15]. Therefore, X-ray absorption spectroscopy (XAS) utilizing synchrotron radiation has been used to identify metal species in MSWI fly ash at low concentration level. In the last two decades, metal species identified by XAS have been reported by many studies [12–27]. However, a limited number of studies focused on metal chelate complex in chelate-treated MSWI fly ash. As far as literature review at present, only Yamamoto et al. directly identified lead chelate complex in chelate-treated MSWI fly ash by XAS [28]. Sequential chemical extraction (SCE) suggested by Tessier et al. [29] has been used to investigate chemical forms of heavy metals. SCE fractionates heavy metals into some fractional patterns (e.g. F1: exchangeable, F2: bound to carbonates, F3: bound to Fe-Mn oxides, F4: bound to organic matter, F5: residual) based on their ease of extractability. Chemical conversions of metal species during chelate treatment have been reported by SCE in a few studies [30,31]. However, heavy metals might be fractionated imperfectly owing to

incomplete dissolution of target phases, the removal of non-target species, and the incomplete removal of dissolved metals by re-adsorption on remaining components and/or re-precipitation with the added reagent [26]. Furthermore, geochemical modeling has been used to simulate leaching behaviors of heavy metals [32–37].

Several studies have been tried to estimate metal species in MSWI fly ash by SEM-EDX [38–42]. SEM-EDX analysis cannot identify valences of heavy metals. However, it can estimate possible metal species at individual particle level even at low concentration. In addition, it can also observe bonding states between heavy metal and ash matrix regardless of crystalline or non-crystalline phase. In this context, a new method to estimate metal species in MSWI fly ash by micro-scale correlation analysis using SEM-EDX was developed. Furthermore, possible metal species and their external matrices were estimated by this method in this chapter.

5.2 Materials and methods

In this chapter, metal-rich particles in raw and chelate-treated MSWI fly ash samples were analyzed. However, it is difficult to detect metal-rich points on the surfaces of MSWI fly ash particles owing to voluminous amount of soluble components. Therefore, residual materials collected after JLT46, TCLP, and JLT19 of chelate-treated MSWI fly ash samples were also analyzed. Metal-rich particles were found by point analysis and the elemental distributions were analyzed by elemental mapping using SEM-EDX as described in subsection 4.2.2.

After elemental mapping, the surface of metal-rich particle was divided into 5 sections from the side to another side horizontally and vertically (see Fig. 5.1). Line profile analysis for each vertical/horizontal section was conducted based on elemental mapping data in order to measure elemental concentrations of constituent elements as intensity

data. Correlation coefficients (r) between constituent elements and heavy metal were calculated based on the intensity data in each vertical/horizontal section. Finally, possible metal species at specific vertical/horizontal section in a metal-rich particle were estimated based on correlation coefficients with supporting references.

5.3 Results and discussion

5.3.1 The effect of leaching experiments on observation of metal-rich particle

Fig. 5.2 shows the number of analysis point in each experimental sample. Metal-rich points were detected at 159 and 88 points in raw and chelate-treated MSWI fly ash particles, respectively. The number of metal-rich points of chelate-treated MSWI fly ash were approximately half in comparison with raw MSWI fly ash. Morphological characteristics of MSWI fly ash particles changed dramatically owing to secondary mineral formation during chelate treatment. Because metal-rich points or surfaces on fly ash particles were masked by the secondary mineral formation, less metal-rich points were found on chelate-treated MSWI fly ash. After the removal of soluble and semi-soluble components by leaching experiments, the number of metal-rich points increased from 88 to 253 points. In this point analysis, metal-rich particles such as Cu, Cr, Fe, Mn, Ti, and Zn were detected. The number of metal-rich particle in each experimental sample is summarized in Table 5.1. Especially, Fe, Ti, and Zi-rich particles were frequently detected owing to their high contents in comparison with other heavy metals (see Table

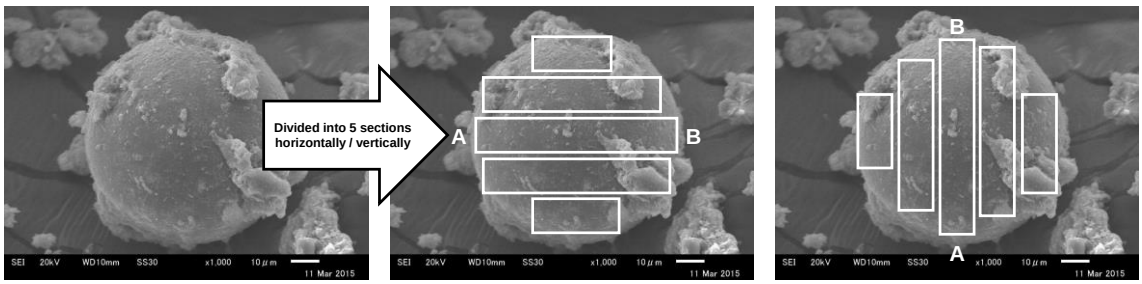

Fig. 5.1 Dividing method of a metal-rich particle for micro-scale correlation analysis

2.1 in chapter 2).

As shown in Table 2.1 and 5.1, various heavy metals could be detected by EDXRF and SEM-EDX analysis. However, XRD analysis could identify only rutile and perovskite as crystalline metal-bearing minerals (see Fig. 3.1). This suggests that metal species in MSWI fly ash are non-crystalline forms or the concentrations of crystalline forms are lower than XRD detection limit.

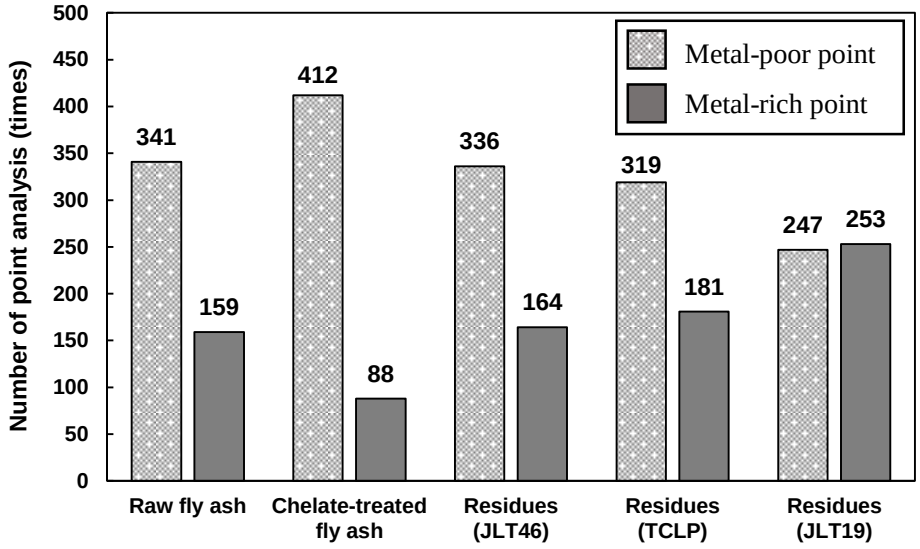

Fig. 5.2 The number of metal-rich point in each experimental sample

Table 5.1 The number of metal-rich particle in each experimental sample

Experimental samples	Heavy metals					
	Cu	Cr	Fe	Mn	Ti	Zn
Raw MSWI fly ash	0	1	6	1	4	12
Chelate-treated MSWI fly ash	0	0	1	0	10	1
Residues collected after JLT46	1	1	7	1	15	0
Residues collected after TCLP	0	2	4	0	14	0
Residues collected after JLT19	0	2	17	0	31	1
Total	1	6	35	2	74	14

5.3.2 Possible metal species and their external matrix estimated by micro-scale correlation analysis

5.3.2.1 Titanium (Ti)

Ti species in MSWI fly ash samples could be identified only rutile and perovskite. According to literature review, titanium dioxide (TiO_2) is widely used in commercial products such as paints, papers, inks, cosmetics, sunscreens, food additives, textiles, and so on [43–49]. Titanium dioxide naturally exists as 3 types of crystalline forms; rutile, anatase, and brookite. Although rutile and anatase are mainly used in commercial products, anatase could not be identified in this study. Previous studies also reported only rutile and perovskite as Ti species in MSWI fly ash [50–54]. Roes et al. reported that most TiO_2 is inert during MSWI process [55], whereas transformation from anatase to rutile around 600 to 700 °C have been reported [47]. Massari et al. also reported that anatase reacts with CaO in fly ash and form perovskite during incineration process [56].

Fig. 5.3 shows elemental distributions and micro-scale correlation analysis along point A to point B on Ti-rich particle in chelate-treated MSWI fly ash. Ti concentrated on the surface of Al/Ca/Si-based spherical particle attached with KCl/NaCl-based components. The spherical particle (calcium aluminosilicate) is commonly observed in MSWI fly ash [40,57,58]. Micro-scale correlation analysis showed that Ti had high correlations with Al, Ca, O, and Si as well as negative correlations with Cl and K. Therefore, the Ti species are estimated to be rutile or perovskite when the Ti exists as crystalline form. Furthermore, positive correlations with Al and Si suggests that the crystalline Ti (rutile or perovskite) or non-crystalline Ti is incorporated or combined with aluminosilicate matrix. Micro-scale correlation analysis also showed differences of dominant Ti species at individual particle level. For example, another Ti-rich particle had Ca-based porous surface as shown in Fig. A.1 (Supplementary material). In this particle, Ti had positive correlations with Al,

Ca, and O as well as negative correlation with Si. Especially, correlation between Ti and Ca was strongly high (correlation coefficient: r = 0.75). Therefore, the Ti speciation is estimated to be perovskite. As shown in Fig. A.2 (Supplementary material), another Ti-rich particle had positive correlations with Al, K, Na, O, and Si as well as negative correlations with Ca and Cl. In contrast to Fig. A.1 (Supplementary material), correlation between Ti and Ca was negative (r = − 0.35). Therefore, the Ti speciation is estimated to be rutile if crystalline form. In addition, Ti is incorporated or combined with aluminosilicate matrix, which is the same with the case shown in Fig. 5.3. As shown in

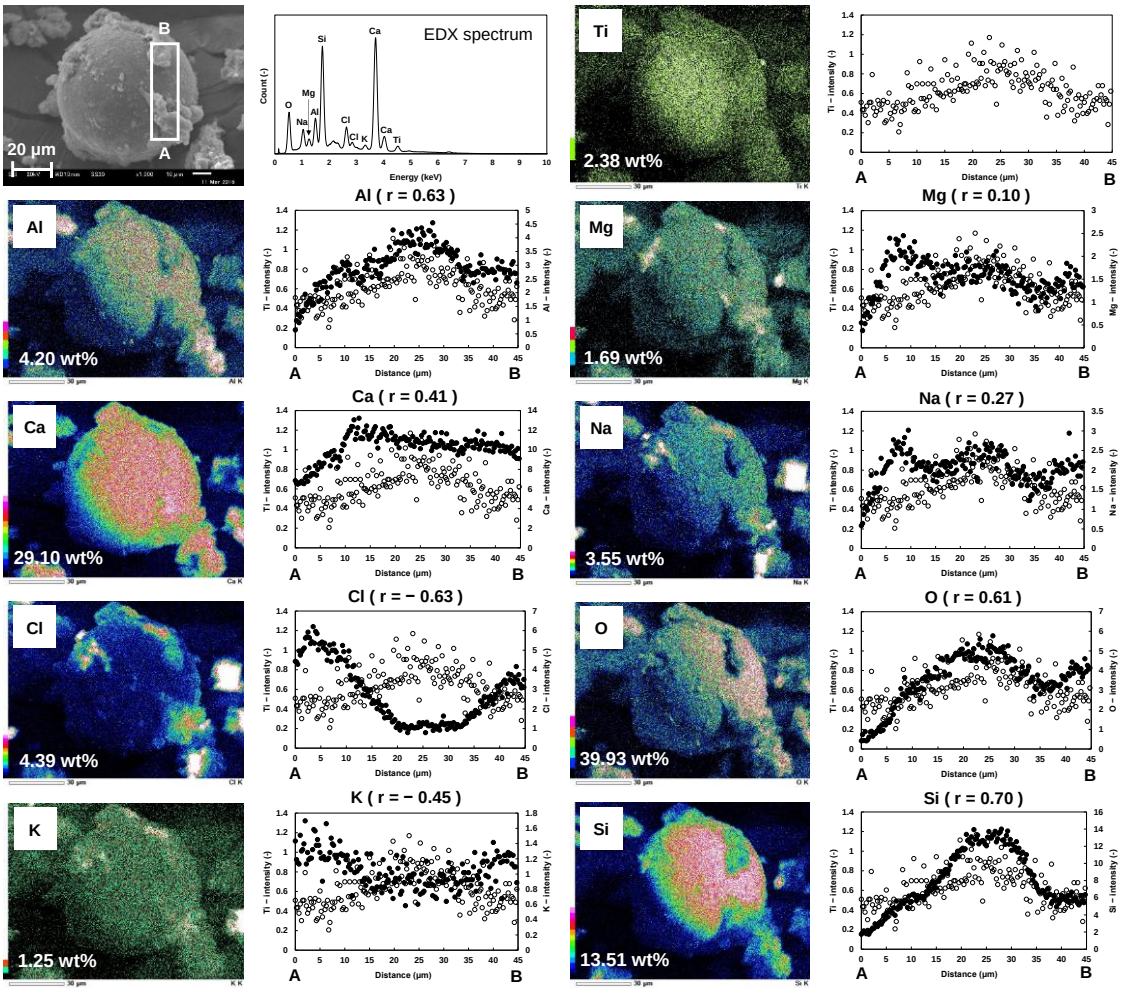

Fig. 5.3 Elemental distributions and micro-scale correlation analysis along point A to point B on Ti-rich particle (rutile or perovskite) in chelate-treated MSWI fly ash (r : correlation coefficient)

Fig. 3.1, XRD analysis identified Ti-bearing minerals (rutile and perovskite) in MSWI fly ash. Furthermore, micro-scale correlation analysis revealed that dominant Ti species and their bonding states with Al/Ca/Si-based ash matrix were different at individual particle level. During MSWI process, TiO_2 is not volatilized and remained particulate owing to high boiling point (2972 °C) [59,60]. Ti reacts with Al, Ca, and Si and then forms ash matrix [61]. Thus, particulate anatase (TiO_2) transforms to rutile or perovskite during MSWI process. Titanium randomly bind to ash particles regardless of their composition [39]. Therefore, original and/or transformed rutile are incorporated or combined with aluminosilicate matrix to form ash matrix as shown in Figs. 5.3 and A.2 (Supplementary material) in some cases.

Fig. 5.4 shows correlation coefficients between Ti and O calculated based on integrated intensity data of all horizontal sections. Although correlation coefficients always have positive values at each horizontal section, correlation coefficient at the whole particle level is negative (see Fig. 5.5). When intensity data of all horizontal sections were integrated simply to one dataset, such pseudo-negative correlation coefficient could be calculated. It suggests that micro-scale correlation analysis should be conducted at

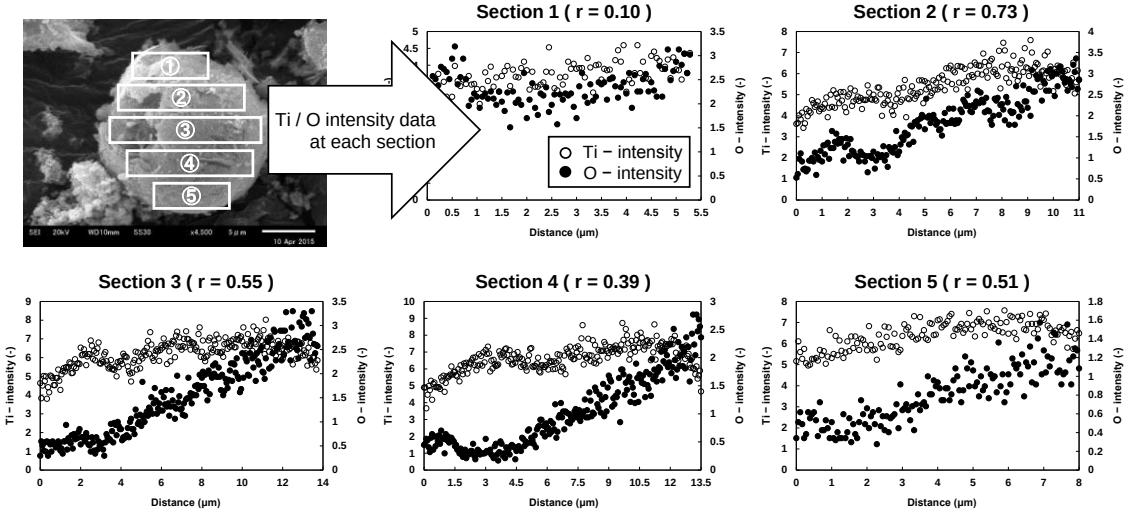

Fig. 5.4 Intensity data of Ti and O at all horizontal sections (r : correlation coefficient)

appropriate scale level to prevent from pseudo-correlation and estimate possible metal species correctly.

5.3.2.2 Copper (Cu)

According to previous studies, XRD analysis identified several Cu species such as $CuCl_2$ [12,16], Cu_2O [12], CuO [12,13,16,40], $Cu(OH)_2$ [16], and $K_2Cu_3O(SO_4)_3$ [40]. XAS analysis also showed existence of Cu chlorides, hydroxides, oxides, and sulfides in MSWI fly ash [12,13,16–20]. Thus, previous studies suggested various Cu species because incineration temperature have impact on Cu species during MSWI process as well as chlorine, moisture, and sulfur contents [3,5,6]. In this study, only one Cu-rich particle was found in residual materials collected after JLT46 (see Fig. 5.6). Micro-scale correlation analysis showed that Cu had positive correlation with Al, Cl, Mg, O, Si, and Zn as well as negative correlation with Ca and S. Because chelate reagent contains S, the negative correlation between Cu and S suggests that the Cu might not form complex with the chelate reagent. The positive correlation among Al, Cl, Cu, O, and Si suggests that Cu species are chloride (e.g. $CuCl_2$) or oxides (e.g. Cu_2O and CuO) and they are incorporated or combined with aluminosilicate matrix. Because Cu was detected in residue samples

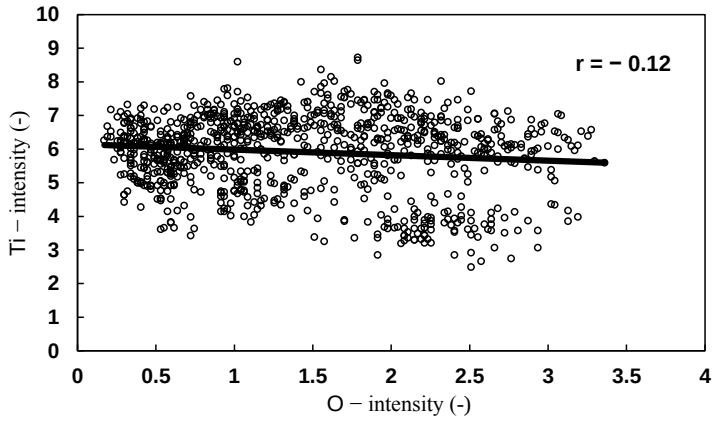

Fig. 5.5 Scatter plot for intensity data of O and Ti (r : correlation coefficient)

after JLT46 and $CuCl_2$ is soluble in water, $CuCl_2$ can be excluded and high correlation with Cl is considered pseudo-positive. Furthermore, Cu also had positive correlation with Zn. Weibel et al. reported that alloy brass ($Cu_{0.6}Zn_{0.4}$) is frequently found in MSWI fly ash by SEM-EDX analysis [42]. Therefore, the Cu species are estimated to be Cu oxides or brass with aluminosilicate matrix.

5.3.2.3 Chromium (Cr)

Major chemical forms of Cr have been fractionated as residual fraction (exceeded

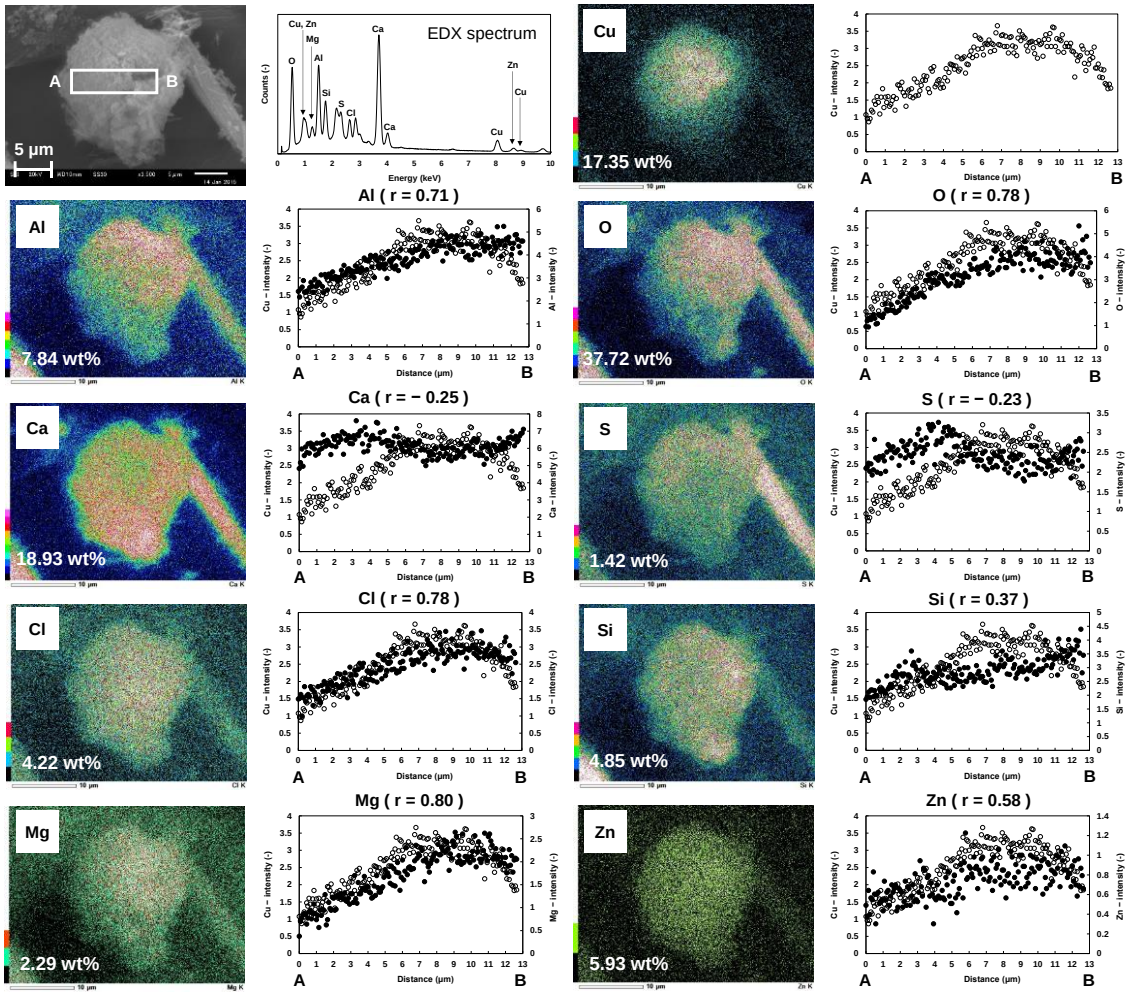

Fig. 5.6 Elemental distributions and micro-scale correlation analysis along point A to point B on Cu-rich particle (Cu oxides or brass) in residues collected after JLT46 (r : correlation coefficient)

50 %) by SCE [30,32,51,54,62–66]. The low leachability of Cr results from incorporation into stable spinel matrix [51,66] and/or formation of chromium oxide (Cr_2O_3) incorporated into Al/Ca/Si-based matrix [32,54]. In this study, 6 Cr-rich particles were detected (see Table 5.1). However, clear Cr distribution could be measured in only 1 particle. SEM-EDX analysis showed that Cr clearly concentrated at center part of the particle. On the other hand, Si relatively concentrated near inner border area of the particle (see Fig. 5.7). Micro-scale correlation analysis showed that Cr had positive correlation with only O as well as negative correlation with Al, Ca, Mg, Na, Si, and Ti. Therefore, Cr speciation is estimated to be Cr_2O_3, not chromate forms like sodium chromate. In addition, low correlations with Al, Ca, and Si suggest that Cr_2O_3 is not incorporated in Al/Ca/Si-based matrix. It is inconsistent with previous studies [32,54]. As reported in following sections, this study found that other metal oxides were usually incorporated in Al/Ca/Si-based matrix. Therefore, Cr_2O_3 behaviors might be greatly different from other meal oxides in MSWI fly ash formation processes.

5.3.2.4 Iron (Fe)

Previous studies identified Fe oxides such as wüstite (FeO) [51], hematite (Fe_2O_3) [12,13,16,41,50–54,58,62], and magnetite (Fe_3O_4) [13,16,50,51] in MSWI fly ash. Thermodynamic analysis showed that Fe chlorides are also possible species [67]. However, Fe chlorides was not identified by XRD. In contrast to XRD analysis, XAS analysis could detect non-crystalline Fe chlorides ($FeCl_2$ and $FeCl_3$) [21]. The results showed that percentage of the Fe species in MSWI fly ash is as follows: 76% Fe_2O_3, 10% $FeCl_3$, 10% $FeCl_2$, and 4% FeO. Therefore, Fe chlorides and oxides are probably major species in MSWI fly ash. SEM-EDX analysis showed that Fe-rich particle had spherical and smooth surface attached with aggregates of smaller particles (see Fig. 5.8). Micro-

scale correlation analysis showed that Fe had positive correlations with Al, Ca, O, and Si as well as no correlations with Cl, K, and Na. Therefore, the Fe species are estimated to be Fe oxides in Al/Ca/Si-based matrix. No correlation with Cl, K, and Na means that Fe oxides do not exist together with KCl/NaCl-based aggregates on the surface. These observations partially suggest fly ash formation mechanisms in MSWI plants. Fe oxides react with and/or are trapped in Al/Ca/Si-based compounds like aluminosilicate in the gas phase and then followed by KCl/NaCl adsorption on the surface.

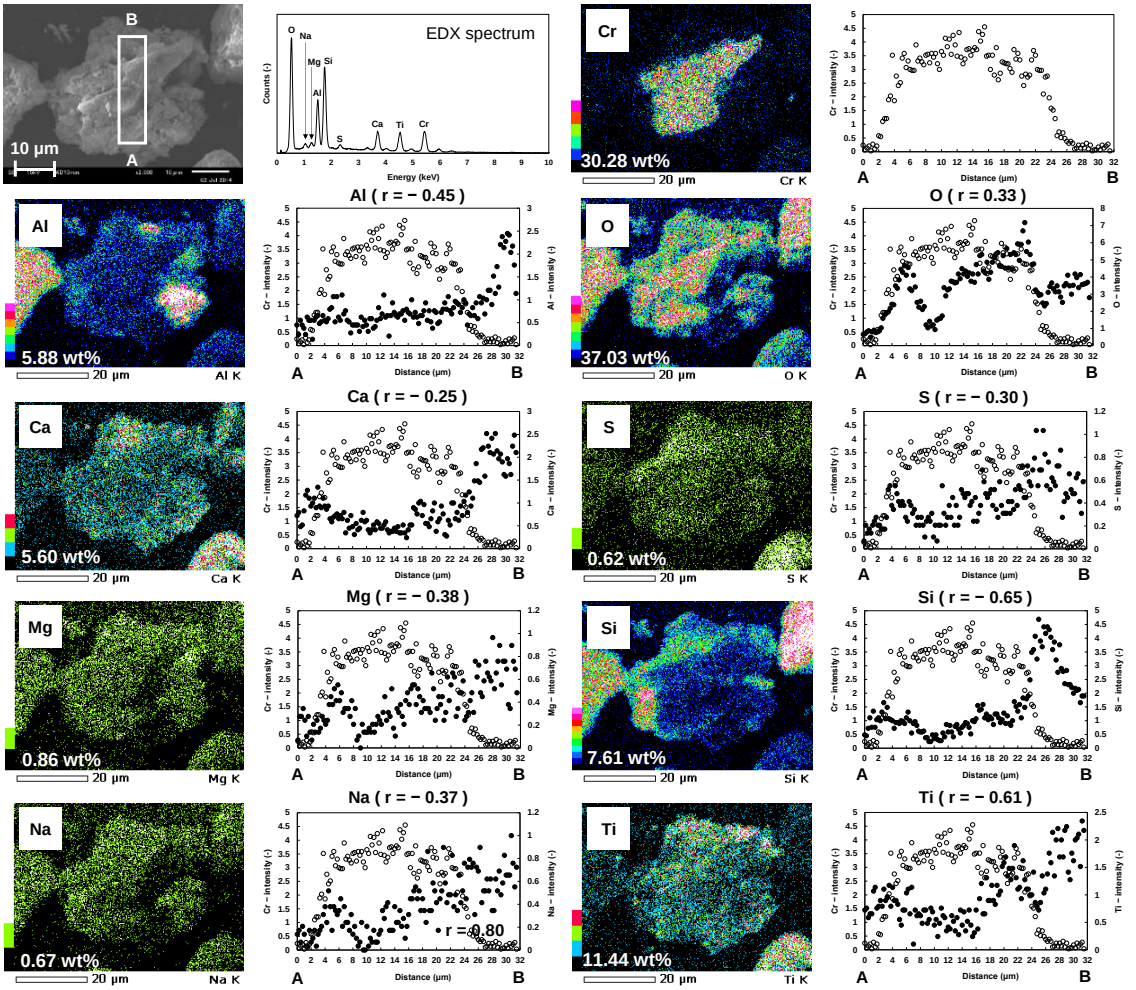

Fig. 5.7 Elemental distributions and micro-scale correlation analysis along point A to point B on Cr-rich particle (Cr_2O_3) in residues collected after JLT19 (r : correlation coefficient)

5.3.2.5 Manganese (Mn)

According to previous studies, possible Mn species are chloride and oxide form because their formation free energy are close at around incineration temperature according to thermodynamic analysis [67]. The study also concluded that most Mn exist as oxide form inside ash matrix because only 20% of Mn dissolved in dilute sulfuric acid. Chang et al. also reported that Mn is not easily dissolved in water because it is strongly bound to the ash matrix [64]. Furthermore, chemical forms of Mn were mainly fractionated to Fe-Mn oxide form by SCE [72,73]. Therefore, major Mn speciation is

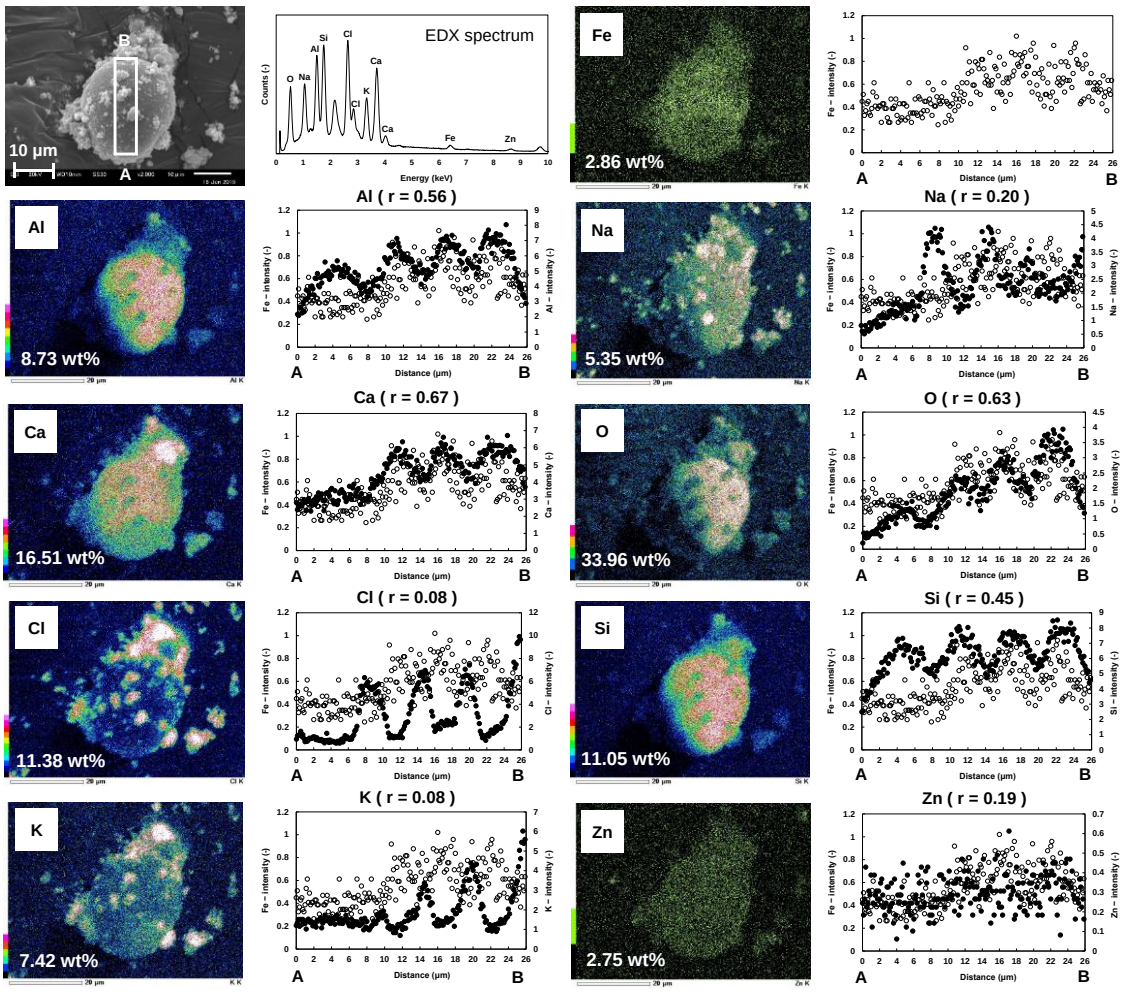

Fig. 5.8 Elemental distributions and micro-scale correlation analysis along point A to point B on Fe-rich particle (Fe oxides) in raw MSWI fly ash (r : correlation coefficient)

probably oxide form. As shown in Fig. 5.9, micro-scale correlation analysis showed that Mn had positive correlation with all constituent elements (Al, Ca, Cl, Mg, O, Si, and Zn). The Mn-rich particle was observed in residual materials collected after JLT46. Because Mn chlorides should be removed from the residues during JLT46 owing to the high solubility to water, high correlation with Cl is considered pseudo-positive. As a result, the Mn speciation is estimated to be Mn oxide (MnO) with Al/Ca/Si-based matrix. Mn leachability might be also controlled by not only MnO lechablity but also the leachability of Al/Ca/Si-based matrix around MnO.

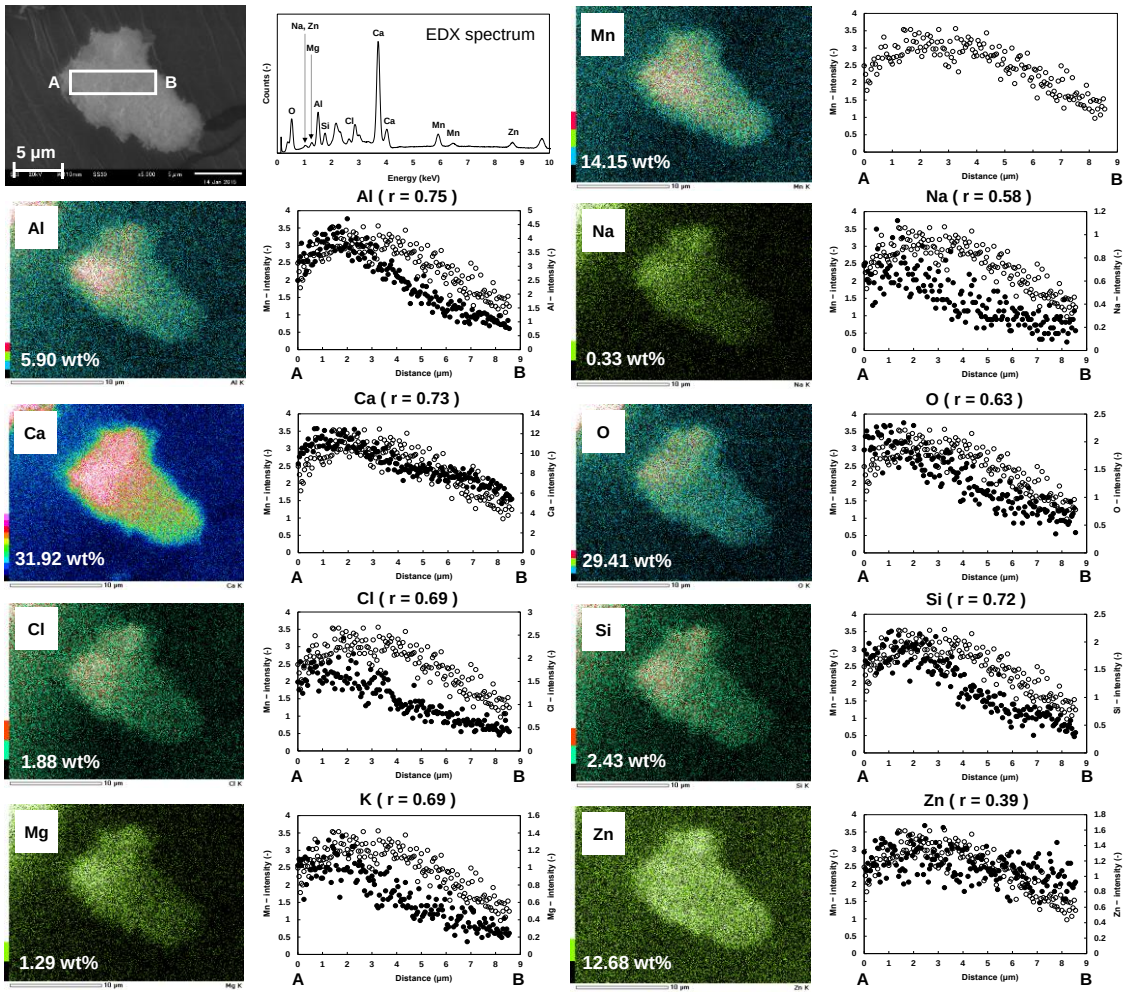

Fig. 5.9 Elemental distributions and micro-scale correlation analysis along point A to point B on Mn-rich particle (MnO) in residues collected after JLT46 (r : correlation coefficient)

5.3.2.6 Zinc (Zn)

According to previous studies, XRD analysis identified various Zn species such as K_2ZnCl_4 [52,74], $ZnAl_2O_4$ [40], $ZnCl_2$ [50], ZnO [13,53,72] , ZnS [52], and Zn_2SiO_4 [65]. XAS analysis also reported such Zn species in MSWI fly ash [14,21–25]. Furthermore, some studies reported that approximately 50% of Zn in MSWI fly ash are soluble forms [75–77], whereas 75% is residual fraction in another study [30]. Therefore, many Zn species and chemical forms have been reported by previous studies. According to thermodynamic analysis, formation of Zn chloride is preferred than Zn oxide because affinity between Zn and Cl increases with temperature [6,67]. However, Zn species also depend on flue gas components such as moisture, chlorine, sulfur, and inorganic particulate (Fe_2O_3, Al_2O_3, and CaO) [2]. Therefore, Zn might exist as various species in MSWI fly ash or major speciation is completely different in each MSWI fly ash sample.

In this study, micro-scale correlation analysis could estimate several Zn species. The first Zn species are $ZnCl_2$ or K_2ZnCl_4. As shown Fig. 5.10, Zn had positive correlation with Cl, K, and Na as well as negative correlation with Al, Ca, Mg, O, and Si. Therefore, the Zn speciation is estimated to be $ZnCl_2$ owing to correlation between Cl and Zn. Furthermore, K_2ZnCl_4 was also identified by XRD analysis in previous studies [52,74]. As shown in Table 2.1, contents of Cl and K in MSWI fly ash were relatively high. The high concentrated Cl and alkali metal in flue gas promote formation of Cl-metal complexes such as K_2ZnCl_4 [42]. Therefore, the Zn speciation is also estimated to be K_2ZnCl_4 owing to correlation among Cl, K, and Zn. Negative correlation with Al, Ca, Mg, O, and Si suggests that both $ZnCl_2$ and K_2ZnCl_4 are not trapped in Al/Ca/Si-based matrix but only adsorbed on the surface as the same with KCl/NaCl-based aggregates. The second Zn species are ZnO with Si-based matrix or Zn_2SiO_4. As shown Fig. A.3 (Supplementary material), Zn had positive correlation with Ca, O, and Si as well as

negative correlation with Cl, K, and Na. Therefore, the Zn speciation is estimated to be ZnO with Si-based matrix. As mentioned above, dominant Zn speciation is chloride form [6,67]. However, presence of moistures in MSW promote oxidization of Zn and reduce volatilization of Zn chlorides [4]. Zinc chlorides also react with CaO under presence of moisture to form ZnO as follows Eq (1) [25]. Furthermore, $ZnCl_2$ and ZnO react with SiO_2 at above 1073 K to form Zn_2SiO_4 as follows Eqs (2) and (3) [25]. Therefore, the Zn speciation is also estimated to be Zn_2SiO_4.

The third Zn species are spinels such as $ZnAl_2O_4$ and $ZnFe_2O_4$. They can be formed at

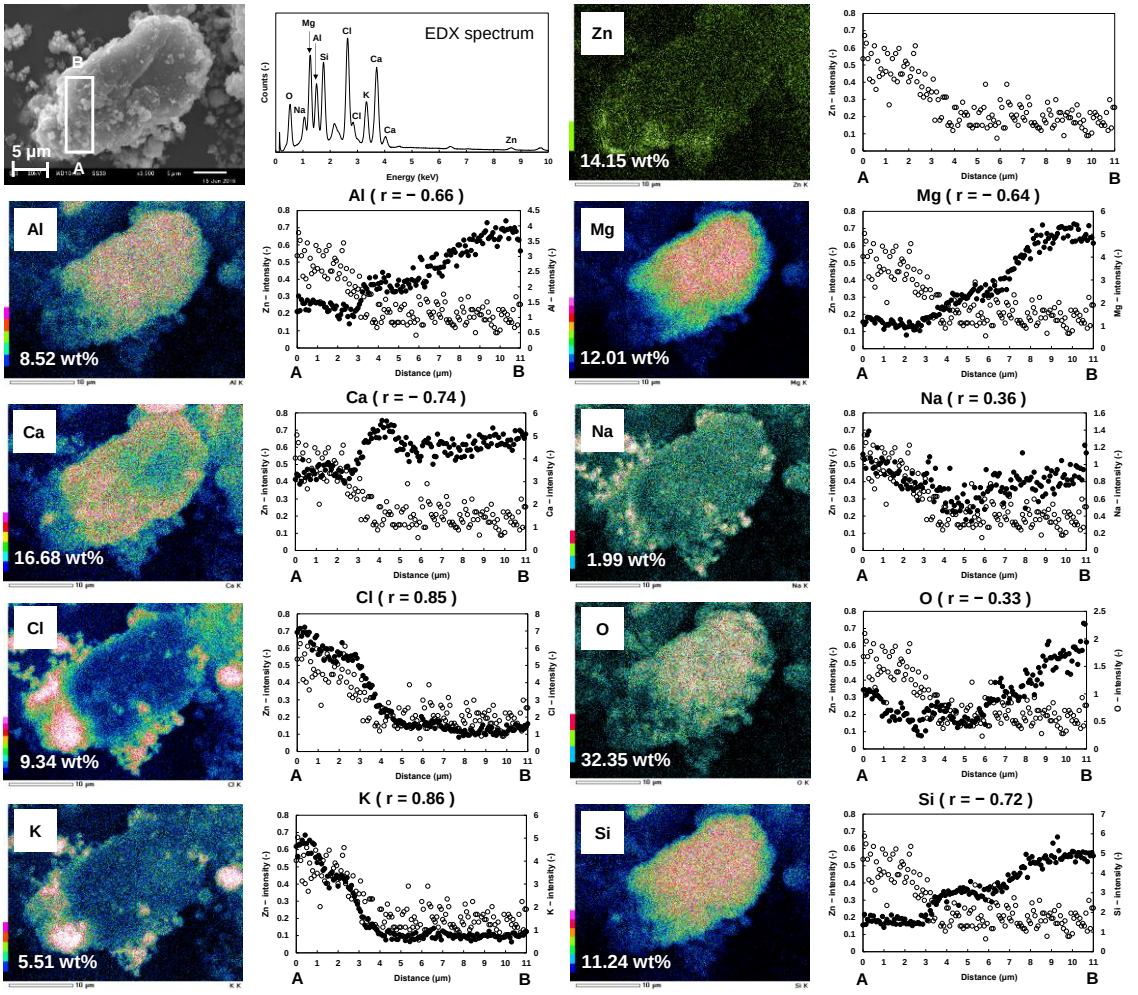

Fig. 5.10 Elemental distributions and micro-scale correlation analysis along point A to point B on Zn-rich particle ($ZnCl_2$ or K_2ZnCl_4) in raw MSWI fly ash (r : correlation coefficient)

1073K under presence of moisture and Al_2O_3 or Fe_2O_3 as follows Eqs (4) and (5) [2,25]. As shown in Fig. A.4 (Supplementary material), Zn had positive correlation with Al, Na, and O as well as negative correlation with Ca, Cl, K, and Si. Negative correlation with Ca and Si suggests that $ZnAl_2O_4$ are not trapped in Al/Ca/Si-based matrix but only adsorbed on the surface. In the case of another Zn-rich particle, Zn had positive correlation with Fe and O as well as negative correlation with Ca, Cl, K, and Na as shown in Fig. A.5 (Supplementary material). As a result, they are estimated to be $ZnFe_2O_4$ on the surface, not in trapped in Al/Ca/Si-based matrix as the same with $ZnAl_2O_4$. Zinc spinels have better resistance against acidic attack in comparison with Zn_2SiO_4 [78,79]. Therefore, formation of Zn spinels under presence of inorganic particulate (Al_2O_3 and Fe_2O_3) can reduce leachability of Zn in MSWI fly ash although they are on the surface not in Al/Ca/Si-based matrix.

$$2ZnCl_2 + CaO + H_2O \rightarrow 2ZnO + CaCl_2 + 2HCl \quad \cdots\cdots (1)$$

$$2ZnCl_2 + SiO_2 + 2H_2O \rightarrow Zn_2SiO_4 + 4HCl \quad \cdots\cdots (2)$$

$$2ZnO + SiO_2 \rightarrow Zn_2SiO_4 \quad \cdots\cdots (3)$$

$$ZnCl_2 + Al_2O_3 + H_2O \rightarrow ZnAl_2O_4 + 2HCl \quad \cdots\cdots (4)$$

$$ZnCl_2 + Fe_2O_3 + H_2O \rightarrow ZnFe_2O_4 + 2HCl \quad \cdots\cdots (5)$$

5.4. Conclusion

Micro-scale correlation analysis was applied to estimate metal species and their external matrix in MSWI fly ash. Estimated metal species are summarized in Table 5.2. Dominant metal species and their bonding states with fly ash matrix are different in each individual fly ash particle. For example, major Ti forms are perovskite ($CaTiO_3$) in some particles and rutile (TiO_2) in others. Micro-scale correlation analysis also suggests heavy

metal behaviors in fly ash formation processes. Metal oxides (Ti, Cu, Fe, Mn, and Zn) likely react with and/or are trapped in Al/Ca/Si-based matrix like aluminosilicate in the gas phase and then followed by KCl/NaCl adsorption on the surface. On the other hand, Cr oxide (Cr_2O_3) is not incorporated in Al/Ca/Si-based matrix. Zn can possibly form other species depending on combustion condition. Zn chlorides ($ZnCl_2$ and/or K_2ZnCl_4) and Zn spinels ($ZnAl_2O_4$ and $ZnFe_2O_4$) are not trapped in Al/Ca/Si-based matrix but adsorbed on the surface together with KCl/NaCl-based aggregates. Because metal oxides are basically incorporated in Al/Ca/Si-based matrix, metal leachability might be controlled by not only metal oxide leachability but also leachability of Al/Ca/Si-based matrix around metal oxides. Although micro-scale correlation analysis makes it possible to estimate dominant metal species and their external matrix regardless of crystalline or non-crystalline forms, this study also found one disadvantage of this method. It should be conducted at appropriate scale level to prevent from detecting pseudo-correlation. This method could estimate major external matrix around metals. It gives useful insights about metal

Table 5.2 Summary of possible metal species estimated by micro-scale correlation analysis

Heavy metals	Estimated metals species
Ti	Rutile (TiO_2), perovskite ($CaTiO_3$)
Cu	Copper oxides (Cu_2O, CuO), brass ($Cu_{0.6}Zn_{0.4}$)
Cr	Chromium oxide (Cr_2O_3)
Fe	Wüstite (FeO), hematite (Fe_2O_3), magnetite (Fe_3O_4)
Mn	Manganese oxide (MnO)
Zn	Zinc chlorides ($ZnCl_2$, K_2ZnCl_4), zinc oxide (ZnO) Willemite (Zn_2SiO_4), spinels ($ZnAl_2O_4$, $ZnFe_2O_4$)

leaching mechanisms in MSWI fly ash.

5.5 References

[1] H. Raclavská, A. Corsaro, S. Hartmann-Koval, D. Juchelková, Enrichment and distribution of 24 elements within the sub-sieve particle size distribution ranges of fly ash from wastes incinerator plants, J. Environ. Manage. 203 (2017) 1169–1177. doi:10.1016/j.jenvman.2017.03.073.

[2] F. Jiao, L. Zhang, W. Song, Y. Meng, N. Yamada, A. Sato, Y. Ninomiya, Effect of inorganic particulates on the condensation behavior of lead and zinc vapors upon flue gas cooling, Proc. Combust. Inst. 34 (2013) 2821–2829. doi:10.1016/j.proci.2012.07.062.

[3] Y. Zhang, Q. Li, J. Jia, A. Meng, Thermodynamic analysis on heavy metals partitioning impacted by moisture during the MSW incineration, Waste Manag. 32 (2012) 2278–2286. doi:10.1016/j.wasman.2012.07.007.

[4] Z. Youcai, S. Stucki, C. Ludwig, J. Wochele, Impact of moisture on volatility of heavy metals in municipal solid waste incinerated in a laboratory scale simulated incinerator, Waste Manag. 24 (2004) 581–587. doi:10.1016/j.wasman.2004.01.004.

[5] K.S. Wang, K.Y. Chiang, S.M. Lin, C.C. Tsai, C.J. Sun, Effects of chlorides on emissions of toxic compounds in waste incineration: Study on partitioning characteristics of heavy metal, Chemosphere. 38 (1999) 1833–1849. doi:10.1016/S0045-6535(98)00398-1.

[6] J.C. Chen, M.Y. Wey, J.L. Su, S.M. Hsieh, Two-stage simulation of the major heavy-metal species under various incineration conditions, Environ. Int. 24 (1998) 451–466. doi:10.1016/S0160-4120(98)00025-7.

[7] K. Chiang, K. Wang, F. Lin, W. Chu, Chloride effects on the speciation and partitioning of heavy metal during the municipal solid waste incineration process, Sci. Total Environ. 203 (1997) 129–140. doi:10.1016/S0048-9697(97)00140-X.

[8] S.K. Durlak, P. Biswas, J. Shi, Equilibrium analysis of the affect of temperature, moisture and sodium content on heavy metal emissions from municipal solid waste incinerators, J. Hazard. Mater. 56 (1997) 1–20. doi:10.1016/S0304-3894(97)00002-2.

[9] H. Sakanakura, Formation and durability of dithiocarbamic metals in stabilized air pollution control residue from municipal solid waste incineration and melting processes, Environ. Sci. Technol. 41 (2007) 1717–1722. doi:10.1021/es062077e.

[10] M. Li, S. Hu, J. Xiang, L.S. Sun, P.S. Li, S. Su, X.X. Sun, Characterization of fly ashes from two chinese municipal solid waste incinerators, Energy & Fuels. 17 (2003) 1487–1491. doi:10.1021/ef030092o.

[11] T. Mangialardi, A.E. Paolini, A. Polettini, P. Sirini, Optimization of the solidification/stabilization process of MSW fly ash in cementitious matrices, J. Hazard. Mater. 70 (1999) 53–70. doi:10.1016/S0304-3894(99)00132-6.

[12] M.C. Hsiao, H.P. Wang, Y.W. Yang, EXAFS and XANES studies of copper in a solidified fly ash, Environ. Sci. Technol. 35 (2001) 2532–2535. doi:10.1021/es001374v.

[13] M.C. Hsiao, H.P. Wang, Y.L. Wei, J.E. Chang, C.J. Jou, Speciation of copper in the incineration fly ash of a municipal solid waste, J. Hazard. Mater. 91 (2002) 301–307. doi:10.1016/S0304-3894(02)00015-8.

[14] R.P.W.J. Struis, C. Ludwig, H. Lutz, A.M. Scheidegger, Speciation of zinc in municipal solid waste incineration fly ash after heat treatment: An X-ray absorption spectroscopy study, Environ. Sci. Technol. 38 (2004) 3760–3767.

doi:10.1021/es0346126.

[15] R.P.W.J. Struis, M. Pasquali, L. Borgese, A. Gianoncelli, M. Gelfi, P. Colombi, D. Thiaudière, L.E. Depero, G. Rizzo, E. Bontempi, Inertisation of heavy metals in municipal solid waste incineration fly ash by means of colloidal silica – a synchrotron X-ray diffraction and absorption study, RSC Adv. 3 (2013) 14339–14351. doi:10.1039/c3ra41792a.

[16] M.C. Hsiao, H.P. Wang, J.E. Chang, C.Y. Peng, Tracking of copper species in incineration fly ashes, J. Hazard. Mater. 138 (2006) 539–542. doi:10.1016/j.jhazmat.2006.05.087.

[17] M. Takaoka, T. Yamamoto, A. Shiono, N. Takeda, K. Oshita, T. Matsumoto, T. Tanaka, The effect of copper speciation on the formation of chlorinated aromatics on real municipal solid waste incinerator fly ash, Chemosphere. 59 (2005) 1497–1505. doi:10.1016/j.chemosphere.2004.12.049.

[18] M.C. Hsiao, H.P. Wang, Y.J. Huang, Y.W. Yang, EXAFS study of copper in waste incineration fly ashes, J. Synchrotron Radiat. 8 (2001) 931. doi:10.1107/S0909049500020987.

[19] M. Takaoka, A. Shiono, K. Nishimura, T. Yamamoto, T. Uruga, N. Takeda, T. Tanaka, K. Oshita, T. Matsumoto, H. Harada, Dynamic change of copper in fly ash during de novo synthesis of dioxins, Environ. Sci. Technol. 39 (2005) 5878–5884. doi:10.1021/es048019f.

[20] S. Tian, M. Yu, W. Wang, Q. Wang, Z. Wu, Investigating the speciation of copper in secondary fly ash by X-ray absorption spectroscopy, Environ. Sci. Technol. 43 (2009) 9084–9088. doi:10.1021/es902039x.

[21] T. Fujimori, Y. Tanino, M. Takaoka, Coexistence of Cu, Fe, Pb, and Zn oxides and chlorides as a determinant of chlorinated aromatics generation in municipal solid

waste incinerator fly ash, Environ. Sci. Technol. 48 (2014) 85–92. doi:10.1021/es403585h.

[22] M. Takaoka, T. Yamamoto, T. Tanaka, N. Takeda, K. Oshita, T. Uruga, Direct speciation of lead, zinc and antimony in fly ash from waste treatment facilities by XAFS spectroscopy, Phys. Scr. T115 (2005) 943–945. doi:10.1238/Physica.Topical.115a00943.

[23] M. Yu, S. Tian, W. Chu, D. Chen, Q. Wang, Z. Wu, Speciation of zinc in secondary fly ashes of municipal solid waste at high temperatures, J. Synchrotron Radiat. 16 (2009) 528–532. doi:10.1107/S0909049509020032.

[24] T. Fujimori, Y. Tanino, M. Takaoka, Role of zinc in MSW fly ash during formation of chlorinated aromatics, Environ. Sci. Technol. 45 (2011) 7678–7684. doi:10.1021/es201810u.

[25] X. Cai, Q. Huang, M. Alhadj-Mallah, Y. Chi, J. Yan, Characterization of zinc vapor condensation in fly ash particles using synchrotron X-ray absorption spectroscopy, J. Zhejiang Univ. Sci. A. 16 (2015) 70–80. doi:10.1631/jzus.A1400178.

[26] A. Funatsuki, M. Takaoka, K. Oshita, N. Takeda, Methods of determining lead speciation in fly ash by X-ray absorption fine-structure spectroscopy and a sequential extraction procedure, Anal. Sci. 28 (2012) 481–490. doi:10.2116/analsci.28.481.

[27] K. Shiota, T. Nakamura, M. Takaoka, K. Nitta, K. Oshita, T. Fujimori, T. Ina, Chemical kinetics of Cs species in an alkali-activated municipal solid waste incineration fly ash and pyrophyllite-based system using Cs K-edge in situ X-ray absorption fine structure analysis, Spectrochim. Acta Part B At. Spectrosc. 131 (2017) 32–39. doi:10.1016/j.sab.2017.03.003.

[28] H. Yamamoto, M. Nagoshi, T. Yokoyama, M. Takaoka, N. Takeda, The chemical states of virgin and kneaded ash with chelating agent, Environ. Eng. Res. 43 (2006) 271–277. doi:10.11532/proes1992.43.271.

[29] A. Tessier, P.G.C. Campbell, M. Bisson, Sequential Extraction Procedure for the Speciation of Particulate Trace Metals, Anal. Chem. 51 (1979) 844–851. doi:10.1021/ac50043a017.

[30] F.H. Wang, F. Zhang, Y.J. Chen, J. Gao, B. Zhao, A comparative study on the heavy metal solidification/stabilization performance of four chemical solidifying agents in municipal solid waste incineration fly ash, J. Hazard. Mater. 300 (2015) 451–458. doi:10.1016/j.jhazmat.2015.07.037.

[31] B. Zhang, W. Zhou, H. Zhao, Z. Tian, F. Li, Y. Wu, Stabilization/solidification of lead in MSWI fly ash with mercapto functionalized dendrimer Chelator, Waste Manag. 50 (2016) 105–112. doi:10.1016/j.wasman.2016.02.001.

[32] H. Zhang, Y. Zhao, J. Qi, Characterization of heavy metals in fly ash from municipal solid waste incinerators in Shanghai, Process Saf. Environ. Prot. 88 (2010) 114–124. doi:10.1016/j.psep.2010.01.001.

[33] Y. Zhang, B. Cetin, W.J. Likos, T.B. Edil, Impacts of pH on leaching potential of elements from MSW incineration fly ash, Fuel. 184 (2016) 815–825. doi:10.1016/j.fuel.2016.07.089.

[34] P. Van Herck, B. Van Der Bruggen, G. Vogels, C. Vandecasteele, Application of computer modelling to predict the leaching behaviour of heavy metals from MSWI fly ash and comparison with a sequential extraction method, Waste Manag. 20 (2000) 203–210. doi:10.1016/S0956-053X(99)00321-9.

[35] Y. Zhang, J. Jiang, M. Chen, MINTEQ modeling for evaluating the leaching behavior of heavy metals in MSWI fly ash, J. Environ. Sci. 20 (2008) 1398–1402.

doi:10.1016/S1001-0742(08)62239-1.

[36] J. Hyks, T. Astrup, T.H. Christensen, Long-term leaching from MSWI air-pollution-control residues: Leaching characterization and modeling, J. Hazard. Mater. 162 (2009) 80–91. doi:10.1016/j.jhazmat.2008.05.011.

[37] T. Astrup, J.J. Dijkstra, R.N.J. Comans, H.A. Van Der Sloot, T.H. Christensen, Geochemical modeling of leaching from MSWI air-pollution-control residues, Environ. Sci. Technol. 40 (2006) 3551–3557. doi:10.1021/es052250r.

[38] S. Gilardoni, P. Fermo, F. Cariati, V. Gianelle, D. Pitea, E. Collina, M. Lasagni, MSWI fly ash particle analysis by scanning electron microscopy-energy dispersive X-ray spectroscopy., Environ. Sci. Technol. 38 (2004) 6669–6675. doi:10.1021/es0494961.

[39] K. Karlfeldt Fedje, S. Rauch, P. Cho, B.M. Steenari, Element associations in ash from waste combustion in fluidized bed, Waste Manag. 30 (2010) 1273–1279. doi:10.1016/j.wasman.2009.09.012.

[40] A. Bogush, J.A. Stegemann, I. Wood, A. Roy, Element composition and mineralogical characterisation of air pollution control residue from UK energy-from-waste facilities, Waste Manag. 36 (2015) 119–129. doi:10.1016/j.wasman.2014.11.017.

[41] J. Zhou, S. Wu, Y. Pan, L. Zhang, Z. Cao, X. Zhang, S. Yonemochi, S. Hosono, Y. Wang, K. Oh, G. Qian, Enrichment of heavy metals in fine particles of municipal solid waste incinerator (MSWI) fly ash and associated health risk, Waste Manag. 43 (2015) 239–246. doi:10.1016/j.wasman.2015.06.026.

[42] G. Weibel, U. Eggenberger, S. Schlumberger, U.K. Mäder, Chemical associations and mobilization of heavy metals in fly ash from municipal solid waste incineration, Waste Manag. 62 (2016) 147–159. doi:10.1016/j.wasman.2016.12.004.

[43] A. Menard, D. Drobne, A. Jemec, Ecotoxicity of nanosized TiO_2. Review of in vivo data, Environ. Pollut. 159 (2011) 677–684. doi:10.1016/j.envpol.2010.11.027.

[44] T. Morishige, Y. Yoshioka, A. Tanabe, X. Yao, S. ichi Tsunoda, Y. Tsutsumi, Y. Mukai, N. Okada, S. Nakagawa, Titanium dioxide induces different levels of IL-1β production dependent on its particle characteristics through caspase-1 activation mediated by reactive oxygen species and cathepsin B, Biochem. Biophys. Res. Commun. 392 (2010) 160–165. doi:10.1016/j.bbrc.2009.12.178.

[45] B. Jovanović, Critical review of public health regulations of titanium dioxide, a human food additive, Integr. Environ. Assess. Manag. 11 (2015) 10–20. doi:10.1002/ieam.1571.

[46] R.J.B. Peters, G. Van Bemmel, Z. Herrera-Rivera, H.P.F.G. Helsper, H.J.P. Marvin, S. Weigel, P.C. Tromp, A.G. Oomen, A.G. Rietveld, H. Bouwmeester, Characterization of titanium dioxide nanoparticles in food products: Analytical methods to define nanoparticles, J. Agric. Food Chem. 62 (2014) 6285–6293. doi:10.1021/jf5011885.

[47] A.K. Tripathi, M.K. Singh, M.C. Mathpal, S.K. Mishra, A. Agarwal, Study of structural transformation in TiO_2 nanoparticles and its optical properties, J. Alloys Compd. 549 (2013) 114–120. doi:10.1016/j.jallcom.2012.09.012.

[48] D.M. Mitrano, S. Motellier, S. Clavaguera, B. Nowack, Review of nanomaterial aging and transformations through the life cycle of nano-enhanced products, Environ. Int. 77 (2015) 132–147. doi:10.1016/j.envint.2015.01.013.

[49] M. Dulger, T. Sakallioglu, I. Temizel, B. Demirel, N.K. Copty, T.T. Onay, C.S. Uyguner-Demirel, T. Karanfil, Leaching potential of nano-scale titanium dioxide in fresh municipal solid waste, Chemosphere. 144 (2016) 1567–1572. doi:10.1016/j.chemosphere.2015.10.037.

[50] L. Le Forestier, G. Libourel, Characterization of Flue Gas Residues from Municipal Solid Waste Combustors, Environ. Sci. Technol. 32 (1998) 2250–2256. doi:10.1021/es980100t.

[51] C.S. Kirby, J.D. Rimstidt, Mineralogy and surface properties of municipal solid waste ash, Environ. Sci. Technol. 27 (1993) 652–660. doi:10.1021/es00001a601.

[52] A.P. Bayuseno, W.W. Schmahl, Characterization of MSWI fly ash through mineralogy and water extraction, Resour. Conserv. Recycl. 55 (2011) 524–534. doi:10.1016/j.resconrec.2011.01.002.

[53] P. Ubbrìaco, P. Bruno, A. Traini, D. Calabrese, Fly ash reactivity: Formation of hydrate phases, J. Therm. Anal. Calorim. 66 (2001) 293–305. doi:10.1023/A:1012468505722.

[54] F. Jiao, L. Zhang, Z. Dong, T. Namioka, N. Yamada, Y. Ninomiya, Study on the species of heavy metals in MSW incineration fly ash and their leaching behavior, Fuel Process. Technol. 152 (2016) 108–115. doi:10.1016/j.fuproc.2016.06.013.

[55] L. Roes, M.K. Patel, E. Worrell, C. Ludwig, Preliminary evaluation of risks related to waste incineration of polymer nanocomposites, Sci. Total Environ. 417–418 (2012) 76–86. doi:10.1016/j.scitotenv.2011.12.030.

[56] A. Massari, M. Beggio, S. Hreglich, R. Marin, S. Zuin, Behavior of TiO_2 nanoparticles during incineration of solid paint waste: A lab-scale test, Waste Manag. 34 (2014) 1897–1907. doi:10.1016/j.wasman.2014.05.015.

[57] H. Kitamura, T. Sawada, T. Shimaoka, F. Takahashi, Geochemically structural characteristics of municipal solid waste incineration fly ash particles and mineralogical surface conversions by chelate treatment, Environ. Sci. Pollut. Res. 23 (2016) 734–743. doi:10.1007/s11356-015-5229-5.

[58] M.J. Quina, R.C. Santos, J.C. Bordado, R.M. Quinta-Ferreira, Characterization of

air pollution control residues produced in a municipal solid waste incinerator in Portugal, J. Hazard. Mater. 152 (2008) 853–869. doi:10.1016/j.jhazmat.2007.07.055.

[59] N.C. Mueller, J. Buha, J. Wang, A. Ulrich, B. Nowack, Modeling the flows of engineered nanomaterials during waste handling, Environ. Sci. Process. Impacts. 15 (2012) 251–259. doi:10.1039/C2EM30761H.

[60] H. Shi, R. Magaye, V. Castranova, J. Zhao, Titanium dioxide nanoparticles: a review of current toxicological data, Part. Fibre Toxicol. 10 (2013) 1–33. doi:10.1186/1743-8977-10-15.

[61] D.H. Klein, A.W. Andren, J.A. Carter, J.F. Emery, C. Feldman, W. Fulkerson, W.S. Lyon, J.C. Ogle, Y. Talmi, R.I. Van Hook, N. Bolton, Pathways of Thirty-seven Trace Elements Through Coal-Fired Power Plant, Environ. Sci. Technol. 9 (1975) 973–979. doi:10.1021/es60108a007.

[62] Z. Tian, B. Zhang, C. He, R. Tang, H. Zhao, F. Li, The physiochemical properties and heavy metal pollution of fly ash from municipal solid waste incineration, Process Saf. Environ. Prot. 98 (2015) 333–341. doi:10.1016/j.psep.2015.09.007.

[63] Y. Xiong, F. Zhu, L. Zhao, H. Jiang, Z. Zhang, Heavy metal speciation in various types of fly ash from municipal solid waste incinerator, J. Mater. Cycles Waste Manag. 16 (2014) 608–615. doi:10.1007/s10163-014-0274-6.

[64] C.Y. Chang, C.F. Wang, D.T. Mui, H.L. Chiang, Application of methods (sequential extraction procedures and high-pressure digestion method) to fly ash particles to determine the element constituents: A case study for BCR 176, J. Hazard. Mater. 163 (2009) 578–587. doi:10.1016/j.jhazmat.2008.07.039.

[65] P.J. He, H. Zhang, C.G. Zhang, D.J. Lee, Characteristics of air pollution control residues of MSW incineration plant in Shanghai, J. Hazard. Mater. 116 (2004)

229–237. doi:10.1016/j.jhazmat.2004.09.009.

[66] F. Liu, Hj. Liu, Q. Yu, Y. Nie, Chemical speciation and mobility of heavy metals in municipal solid waste incinerator fly ash, J. Environ. Sci. 16 (2004) 885–888.

[67] M.A. Fernandez, L. Martinez, M. Segarra, J.C. Garcia, F. Espiell, Behavior of heavy metals in the combustion gases of urban waste incinerators, Environ. Sci. Technol. 26 (1992) 1040–1047. doi:10.1021/es00029a026.

[68] C.H. Jung, T. Matsuto, N. Tanaka, T. Okada, Metal distribution in incineration residues of municipal solid waste (MSW) in Japan, Waste Manag. 24 (2004) 381–391. doi:10.1016/S0956-053X(03)00137-5.

[69] H. Belevi, H. Moench, Factors determining the element behavior in municipal solid waste incinerators. 1. Field studies, Environ. Sci. Technol. 34 (2000) 2501–2506. doi:10.1021/es991078m.

[70] Y. Wei, T. Shimaoka, A. Saffarzadeh, F. Takahashi, Alteration of municipal solid waste incineration bottom ash focusing on the evolution of iron-rich constituents, Waste Manag. 31 (2011) 1992–2000. doi:10.1016/j.wasman.2011.04.021.

[71] P. Piantone, F. Bodenan, L. Chatelet-Snidaro, Mineralogical study of secondary mineral phases from weathered MSWI bottom ash: Implications for the modelling and trapping of heavy metals, Appl. Geochemistry. 19 (2004) 1891–1904. doi:10.1016/j.apgeochem.2004.05.006.

[72] J. Jiang, M. Chen, Y. Zhang, X. Xu, Pb stabilization in fresh fly ash from municipal solid waste incinerator using accelerated carbonation technology, J. Hazard. Mater. 161 (2009) 1046–1051. doi:10.1016/j.jhazmat.2008.04.051.

[73] S.J. Huang, C.Y. Chang, D.T. Mui, F.C. Chang, M.Y. Lee, C.F. Wang, Sequential extraction for evaluating the leaching behavior of selected elements in municipal solid waste incineration fly ash, J. Hazard. Mater. 149 (2007) 180–188.

doi:10.1016/j.jhazmat.2007.03.067.

[74] Y. Yang, Y. Xiao, N. Wilson, J.H.L. Voncken, Thermal behaviour of ESP ash from municipal solid waste incinerators, J. Hazard. Mater. 166 (2009) 567–575. doi:10.1016/j.jhazmat.2008.11.086.

[75] K. Polyak, J. Hlavay, Chemical fractionation of a fly ash sample by a sequential leaching method, Anal. Bioanal. Chem. 371 (2001) 838–842. doi:10.1007/s00216-001-1094-9.

[76] X. Wan, W. Wang, T. Ye, Y. Guo, X. Gao, A study on the chemical and mineralogical characterization of MSWI fly ash using a sequential extraction procedure, J. Hazard. Mater. 134 (2006) 197–201. doi:10.1016/j.jhazmat.2005.10.048.

[77] S. Wu, Y. Xu, J. Sun, Z. Cao, J. Zhou, Y. Pan, G. Qian, Inhibiting evaporation of heavy metal by controlling its chemical speciation in MSWI fly ash, Fuel. 158 (2015) 764–769. doi:10.1016/j.fuel.2015.06.003.

[78] K. Shih, Y. Tang, Incorporating simulated zinc ash by kaolinite- and sludge-based ceramics: Phase transformation and product leachability, Chinese J. Chem. Eng. 20 (2012) 411–416. doi:10.1016/S1004-9541(11)60147-X.

[79] M. Li, P. Su, Y. Guo, W. Zhang, L. Mao, Effects of SiO_2, Al_2O_3 and Fe_2O_3 on leachability of Zn, Cu and Cr in ceramics incorporated with electroplating sludge, J. Environ. Chem. Eng. 5 (2017) 3143–3150. doi:10.1016/j.jece.2017.06.019.

5.6 Supplementary material

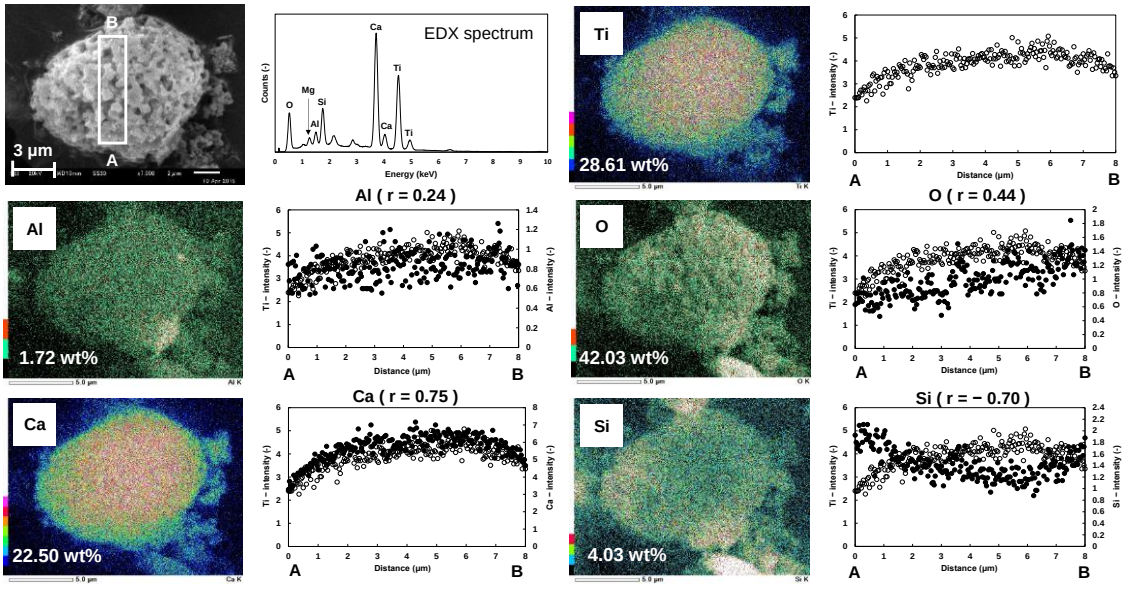

Fig. A.1 Elemental distributions and micro-scale correlation analysis along point A to point B on Ti-rich particle (perovskite) in residues collected after JLT19 (r = correlation coefficient)

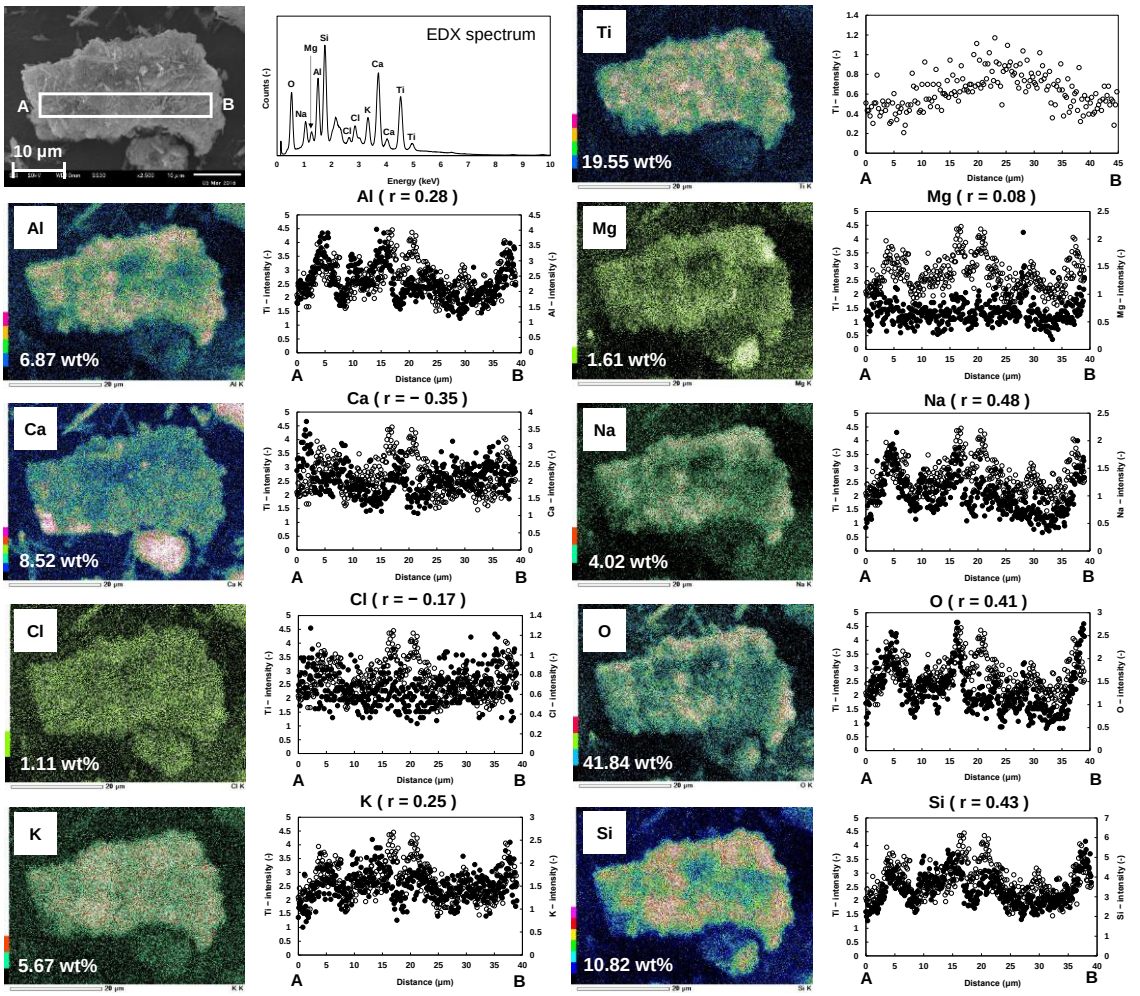

Fig. A.2 Elemental distributions and micro-scale correlation analysis along point A to point B on Ti-rich particle (rutile) in residues collected after JLT46 (r = correlation coefficient)

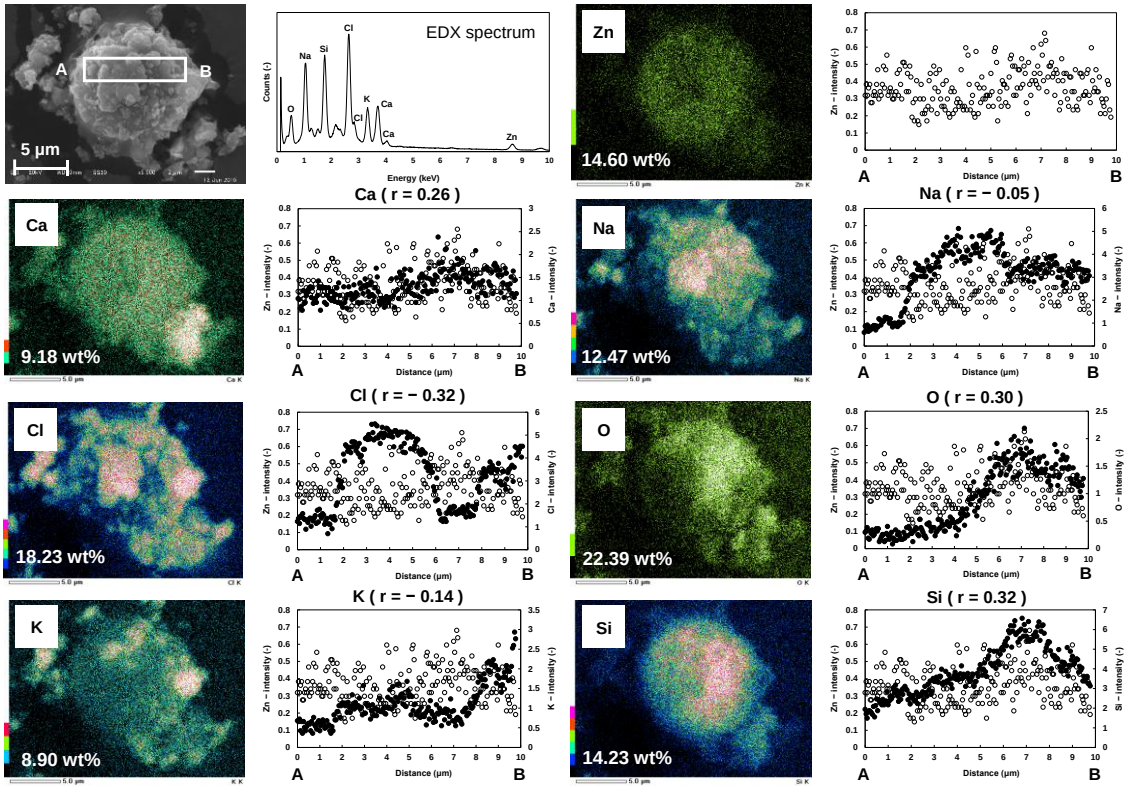

Fig. A.3 Elemental distributions and micro-scale correlation analysis along point A to point B on Zn-rich particle (ZnO or Zn_2SiO_4) in raw MSWI fly ash (r : correlation coefficient)

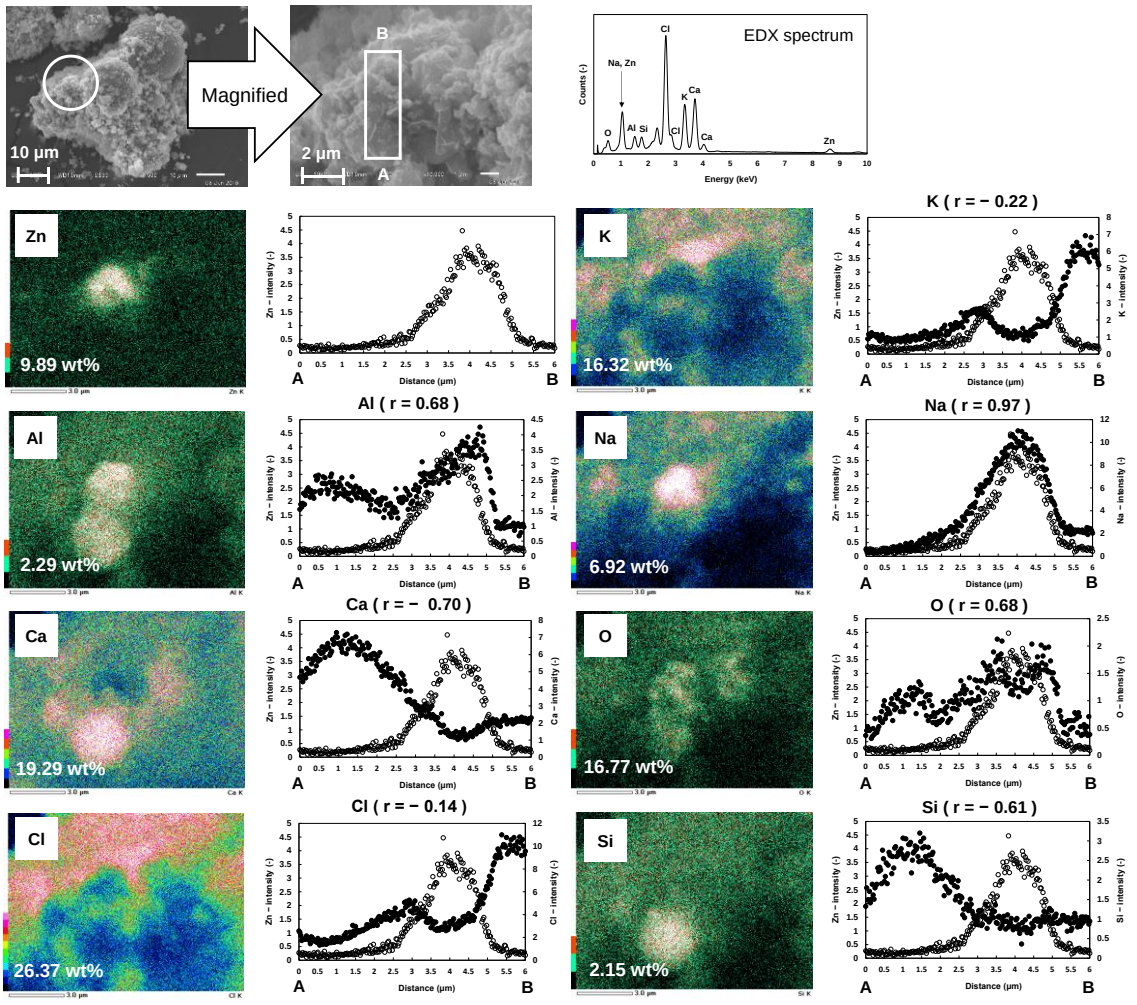

Fig. A.4 Elemental distributions and micro-scale correlation analysis along point A to point B on Zn-rich part ($ZnAl_2O_4$) on raw MSWI fly ash particle (r : correlation coefficient)

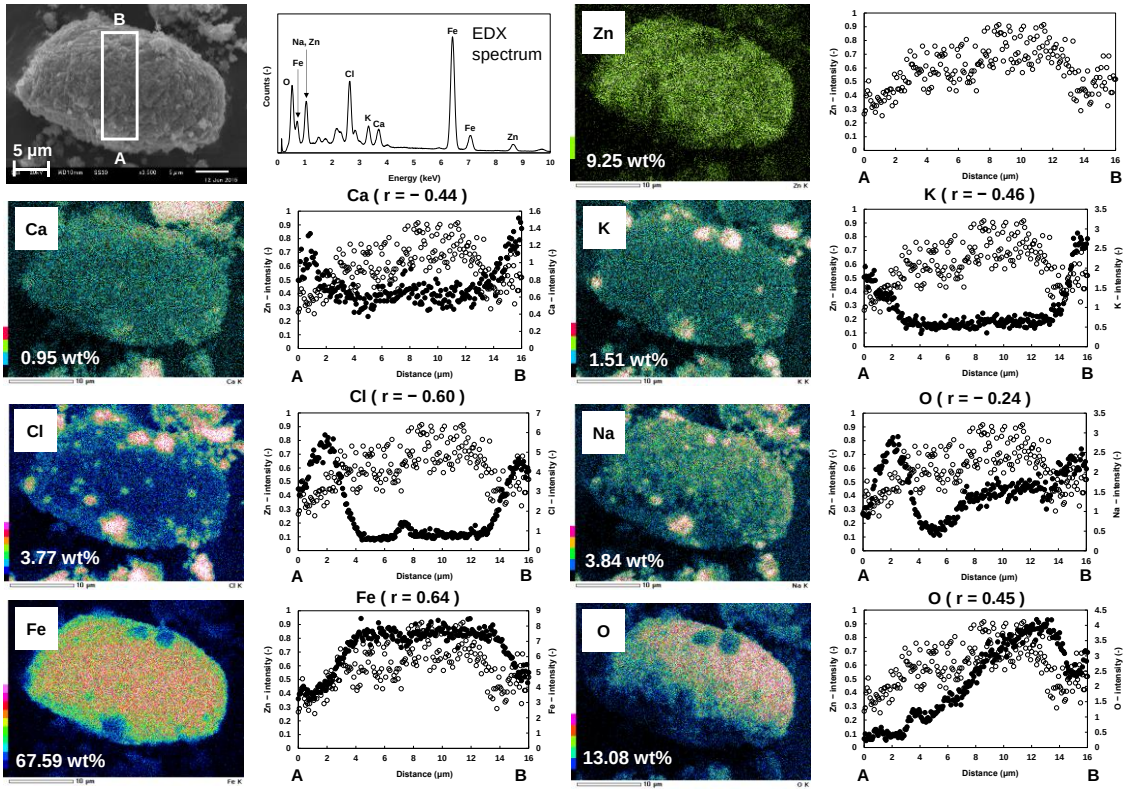

Fig. A.5 Elemental distributions and micro-scale correlation analysis along point A to point B on Zn-rich particle ($ZnFe_2O_4$) in raw MSWI fly ash (r : correlation coefficient)

CHAPTER

6

INTRA- AND INTER-PARTICLE HETEROGENEITY OF MSWI FLY ASH PARTICLES

Abstract: In this chapter, 2 types of elemental heterogeneities of MSWI fly ash particle were measured focusing on three structural components of fly ash particles. These results suggested that MSWI fly ash particles have both internal heterogeneities inside their bodies and also are heterogeneous in inter-particle level.

6.1 Introduction

MSWI fly ash consists of crystalline and non-crystalline phases (e.g. poor crystalline, amorphous, glassy phases). XRD analysis showed that crystalline phases of MSWI fly ash consist of complex minerals [1–6]. Furthermore, a high content of non-crystalline phases (approximately 33 to 72 %) were found in MSWI fly ash [7–14]. For these reasons, XRD cannot identify compositions of MSWI fly ash in some cases.

Microscopic observation equipped with elemental analyzer is applied for single-particle characterization of MSWI fly ash particles [15,16]. The main advantage of this technique is that crystalline and non-crystalline matrices of MSWI fly ash particles can be analyzed simultaneously. Microscopic observation and elemental analysis showed that individual MSWI fly ash particles consist of a few and/or several compositions [5,6,16,17]. According to these studies, Mahieux et al. reported that MSWI fly ash particles are heterogeneous [17] while Rémond et al. reported that individual particles are homogeneous although their mineral compositions are quite heterogeneous [5,6]. As described in Chapter 2 and 3, MSWI fly ash particles have specific geochemical structure. They likely consist of Si-based insoluble core structure, Al/Ca/Si-based matrices inside the body, and soluble KCl/NaCl-based aggregates on the surface. Furthermore, morphological characteristics of MSWI fly ash particles changed dramatically owing to secondary mineral formation during chelate treatment process. Therefore, the surface and inner matrices of MSWI fly ash particles seem to be greatly heterogeneous at micro-scale level.

Because the heterogeneity of MSWI fly ash has not been measured quantitatively, elemental heterogeneity of MSWI fly ash particles were quantitatively investigated focusing on geochemical structures in this chapter. Two types of elemental heterogeneities would be reported. The first type is internal heterogeneities of individual

MSWI fly ash particles. They are inner heterogeneities within body components of each MSWI fly ash particle; surface, semi-soluble Al/Ca/Si-based matrix, and insoluble inner core. The other type is inter-particle heterogeneities among MSWI fly ash particles. Heterogeneity analysis also focused on each body component of MSWI fly ash particles (surfaces, Al/Ca/Si-based matrices, and insoluble inner cores). In this analysis, SEM-EDX was applied for the heterogeneity analysis.

6.2 Materials ane method

6.2.1 Experimental samples

Raw and chelate-treated MSWI fly ash were used for elemental heterogeneity analysis. In this chapter, internal heterogeneity of individual MSWI fly ash particles are called intra-particle heterogeneity. Raw MSWI fly ash samples were used only for intra-particle and inter-particle heterogeneities of the surface. Because wet conditions during chelate treatment changed morphological characteristics of fly ash particle surfaces owing to secondary mineral formation, raw MSWI fly ash were also analyzed to investigate the impact of wet condition on surface heterogeneity. Residual materials of chelate-treated MSWI fly ash collected after JLT46, TCLP, and JLT19 were also used for elemental heterogeneity analysis of Al/Ca/Si-based matrices and insoluble inner cores. In this chapter, 100 particles for each experimental sample were analyzed by SEM-EDX.

6.2.2 Intra-particle and inter-particle heterogeneity analysis

Intra-particle heterogeneity analysis aims to measure heterogeneity of individual fly ash particles. After elemental mapping of individual MSWI fly ash particle/residual material particle, the measured particle was divided into 5 sections horizontally (see Fig.

6.1-A). Line profile analysis was conducted at each section in order to measure variations of constituent element concentrations along the horizontal side of each section. After the line profile analysis of all sections, coefficient of variation (CV value) was calculated for each element. In this analysis, weighted average of CV values was used as a quantitative indicator of the intra-particle heterogeneity. In this analysis, inter-particle heterogeneity was also investigated. This analysis aims to measure heterogeneity among fly ash particles. At first, average elemental concentrations of each sample as weight percent [wt%] were measured using elemental mapping data (see Fig. 6.1-B). For each particle sample, the average data of each elemental concentration was calculated. The weight percent data were plotted in histogram in order to visualize inter-particle heterogeneity quantitatively. CV values of element concentrations were used as a quantitative indicator of inter-particle heterogeneity of MSWI fly ash particles.

6.3 Results and discussion

6.3.1 Intra-particle heterogeneity of MSWI fly ash particle surface

The CV values of major elements in raw and chelate-treated MSWI fly ash particles

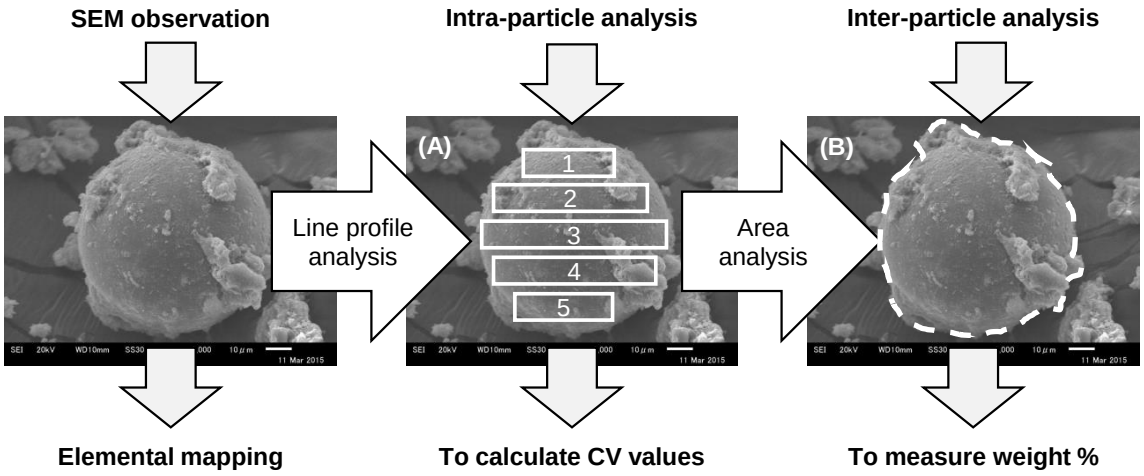

Fig. 6.1 Example of analysis area for line profile analysis and area analysis. (A) Inter-particle heterogeneity analysis (B) Inter-particle heterogeneity analysis

are shown in Fig. 6.2. In the case of Al, Ca, and Si, their CV values of both raw and chelate-treated MSWI fly ash particles were almost in the range of 0 to 1.0. Especially, CV values of Ca were much lower than those of other elements in both MSWI fly ash

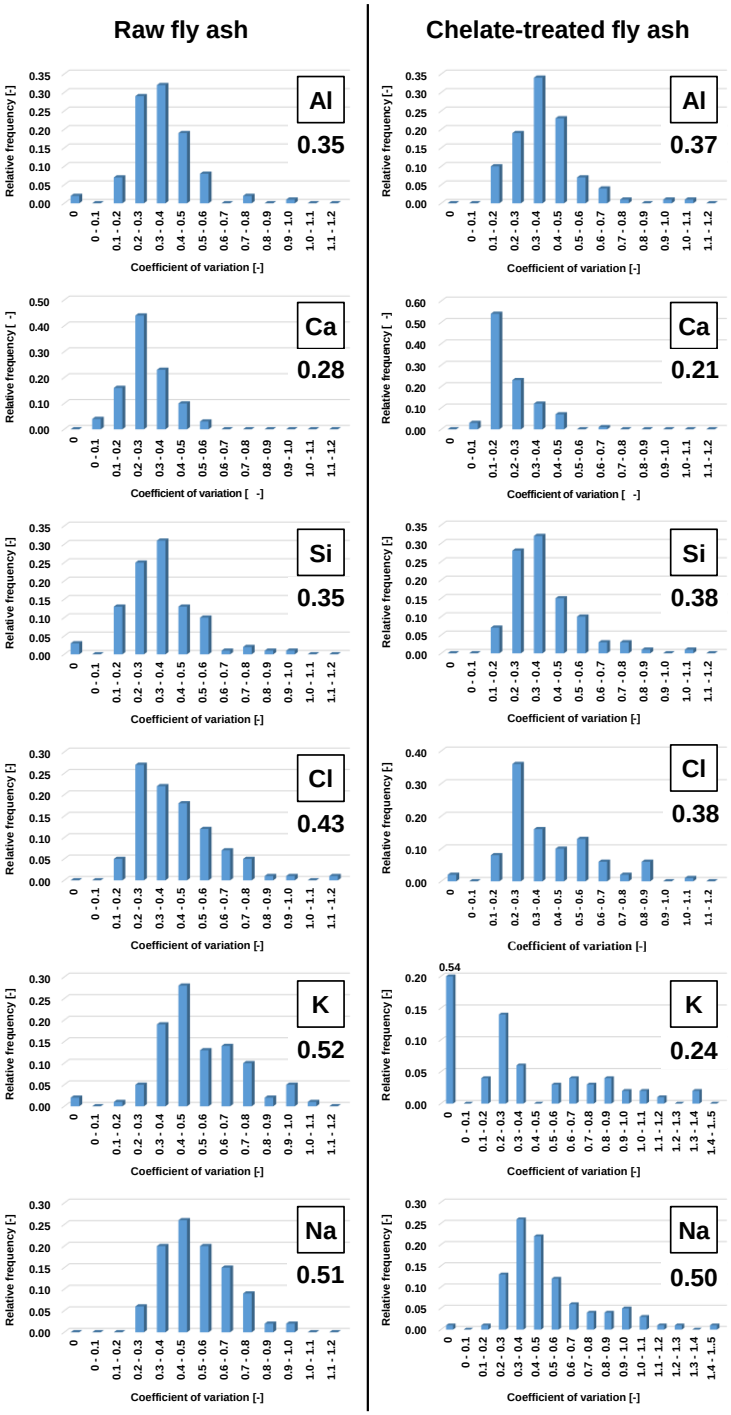

Fig. 6.2 CV values of major elements in raw and chelate-treated MSWI fly ash particles (Values shown in each figure are weighted average CV values of each element)

particles. As mentioned in subsection 2.2.1, acidic gas neutralization is conducted by $Ca(OH)_2$ slurry injection. The neutralization reaction between $Ca(OH)_2$ and HCl generates $CaCl_2$ and some of unreacted $Ca(OH)_2$ remains. Therefore, detected Ca on the surface of MSWI fly ash particles seem to be derived from $CaCl_2$, $Ca(OH)_2$ and/or exposed surface of semi-soluble Al/Ca/Si-based matrices. The lowest Ca heterogeneity among major elements implies that a major form of surface Ca is unreacted $Ca(OH)_2$ and/or semi-soluble Al/Ca/Si-based matrices if Ca-containing materials are major in Al/Ca/Si-based matrices. It would be discussed again in next subsection. In the case of Cl, K, and Na, the CV values of both MSWI fly ash particles were almost in the range of 0 to 1.5, which is wider than Al, Ca, and Si. Their weighted average CV values were 0-82% higher than those of Al, Ca, and Si except for K of chelate-treated MSWI fly ash particles. As mentioned in Chapter 2 and 3, soluble KCl/NaCl-based aggregates attach on the surface of MSWI fly ash particles. Because KCl/NaCl-based aggregates generates hotspots of Cl/K/Na on the surface, it increases intra-particle heterogeneity of Cl, K, and Na on the surface.

In order to investigate the impact of moistening condition during chelate treatment on intra-particle heterogeneity exactly, the surface of the same raw MSWI fly ash particle was monitored before and after the moistening treatment (see Fig. 6.3). SEM-EDX analysis showed that Cl, K, and Na were locally concentrated in inner edge of the particle surface before the moistening treatment (see Fig. 6.3-A1). The CV values of Cl, K, and Na were 0.40, 0.64, and 0.52, respectively (see Fig. 6.4-A). After the moistening treatment, they were dissolved and distributed on the whole surface (see Fig. 6.3-A2). As a result, CV values of Cl, K, and Na decreased to 0.32, 0.36, and 0.50, respectively (see Fig. 6.4-A). CV value of Ca also decreased after the moistening treatment. This means

that these elements became less heterogeneous on the surface by dissolution and

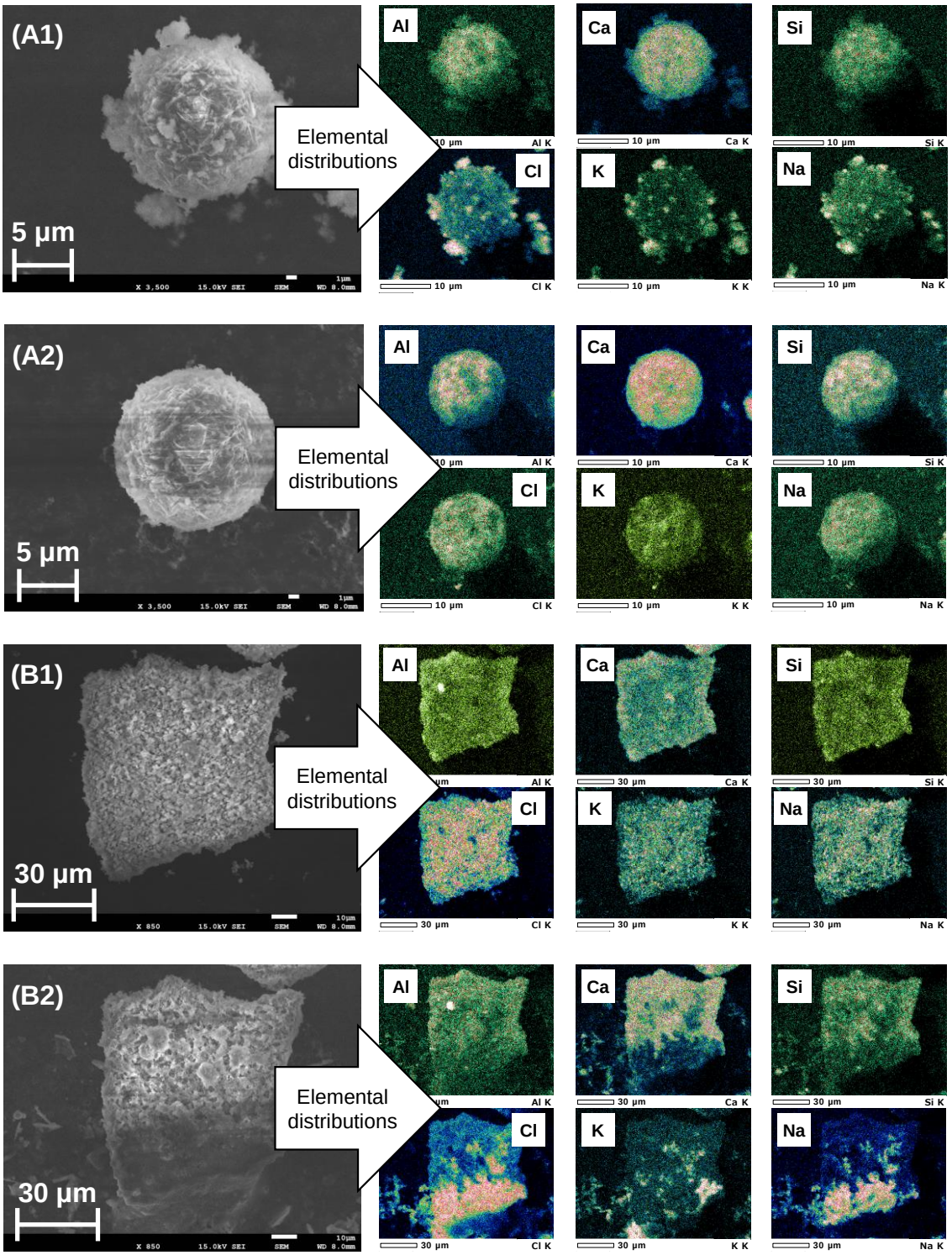

Fig. 6.3 Morphological characteristics and elemental distributions of the same MSWI fly ash particle surface (Particle A and B) (A1 and B1: Before the moistening treatment, A2 and B2: Aftter the moistening treatment)

precipitation/recrystallization under wet condition of the moistening treatment. These results are consistent with CV differences between raw and chelate-treated MSWI fly ash particles shown in Fig. 6.2. According to 100 particle observations shown in Fig. 6.2, decrease of intra-particle heterogeneity on the surface under wet condition seems to be general. However, some specific cases were also found (see Fig. 6.3-B). In these cases, CV values of Ca, Cl and K increased by more than 64% (see Fig. 4-B). It means that dissolution/recrystallization of soluble elements and/or other secondary mineral formation under wet condition of chelate-treatment sometime increase intra-particle heterogeneities of these elements.

6.3.2 Intra-particle heterogeneities of semi-soluble Al/Ca/Si-based matrices and insoluble inner core

The CV values of major elements in all residual materials are shown in Fig. 6.5. In the case of Al and Si, weighted average CV values of all residual materials were 14% lower for Al and 21% lower for Si than those of fly ash particle surfaces. This means that Al and Si intra-particle heterogeneity on the surface is higher than those of inner particle

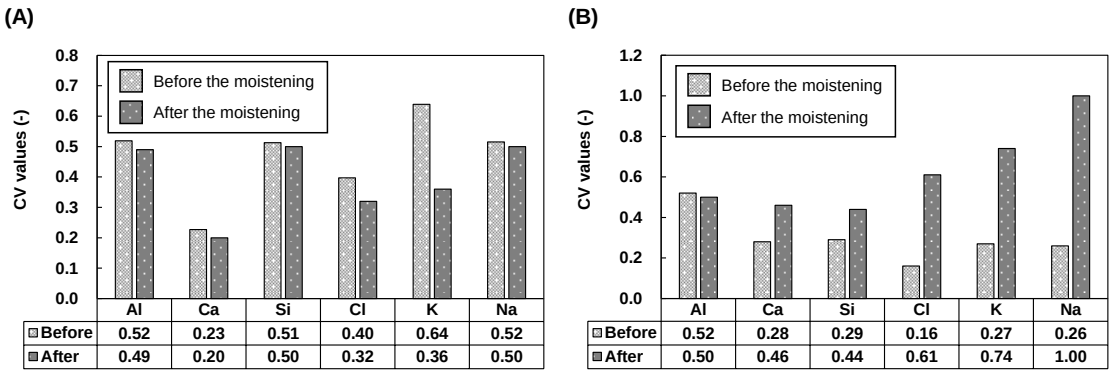

Fig. 6.4 CV values of major elements on the same MSWI fly ash particle surface before and after the moistening treatment ((A) Particle A shown in Fig. 6.3-A, (B) Particle B shown in Fig. 6.3-B)

body. In the case of Ca, weighted average CV values of all residual materials were lower than those of Al and Si. This means that Ca included in semi-soluble component and insoluble inner core are less heterogeneous than Al and Si. Although semi-soluble

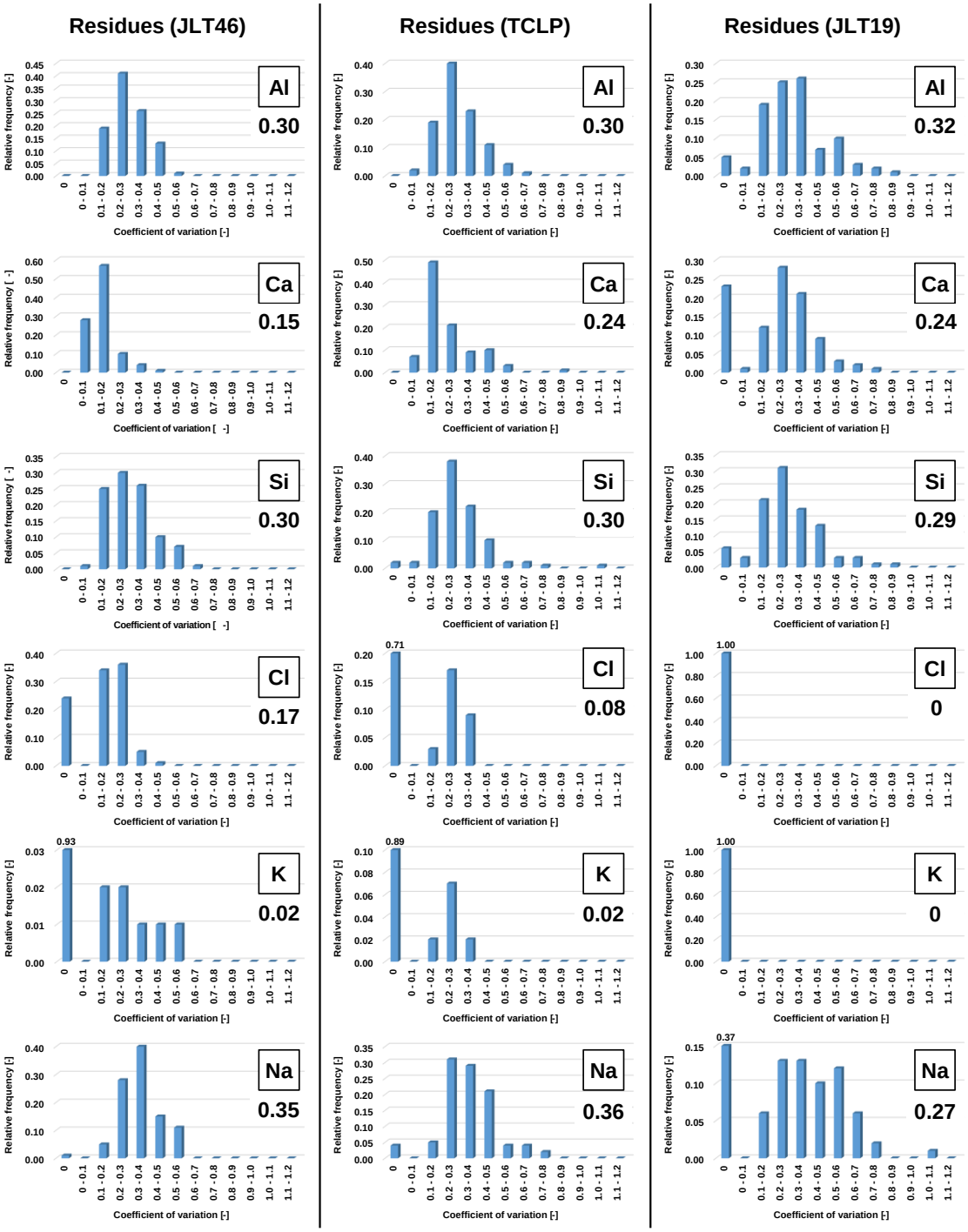

Fig. 6.5 CV values of major elements in all residual materials (Values shown in each figure are weighted average CV values of each element)

component mainly consists of Al, Ca, and Si, binding characteristics of these elements in Al/Ca/Si-based matrices are still uncertain. It might suggest that semi-soluble component is mainly Ca-based matrices like $CaCl_2$, $CaCO_3$ and unreacted $Ca(OH)_2$ in which aluminosilicate domains are included. In the case of Cl, K, and Na, they were not detected in almost residual materials owing to removal of soluble components (e.g. KCl and NaCl). When limited samples in which these elements were detectable were focused on, the average CV values of Cl, K, and Na in all residual materials were more than 28% lower than those of fly ash particle surfaces. Cl, K, and Na included in semi-soluble and insoluble components seem to be geochemically bound to Al, Ca, and/or Si-based matrices. Physical encapsulation of fine KCl/NaCl aggregates inside Al/Ca/Si-based matrices might be negligible owing to lower intra-particle heterogeneity than the surface.

6.3.3 Inter-particle heterogeneity of the surfaces among MSWI fly ash particles

Major element concentrations of the surfaces of raw and chelate-treated MSWI fly ash particles are shown in Fig. 6.6. In the case of Cl, K, and Na, Cl particularly had wide distributions in both raw and chelate-treated MSWI fly ash particles. In the case of Al, Ca, and Si, only Ca distributed widely from 0 to 60.0 wt%. In addition, surface Ca concentrations are clearly higher than those of Al and Si for both raw and chelate-treated MSWI fly ash particles. In the previous subsections, semi-soluble Al/Ca/Si-based matrices were estimated to be Ca-based materials including aluminosilicate domains. In addition, major form of surface Ca was estimated to be exposed surface of semi-soluble Al/Ca/Si-based matrices and/or unreacted $Ca(OH)_2$. Higher concentrations of surface Ca than those of Al and Si, shown in Fig. 6.6, supports this estimation. As a next step, raw and chelate-treated MSWI fly ash particles were compared in order to detect the impacts of wet conditions during chelate-treatment. Average concentrations of surface Al, Ca, and

Si in chelate-treated MSWI fly ash particles increased by 30-61%. On the other hand, CV values of these elements decreased by 43-53% compared to raw MSWI fly ash particles.

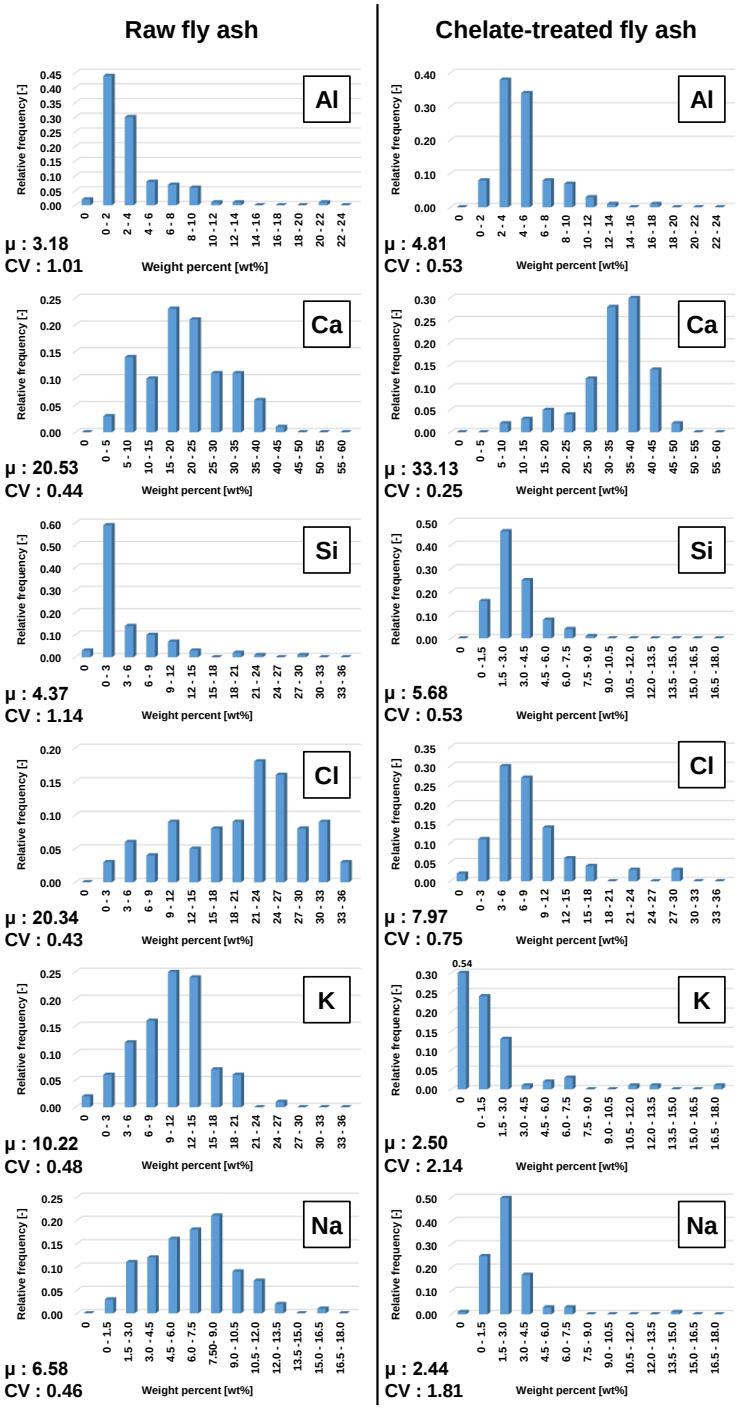

Fig. 6.6 Major element concentrations of the surfaces of raw and chelate-treated MSWI fly ash particles (Unit: weight percent) (μ: average concentration, CV: coefficient of variation)

In contrast to the decrease of inter-particle heterogeneities of surface Al, Ca, and Si by wet condition, those of surface Cl, K, and Na increased. CV values of these elements of chelate-treated MSWI fly ash particles were 60-345% higher than those of raw fly ash particles. Average concentrations of surface Cl, K, and Na in chelate-treated MSWI fly ash particles decreased by 61-75%. Dissolution and transfers of these elements from one fly ash particle to other particles under wet condition of chelate-treatment might have contributed into increase/decrease of inter-particle heterogeneity, internal changes within individual MSWI fly ash particles also seem to promote them to some extent. Fig. 6.7 shows major element concentrations of two raw MSWI fly ash particles, shown in Fig. 6.3, before and after the moistening treatment. The weight percent of surface Cl, K, and Na decreased after the moistening treatment owing to exposure of Al/Ca/Si-based matrices. As a result, weight percent of Al, Ca, and Si slightly increased after the moistening treatment. These results are consistent with the results shown in Fig. 6.6 although it might be specific cases.

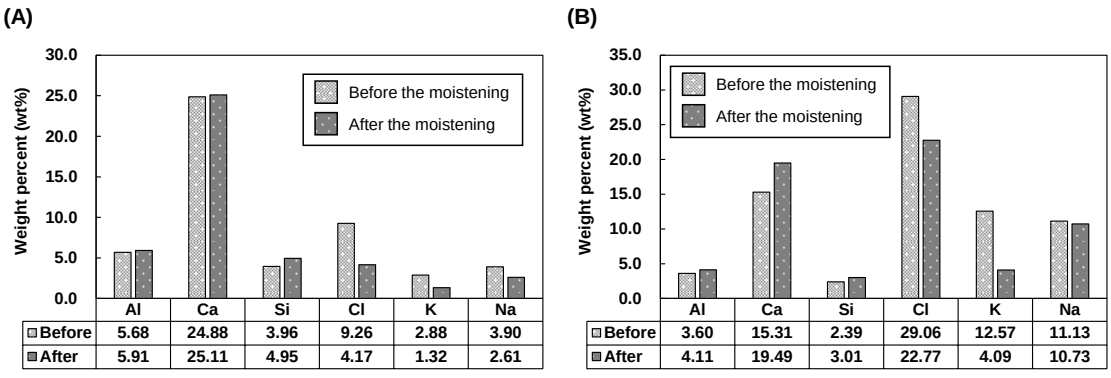

Fig. 6.7 Weight percent of major elements on the same MSWI fly ash particle surface before and after the moistening treatment ((A) Particle A shown in Fig. 6.3-A, (B) Particle B shown in Fig. 6.3-B)

6.3.4 Inter-particle heterogeneities of semi-soluble Al/Ca/Si-based matrices and insoluble inner core

Element concentration as weight percent of major elements in all residual materials are shown in Fig. 6.8. In the case of Cl, K, and Na, their concentrations in semi-soluble and insoluble components were within slightly smaller range in comparison with their surface concentrations. In addition, average concentrations of these elements were more than 32% lower than those on the surface. Except for Cl in semi-soluble component exposed by JLT46, CV values of Cl and K in semi-soluble components were 65-132% higher than those of the surface. It is contrast to lower intra-particle heterogeneity of Cl and K in semi-soluble components. On the other hand, CV values of Na in semi-soluble components were more than 18% lower compared to the surface. In the case of Al, Ca, and Si, CV values of these elements in semi-soluble components exposed by TCLP and insoluble components were higher than those of the surface. They are 9-40% increase in semi-soluble components and 49-352% increase in insoluble components. This means that inter-particle heterogeneity of these elements in insoluble component is particularly high. Although results in Chapter 3 suggested structure model of a MSWI fly ash particle including Si-based insoluble core, large inter-particle heterogeneity of Al and Ca in insoluble components suggest that Al-rich and/or Ca-rich cores are also possible. In order to visualize inter-particle heterogeneity of Al, Ca, and Si in each fly ash particle component, 100 particles observation results are plotted in ternary diagrams (see Fig. 6.9). As expected above, Fig. 6.9-E clearly shows Al-rich and Ca-rich insoluble cores as well as Si-rich core. Elemental distributions of Al-, Ca-, and Si-rich insoluble cores are shown in Fig 6.10. SEM-EDX analysis showed that Al and Si-rich insoluble cores, which are considered as Al_2O_3 and SiO_2 as identified by XRD analysis, had smooth and non-porous surface (see Fig. 6.10-A and B). SEM-EDX analysis also showed that Ca-rich particles

seem to be aggregates of smaller particles (see Fig. 6.10-C). Furthermore, Ti was frequently concentrated on Ca-rich particles. Therefore, they seem to be $CaTiO_3$ as identified by XRD analysis. In this analysis, Fe-rich particles, which are considered as Fe

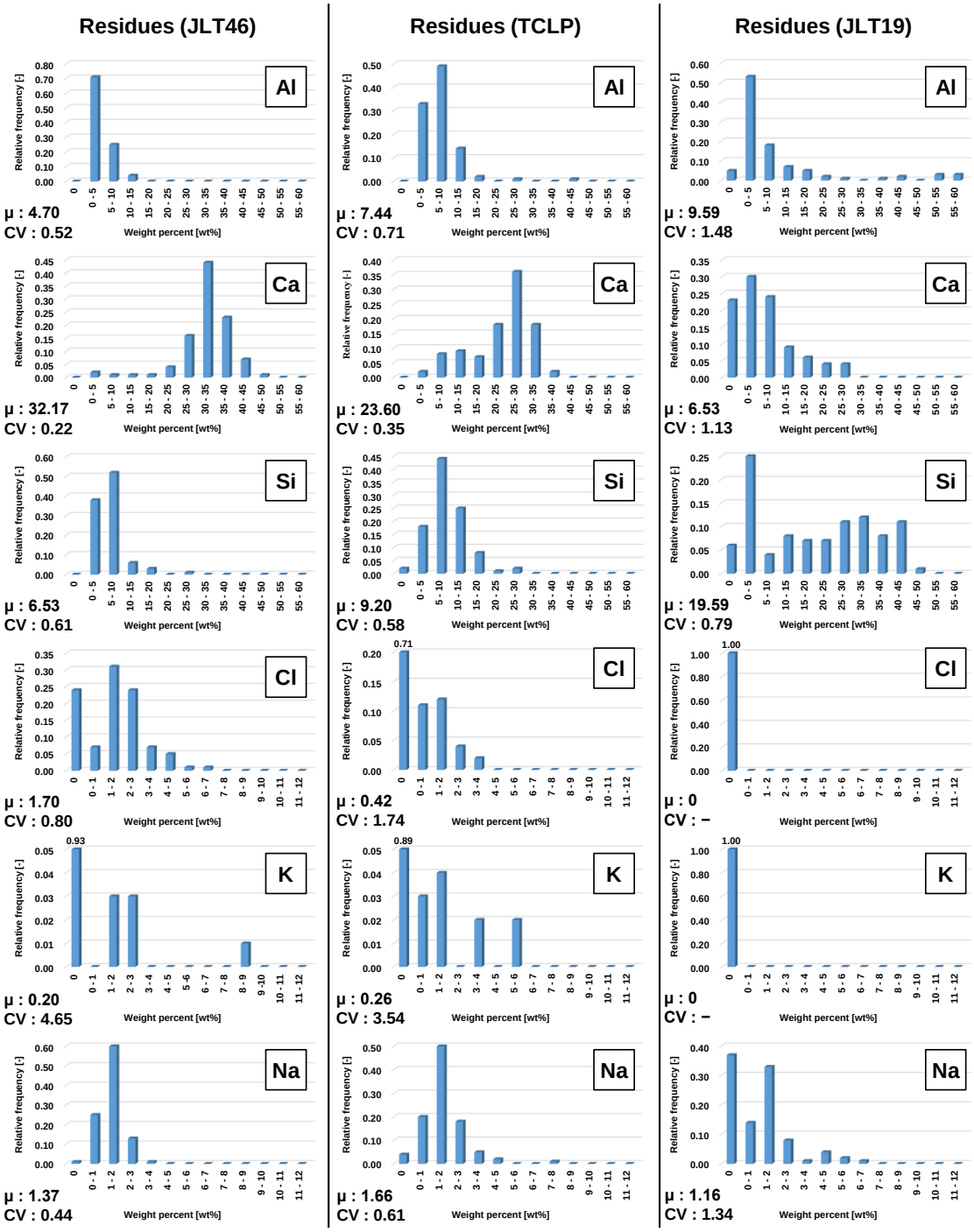

Fig. 6.8 Major element concentrations in all residual materials (Unit: weight percent) (μ: average concentration, CV: coefficient of variation)

oxides, were also observed in the residual materials (see Fig. 6.10-D). Therefore, Al-, Ca-, and Si-rich materials, which sometimes or frequently include Fe and Ti, form insoluble core of a MSWI fly ash particle. Fig. 6.9-C and D supports that semi-soluble Al/Ca/Si-based matrices consist mainly of Ca-based materials including aluminosilicate domains. When aluminosilicate is rich in semi-soluble component, it would increase inter-particle heterogeneity of Al and Si. Leaching behaviours of heavy metals in MSWI fly ash are partially or greatly controlled by complexation or sorption to Al/Ca/Si-based matrices like hydrous aluminium oxides and calcium carbonate [19–21]. Inter-particle and intra-particle heterogeneity of semi-soluble Al/Ca/Si-based matrices might change sorption characteristics and thus give non-negligible impact on leaching behaviours at micro-level local scale.

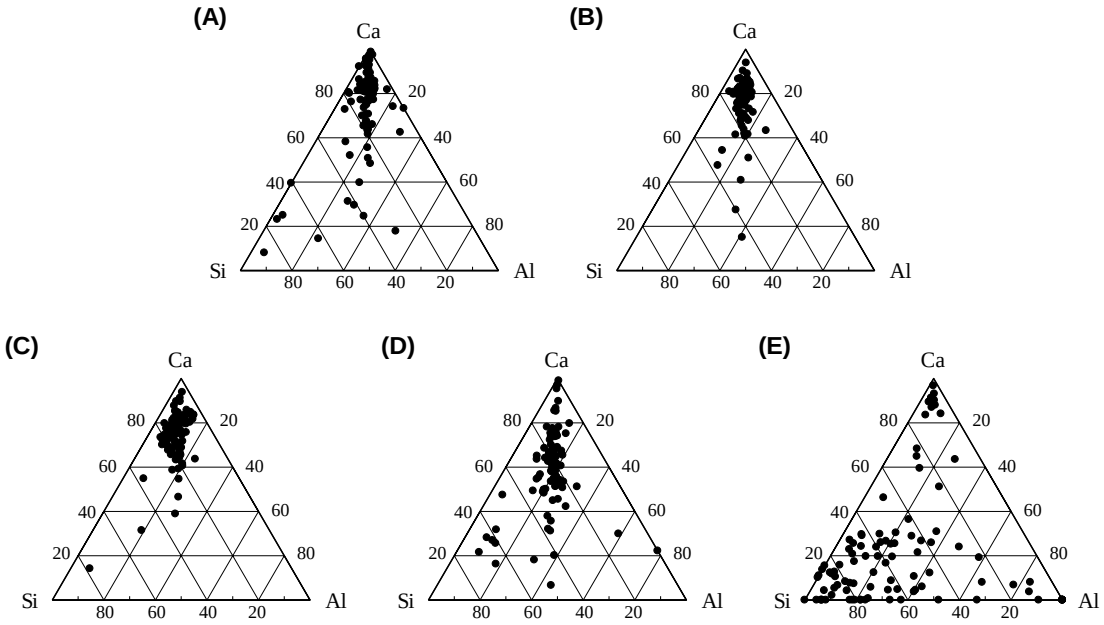

Fig. 6.9 Ternary diagram of MSWI fly ash particle components. (A) Surface of raw MSWI fly ash particles (B) Surface of chelate-treated MSWI fly ash particles (C) Semi-soluble component exposed by JLT46 (D) Semi-soluble component exposed by TCLP (E) Insoluble component exposed by JLT19

6.4 Conclusion

Two types of elemental heterogeneities of MSWI fly ash particle were measured focusing on three structural components of fly ash particles. They are internal heterogeneity of individual fly ash particles (intra-particle heterogeneity) and inter-particle heterogeneities among fly ash particles. The impact of wet condition during

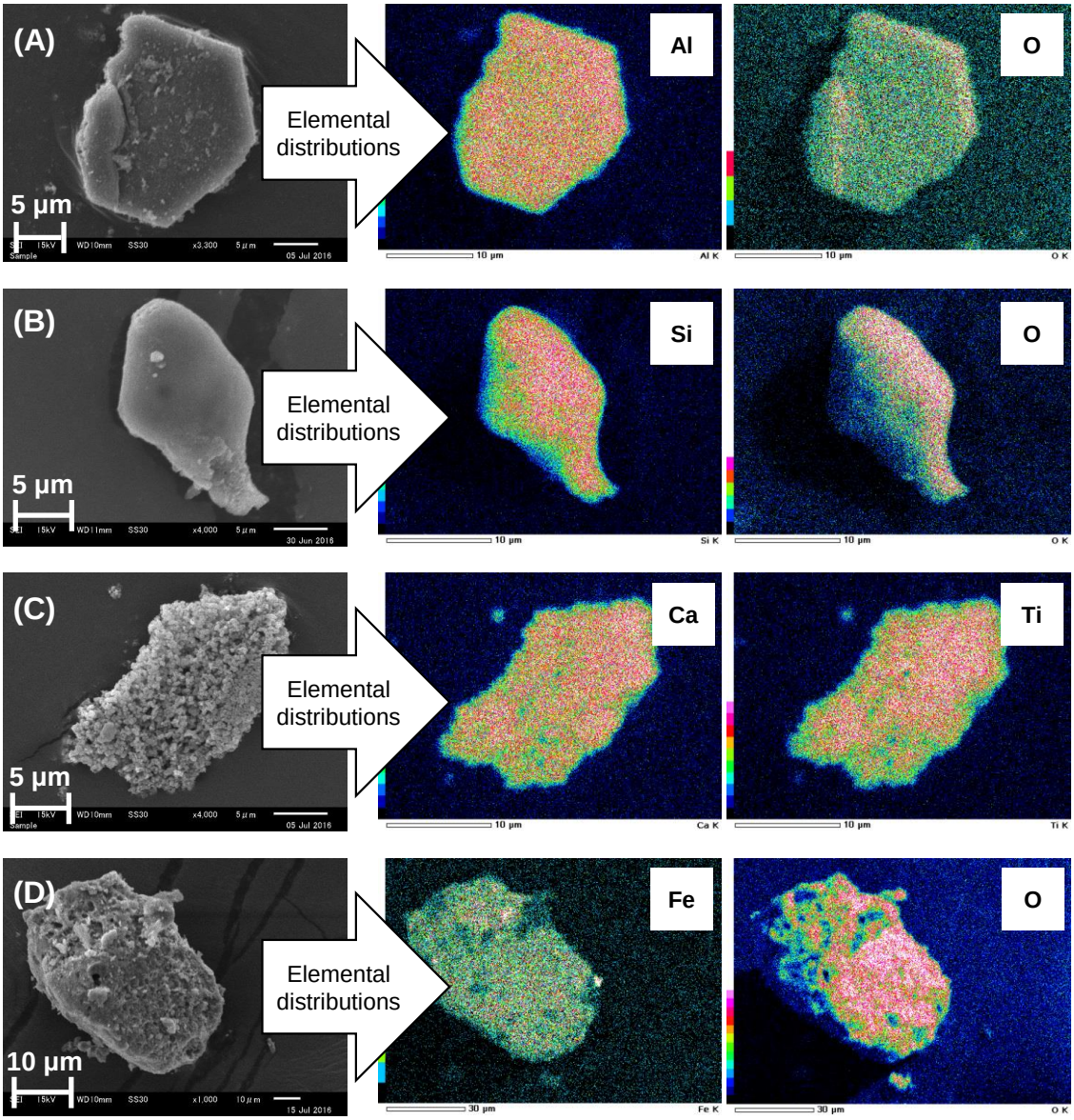

Fig. 6.10 Morphological characteristics and elemental distributions of residual materials collected after JLT19. (A) Aluminum-rich particle (B) Silicon-rich particle (C) Calcium and titanium-rich particle (D) Iron-rich particle

chelate-treatment on intra- and inter-particle heterogeneity of fly ash particle surfaces were also investigated. On the surface of fly ash particles, Cl, K, and Na have 0-82% larger intra-particle heterogeneities than Al, Ca, and Si owing to KCl/NaCl-based aggregates. Wet condition of chelate treatment decreased intra-particle heterogeneities of Cl, K, and Na by 2-54% owing to dissolution and precipitation. Smaller intra-particle heterogeneity of Ca in semi-soluble component than those of Al and Si suggest that semi-soluble Al/Ca/Si-based matrices around insoluble cores are Ca-based materials including aluminosilicate domains. It was also supported by inter-particle heterogeneity analysis of fly ash particle surfaces. In addition, wet condition of chelate treatment increased inter-particle heterogeneities of Al, Ca, and Si by 30-61% but decrease those of Cl, K, and Na by 61-75%. Inter-particle heterogeneities of Al, Ca, and Si in semi-soluble components and insoluble components are 9-40% and 49-352% higher than those of fly ash particle surface, respectively. Inter-particle heterogeneity analysis clearly suggests that insoluble components are not only Si-rich cores but also Al-rich and Ca-rich cores. MSWI fly ash particles have both internal heterogeneities inside their bodies and also are heterogeneous in inter-particle level.

6.5 References

[1] M.C. Hsiao, H.P. Wang, Y.L. Wei, J.E. Chang, C.J. Jou, Speciation of copper in the incineration fly ash of a municipal solid waste, J. Hazard. Mater. 91 (2002) 301–307. doi:10.1016/S0304-3894(02)00015-8.

[2] M.C. Hsiao, H.P. Wang, Y.W. Yang, EXAFS and XANES studies of copper in a solidified fly ash, Environ. Sci. Technol. 35 (2001) 2532–2535. doi:10.1021/es001374v.

[3] M. Li, S. Hu, J. Xiang, L.S. Sun, P.S. Li, S. Su, X.X. Sun, Characterization of fly ashes from two chinese municipal solid waste incinerators, Energy & Fuels. 17 (2003) 1487–1491. doi:10.1021/ef030092o.

[4] T. Mangialardi, A.E. Paolini, A. Polettini, P. Sirini, Optimization of the solidification/stabilization process of MSW fly ash in cementitious matrices, J. Hazard. Mater. 70 (1999) 53–70. doi:10.1016/S0304-3894(99)00132-6.

[5] S. Rémond, D. Bentz, P. Pimienta, Effects of the incorporation of Municipal Solid Waste Incineration fly ash in cement pastes and mortars: II: Modeling, Cem. Concr. Res. 32 (2002) 565–576. doi:10.1016/S0008-8846(01)00722-0.

[6] S. Rémond, P. Pimienta, D. Bentz, Effects of the incorporation of Municipal Solid Waste Incineration fly ash in cement pastes and mortars: I. Experimental study, Cem. Concr. Res. 32 (2002) 303–311. doi:10.1016/S0008-8846(01)00674-3.

[7] A.P. Bayuseno, W.W. Schmahl, Characterization of MSWI fly ash through mineralogy and water extraction, Resour. Conserv. Recycl. 55 (2011) 524–534. doi:10.1016/j.resconrec.2011.01.002.

[8] F. Bodénan, P. Deniard, Characterization of flue gas cleaning residues from European solid waste incinerators: Assessment of various Ca-based sorbent processes, Chemosphere. 51 (2003) 335–347. doi:10.1016/S0045-6535(02)00838-X.

[9] L. Le Forestier, G. Libourel, Characterization of Flue Gas Residues from Municipal Solid Waste Combustors, Environ. Sci. Technol. 32 (1998) 2250–2256. doi:10.1021/es980100t.

[10] C.S. Kirby, J.D. Rimstidt, Mineralogy and surface properties of municipal solid waste ash, Environ. Sci. Technol. 27 (1993) 652–660. doi:10.1021/es00001a601.

[11] S. Nam, W. Namkoong, Irradiation effect on leaching behavior and form of heavy

metals in fly ash of municipal solid waste incinerator, J. Hazard. Mater. 199–200 (2012) 440–447. doi:10.1016/j.jhazmat.2011.11.049.

[12] H. Raclavská, A. Corsaro, S. Hartmann-Koval, D. Juchelková, Enrichment and distribution of 24 elements within the sub-sieve particle size distribution ranges of fly ash from wastes incinerator plants, J. Environ. Manage. 203 (2017) 1169–1177. doi:10.1016/j.jenvman.2017.03.073.

[13] R.P.W.J. Struis, M. Pasquali, L. Borgese, A. Gianoncelli, M. Gelfi, P. Colombi, D. Thiaudière, L.E. Depero, G. Rizzo, E. Bontempi, Inertisation of heavy metals in municipal solid waste incineration fly ash by means of colloidal silica – a synchrotron X-ray diffraction and absorption study, RSC Adv. 3 (2013) 14339–14351. doi:10.1039/c3ra41792a.

[14] G. Weibel, U. Eggenberger, S. Schlumberger, U.K. Mäder, Chemical associations and mobilization of heavy metals in fly ash from municipal solid waste incineration, Waste Manag. 62 (2016) 147–159. doi:10.1016/j.wasman.2016.12.004.

[15] S. Gilardoni, P. Fermo, F. Cariati, V. Gianelle, D. Pitea, E. Collina, M. Lasagni, MSWI fly ash particle analysis by scanning electron microscopy-energy dispersive X-ray spectroscopy., Environ. Sci. Technol. 38 (2004) 6669–6675. doi:10.1021/es0494961.

[16] H. Hwang, C.-U. Ro, Single-particle characterization of municipal solid waste (MSW) ash particles using low-Z particle electron probe X-ray microanalysis, Atmos. Environ. 40 (2006) 2873–2881. doi:10.1016/j.atmosenv.2006.01.004.

[17] P.Y. Mahieux, J.E. Aubert, M. Cyr, M. Coutand, B. Husson, Quantitative mineralogical composition of complex mineral wastes - Contribution of the Rietveld method, Waste Manag. 30 (2010) 378–388. doi:10.1016/j.wasman.2009.10.023.

[18] H. Kitamura, T. Sawada, T. Shimaoka, F. Takahashi, Geochemically structural characteristics of municipal solid waste incineration fly ash particles and mineralogical surface conversions by chelate treatment, Environ. Sci. Pollut. Res. 23 (2016) 734–743. doi:10.1007/s11356-015-5229-5.

[19] J. Hyks, T. Astrup, T.H. Christensen, Long-term leaching from MSWI air-pollution-control residues: Leaching characterization and modeling, J. Hazard. Mater. 162 (2009) 80–91. doi:10.1016/j.jhazmat.2008.05.011.

[20] G. Cappai, S. Cara, A. Muntoni, M. Piredda, Application of accelerated carbonation on MSW combustion APC residues for metal immobilization and CO2 sequestration, J. Hazard. Mater. 207–208 (2012) 159–164. doi:10.1016/j.jhazmat.2011.04.013.

[21] L. Wang, Y. Jin, Y. Nie, Investigation of accelerated and natural carbonation of MSWI fly ash with a high content of Ca, J. Hazard. Mater. 174 (2010) 334–343. doi:10.1016/j.jhazmat.2009.09.055.

CHAPTER

7

CONCLUSION AND RECOMMENDATION

Abstract: In this chapter, the findings from the present study are summarized as conclusions. Following the conclusions, recommendations in association with conclusions are outlined.

7.1 Conclusion

From the viewpoint of safty management for MSWI fly ash, the present study investigated geochemical characteristics of MSWI fly ash at micro-scale level using mainly SEM-EDX analysis. The findings of the present study are concluded as follows.

7.1.1 Mineralogical characteristics

XRD results showed that chelate treatment did not generate new secondary minerals in detectable level of XRD analysis (approximately 5-10 wt%) for MSWI fly ash. However, SEM observation showed secondary mineral formation such as ettringite by moistening in chelate-treated MSWI fly ash. These results suggest that chelate treatment has non-negligible impacts on mineralogical characteristics. Leaching experiments (JLT46 and TCLP) also promote ettringite formation by hydration reaction. These results suggestted that MSWI fly ash is mineralogically active.

7.1.2 Morphological characteristics

SEM observation showed that raw MSWI fly ash particles could be categorized to 4 types based on their morphological characteristics. SEM-EDX analysis showed that elemental composition of raw MSWI fly ash particles was strongly dependent on particle size. Because chelate treatment changed the surface of fly ash particles dramatically owing to secondary mineral formations, two more types could be categorized for chelate-treated MSWI fly ash particles. Three types of leaching experiments and heterogeneity analysis revealed that a MSWI fly ash particle likely consists of Al-rich, Ca-rich, or Si-rich insoluble core structure, Al/Ca/Si-based semi-soluble matrices inside the body, and soluble KCl/NaCl-based aggregates on the surface. The Al/Ca/Si-based semi-soluble matrices around insoluble cores are estimated to be Ca-based materials including

aluminosilicate domains.

7.1.3 Heterogeneous characteristics

On the surface of fly ash particles, Cl, K, and Na have 0-82% larger intra-particle heterogeneities than Al, Ca, and Si owing to KCl/NaCl-based aggregates. Wet condition of chelate treatment decreased intra-particle heterogeneities of Cl, K, and Na by 2-54% owing to dissolution and precipitation. It also increased inter-particle heterogeneities of Al, Ca, and Si by 30-61% but decrease those of Cl, K, and Na by 61-75%. Inter-particle heterogeneities of Al, Ca, and Si in semi-soluble components and insoluble components are 9-40% and 49-352% higher than those of fly ash particle surface, respectively. These results showed that MSWI fly ash particles have both internal heterogeneities inside their bodies and also are heterogeneous in inter-particle level.

7.1.4 Metal leachability and immobilization

SEM-EDX analysis showed that additional immobilization effects of secondary mineral formation are limited for chelate-treated MSWI fly ash. The durability of toxic metal immobilization by chelate treatment is almost equal to the stability of metal chelate complex. Micro-scale correlation analysis showed that metal oxides (Ti, Cu, Fe, Mn, and Zn) likely react with and/or are trapped in Al/Ca/Si-based matrix like aluminosilicate in the gas phase and then followed by KCl/NaCl adsorption on the surface. These results suggest that metal leachability might be controlled by not only metal oxide leachability but also leachability of Al/Ca/Si-based matrix around metal oxides.

7.2 Recommendation

The present study still could not conclude the impacts of intra and inter-particle

heterogeneity of MSWI fly ash particles on leaching behaviors of heavy metals. Geochemical modeling is one possibility in order to describe leaching behaviors of heavy metals. Geochemical modeling software such as MINTEQA2 [1–6], Visual MINTEQ [7–9], PHREEQC [9,10], ORCHESTRA [4], and LeachXS [4,11] was applied to simulate leaching behaviors of heavy metals in MSWI fly ash. These techniques might quantify the impacts of heterogeneity on metal leachabilities.

As described in subsection 2.2.1, the present study investigated only one sample lot in order to know possible diversity of micro-characteristics of MSWI fly ash particles from the same sample lot. However, composite samples made of different sample lots are usually recommended to generalize analysis results because characteristics of MSWI fly ash depend on waste stream and incineration conditions. Therefore, characterization of composite samples as well as other MSWI fly ash samples collected from different type incinerators are required for generalized conclusions.

As described in Chapter 1, chelate treatment for MSWI fly ash is preferred by a number of municipalities. In order to close and reuse landfill site, leachate treatment is required. Chemical oxygen demand (COD), which is an indicator of the amount of organic matters in leachate, should be monitored for the leachate treatment. However, chelate reagent contains hardly decomposable COD components [12]. Therefore, chelate treatment causes delay of stabilizing landfill site. Thus, inorganic treatment might be preferred. In recent years, geopolymer, which is obtained by the reaction between a solid aluminosilicate and a highly concentrated alkaline solution, has been proposed in order to immobilize heavy metals in MSWI fly ash [13–16]. Furthermore, clay minerals consisted mainly of Al and Si can immobilize heavy metals by ion exchange, adsorption, and intercalation [17]. Therefore, inorganic treatment for selective clay mineral formation in MSWI fly ash might achieve immobilization of heavy metals as well as stabilization

of landfill site simultaneously. Therefore, such technology is one of the promising treatment for MSWI fly ash in the future.

7.3 References

[1] T.T. Eighmy, J.D. Eusden, J.E. Krzanowski, D.S. Domingo, D. Stampfli, J.R. Martin, P.M. Erickson, Comprehensive approach toward understanding element speciation and leaching behavior in municipal solid waste incineration electrostatic precipitator ash, Environ. Sci. Technol. 29 (1995) 629–646. doi:10.1021/es00003a010.

[2] T.T. Eighmy, B.S. Crannell, L.G. Butler, F.K. Cartledge, E.F. Emery, D. Oblas, J.E. Krzanowski, J.D. Eusden, E.L. Shaw, C.A. Francis, Heavy metal stabilization in municipal solid waste combustion dry scrubber residue using soluble phosphate, Environ. Sci. Technol. 31 (1998) 3330–3338. doi:10.1021/es970407c.

[3] P. Van Herck, B. Van Der Bruggen, G. Vogels, C. Vandecasteele, Application of computer modelling to predict the leaching behaviour of heavy metals from MSWI fly ash and comparison with a sequential extraction method, Waste Manag. 20 (2000) 203–210. doi:10.1016/S0956-053X(99)00321-9.

[4] T. Astrup, J.J. Dijkstra, R.N.J. Comans, H.A. Van Der Sloot, T.H. Christensen, Geochemical modeling of leaching from MSWI air-pollution-control residues, Environ. Sci. Technol. 40 (2006) 3551–3557. doi:10.1021/es052250r.

[5] H. Zhang, Y. Zhao, J. Qi, Characterization of heavy metals in fly ash from municipal solid waste incinerators in Shanghai, Process Saf. Environ. Prot. 88 (2010) 114–124. doi:10.1016/j.psep.2010.01.001.

[6] Y. Zhang, B. Cetin, W.J. Likos, T.B. Edil, Impacts of pH on leaching potential of elements from MSW incineration fly ash, Fuel. 184 (2016) 815–825.

doi:10.1016/j.fuel.2016.07.089.

[7] Y. Zhang, J. Jiang, M. Chen, MINTEQ modeling for evaluating the leaching behavior of heavy metals in MSWI fly ash, J. Environ. Sci. 20 (2008) 1398–1402. doi:10.1016/S1001-0742(08)62239-1.

[8] A. Funatsuki, M. Takaoka, K. Oshita, N. Takeda, Methods of determining lead speciation in fly ash by X-ray absorption fine-structure spectroscopy and a sequential extraction procedure, Anal. Sci. 28 (2012) 481–490. doi:10.2116/analsci.28.481.

[9] R.M. Santos, G. Mertens, M. Salman, Ö. Cizer, T. Van Gerven, Comparative study of ageing, heat treatment and accelerated carbonation for stabilization of municipal solid waste incineration bottom ash in view of reducing regulated heavy metal/metalloid leaching, J. Environ. Manage. 128 (2013) 807–821. doi:10.1016/j.jenvman.2013.06.033.

[10] J. Hyks, T. Astrup, T.H. Christensen, Long-term leaching from MSWI air-pollution-control residues: Leaching characterization and modeling, J. Hazard. Mater. 162 (2009) 80–91. doi:10.1016/j.jhazmat.2008.05.011.

[11] F. Takahashi, T. Kanou, T. Shimaoka, Lead solubility and chemical conversions of lead species in insoluble residues of municipal solid waste incineration fly ash during pH-dependent leaching test, J. Japan Soc. Civ. Eng. Div. G Environ. Syst. Eng. 67 (2011) III_517-III_523 (in Japanese).

[12] S. Higuchi, Technical transitions and future trends at MSW landfill site, Mater. Cycles Waste Manag. Res. 26 (2015) 3–11 (in Japanese).

[13] L. Zheng, W. Wang, Y. Shi, The effects of alkaline dosage and Si/Al ratio on the immobilization of heavy metals in municipal solid waste incineration fly ash-based geopolymer, Chemosphere. 79 (2010) 665–671.

doi:10.1016/j.chemosphere.2010.02.018.

[14] Y. Luna Galiano, C. Fernández Pereira, J. Vale, Stabilization/solidification of a municipal solid waste incineration residue using fly ash-based geopolymers, J. Hazard. Mater. 185 (2011) 373–381. doi:10.1016/j.jhazmat.2010.08.127.

[15] A. Zacco, L. Borgese, A. Gianoncelli, R.P.W.J. Struis, L.E. Depero, E. Bontempi, Review of fly ash inertisation treatments and recycling, Environ. Chem. Lett. 12 (2014) 153–175. doi:10.1007/s10311-014-0454-6.

[16] L. Zheng, W. Wang, X. Gao, Solidification and immobilization of MSWI fly ash through aluminate geopolymerization: Based on partial charge model analysis, Waste Manag. 58 (2016) 270–279. doi:10.1016/j.wasman.2016.08.019.

[17] K.G. Bhattacharyya, S. Sen Gupta, Adsorption of a few heavy metals on natural and modified kaolinite and montmorillonite: A review, Adv. Colloid Interface Sci. 140 (2008) 114–131. doi:10.1016/j.cis.2007.12.008.

Acknowledgement

I would like to express my gratitude to my supervisor Associate Professor Fumitake Takahashi. I deeply appreciate his kind cooperation for my research during my master's and doctoral programs. I was able to have many great experiences throughout attendance of domestic / international conferences, application for research grants, writing papers for journal in Japanese / English, and planning some activities as a member of young generation meeting branch in Japan Society of Material Cycles and Waste Management (JSMSWM). I'm looking forward to joint research with you in the future as a researcher.

I'm grateful to Professor Kunio Yoshikawa for meaningful discussion of my research during seminar. I'm also very thankful for giving me opportunities to make good relationship with foreign students throughout annual Japan-China-Korea joint symposium.

I'm grateful to Associate Professor Koji Tokimatsu for introducing me some professors and/or officers to make good connection with them. I'm very thankful for your kind consideration. I also enjoyed communicating with you through drinking together.

I thank to laboratory staffs, seniors, colleagues, and juniors. I could really enjoy my life in Tokyo Institute of Technology. The memorable events such as travels during conferences, graduation trip for master's program, and attending pop music concerts cannot be forgotten.

I acknowledge financial support by “130th anniversary scholarship for doctor course access encouragement” granted by a fund established by Tokyo Institute of Technology (From Oct. 2014 to Mar. 2015). I also acknowledge financial support by Research Fellowships of Japan Society for the Promotion of Science (JSPS) for Young Scientists (From Apr. 2016 to Mar. 2018).

Hiroki Kitamura

List of publication

1. **Hiroki Kitamura**, Takaya Sawada, Takayuki Shimaoka, Fumitake Takahashi (2016) Geochemically structural characteristics of municipal solid waste incineration fly ash particles and mineralogical surface conversions by chelate treatment, *Environmental Science and Pollution Research,* Vol.23, No.1, 734-743. DOI: 10.1007/s11356-015-5229-5.

2. **Hiroki Kitamura**, Fumirake Takahashi (2015) Impact of secondary mineral formation on immobilizing hazardous elements for municipal solid waste incineration fly ash particles, *Journal of Japan Society of Civil Engineers-G:Environment,* Vol.71, No.7, II_239-III_245. DOI:10.2208/jscejer.71.III_239 (in Japanese).

3. **Hiroki Kitamura**, Astryd Viandila Dahlan, Yu Tian, Takayuki Shimaoka, Takashi Yamamoto, Fumirake Takahashi (2017) Geochemical form analysis of titanium in chelate-treated municipal solid waste incineration fly ash particles employing correlation analysis of elemental distribution line profiles, *Journal of Japan Society of Civil Engineers-G:Environment,* Vol.73, No.7, III_287-III_295 (in Japanese).

4. **Hiroki Kitamura**, Astryd Viandila Dahlan, Yu Tian, Takayuki Shimaoka, Takashi Yamamoto, Fumirake Takahashi, Impact of secondary generated minerals on toxic element immobilization for air pollution control fly ash of a municipal solid waste incinerator, *Environmental Science and Pollution Research* (under review).

5. **Hiroki Kitamura**, Astryd Viandila Dahlan, Yu Tian, Takayuki Shimaoka, Takashi Yamamoto, Fumirake Takahashi, Possible metal species and their external matrix in municipal solid waste incineration fly ash estimated by micro-scale correlation analysis, *Journal of Hazardous Materials* (submitted).

6. **Hiroki Kitamura**, Astryd Viandila Dahlan, Yu Tian, Takayuki Shimaoka, Takashi Yamamoto, Fumirake Takahashi, Intra- and inter-particle heterogeneity of municipal solid waste incineration fly ash particles, *Journal of Material Cycles and Waste Management* (submitted).